COMPARATIVE ADSORPTION STUDIES OF HEAVY METAL IONS ON CHITIN AND CHITOSAN BIOPOLYMERS

A Thesis Submitted to
the Graduate School of Engineering and Science of
İzmir Institute of Technology
in Partial Fulfillment of the Requirements for the Degree of

MASTER OF SCIENCE

in Chemistry

by
Serkan KELEŞOĞLU

July 2007
İZMİR

We approve the thesis of **Serkan KELEŞOĞLU**

Date of Signature

……..……
Assoc. Prof. Dr. Hürriyet POLAT
Supervisor
Department of Chemistry
Izmir Institute of Technology

20 July 2007

……..……
Assoc. Prof. Dr. Talal SHAHWAN
Department of Chemistry
Izmir Institute of Technology

20 July 2007

……..……
Prof. Dr. Mehmet POLAT
Department of Chemical Engineering
Izmir Institute of Technology

20 July 2007

……..……
Prof. Dr. Şükran ÇAKLI
Department of Fish Processing Technology
Ege University

20 July 2007

……..……
Assoc. Prof. Dr. Talat YALÇIN
Department of Chemistry
Izmir Institute of Technology

20 July 2007

……..……
Prof. Dr. Levent ARTOK
Head of Department
Izmir Institute of Technology

……..……
Prof. Dr. M. Barış ÖZERDEM
Head of The Graduate School

ACKNOWLEDGEMENTS

I would like to thank the people who have assisted me in preparing this thesis. First I would like to express my grateful thanks to my supervisor Assoc. Prof. Dr. Hürriyet POLAT for her guidance, motivation and endless supports during this project. I am also grateful to Assoc. Prof. Dr. Talal SHAHWAN and Prof. Dr. Mehmet POLAT for their valuable cricism.

I am also thankful to Assoc. Prof. Dr. Cihangir DURAN in Material Science Department at Gebze Institute of Technology for his help in zeta potential and particle size analysis measurements.

I also would like to thank to Research Scientist Sinan YILMAZ for his help in the AAS measurements, and The Center of Material Research for their assistance in the SEM, XRD, TGA/DTA and Elemental Analysis measurements.

Special thanks are to Research Assistants, Mürşide KES and Demet ERDOĞAN for their helps and valuable comments during the experimental period.

Special thanks go to all friends, research assistants and technicians in İzmir Institute of Technology for their helps and friendships.

Finally, I would like to thank my family for their endless support, continued patience and encouragement throughout the course of my studies.

ABSTRACT

COMPARATIVE ADSORPTION STUDIES OF HEAVY METAL IONS ON CHITIN AND CHITOSAN BIOPOLYMERS

In this study comparative adsorption studies of heavy metal ions (Cu^{2+}, Pb^{2+}, Cd^{2+}, Ni^{2+}) on chitin and chitosan biopolymers were performed to investigate the uptake performances. For this purpose chitosan was prepared from chitin in controlled experimental conditions and then these biopolymers were characterized with Elemental Analysis, Viscosity, FT-IR, Potentiometric Titration, XRD, SEM, Zeta Potential, Particle Size Distribution and TGA/DTA measurements.

Batch adsorption experiments were performed at eight different initial heavy metal ion concentrations (10, 25, 50, 100, 250, 500, 750, 1000 m/L), two different temperatures (298.15 K and 328.15 K), time period ranging from 5 minutes to 1 day and pH of solutions ranging from 1 to 7. The results indicated that the uptake performence of chitin and chitosan biopolymer significantly changed with pH, adsorbent dosage, concentration and temperature. In general, chitosan biopolymer demonstrated greater fixation abbility for heavy metal ions than chitin. However the fixation trend of heavy metal ions on chitin and chitosan biopolymers was the same ($Cu^{2+} > Pb^{2+} > Cd^{2+} > Ni^{2+}$). Moreover Irwing-Williams Series support the dominancy of the binding mechanism for Cu^{2+}, Cd^{2+} and Ni^{2+} ions on both biopolymers.

Adsorption of heavy metal ions on both chitin and chitosan biopolymers followed pseudo second order kinetics with the rate constant indicating faster adsorption on chitin for Cu^{2+} and Pb^{2+} ions and faster adsorption on chitosan for Cd^{2+} and Ni^{2+} ions.

Both of the Freundlich and Langmuir adsorption isotherms seem to adequately represent the adsorption data obtained in this study.

The positive value of enthalpy change (ΔH^{o}) and negative value of free energy change (ΔG^{o}) shows the adsorption process is endothermic and spontaneous. Moreover obtained positive entropy changes (ΔS^{o}) show that an increase in randomness, is associating the adsorption of metal ions onto chitin and chitosan biopolymers.

ÖZET

KİTİN VE KİTOSAN BİYOPOLİMERLERİ ÜZERİNE AĞIR METAL İYONLARININ KARŞILAŞTIRMALI ADSORPSİYON ÇALIŞMALARI

Bu çalışmada ağır metal iyonlarının (Cu^{2+}, Pb^{2+}, Cd^{2+}, Ni^{2+}) kitin ve kitosan biyopolimerlerince tutunma performansları karşılaştırılmalı olarak incelenmiştir. Bu amaç doğrultusunda kitosan biyopolimeri kitinden elde edilmiş ve her iki biyopolimerde adsorpsiyon deneyleri öncesi çeşitli analitik ve enstrumental yöntemlerle karakterize edilmiştir.

Adsorpsiyon deneyleri 5 dakikadan 24 saate kadar değişen çalkalama süresi, sekiz farklı başlangıç konsantrasyonu ve iki farklı sıcaklık ortamlarında gerçekleştirilmiştir.

Elde edilen veriler ağır metal iyonlarının heriki biyopolimer tarafından tutunma kapasitelerinin pH, katı-sıvı oranı, konsantrasyon ve sıcaklıkla önemli derecede değiştiğini göstermiş ve kitosan biyopolimerinin çalışılan bütün ağır metalleri tutma kapasitesi kitin biyopolimerine göre oldukça fazla olduğunu görülmüştür. Öbür yandan kitin ve kitosan biyopolimerlerinin ağır metal iyonlarını tutma sıralamasının aynı olduğu görülmüştür. (Cu^{2+} > Pb^{2+} > Cd^{2+}> Ni^{2+}). Bu sıralamada Cu^{2+}, Cd^{2+} ve Ni^{2+} iyonlarının her iki biyopolimer üzerine Irwing-Williams Serisine uygun olarak tutunduğu saptanmıştır.

Ağır metal iyonlarının kitin ve kitosan biyopolimerleri üzerine tutunma kinetiği incelenmiş ve her iki biyopolimer içinde ağır metal iyonlarının ikinci dereceden hız izleyerek tutunduğunu göstermiştir ve hız sabitlerinin aktivasyon enerjilerininde hesaplanmasıyla Cu^{2+} ve Pb^{2+} iyonları için kitin biyopolimer üzerine daha hızlı tutunduğunu saptanmıştır.

Freundlich ve Langmuir izotermlerinin çalışılan bütün ağır metal iyonları için her iki biyopolimer üzerine adsorpsiyonuna uygulanabilirliği görülmüştür.

Ağır metal iyonlarının kitin ve kitosan biyopolimerleri tarafından adsorpsiyonu thermodinamik açıdan incelenmiş ve ağır metal iyonlarının her iki biyopolimer üzerinede tutunmasının kendiliğinden ve endotermik olduğu saptanmıştır.

TABLE OF CONTENTS

LIST OF FIGURES

LIST OF TABLES

CHAPTER 1

INTRODUCTION

1.1. Statement of Pollution Problem

The greatest demand for metal sequestration today comes from the need to immobilize the metals released to the environment or mobilized by and partially lost through human technological activities. It has been established that dissolved metals (particularly heavy metals) escaping into the environment pose a serious health hazard. They accumulate in living tissues throughout the food chain, which has humans at its top, multiplying the danger. Thus, it is necessary to control emissions of heavy metals into the environment.

Due to increase in the world population and development of industrial applications, environmental pollution problem became important. Communities produce both liquid and solid wastes. The liquid waste-wastewater- is essentially the water supply of the community after it has been used in a variety of applications. In recent years, heavy metal concentrations, besides other pollutants, have increased to reach dangerous levels for living environment in many regions.

The presence of toxic and polluting heavy metals in wastewaters from industrial effluents, water supplies and mine waters and their removal has received much attention in recent years. The amount of heavy metals that industrial wastewaters often contain is considerable and would endanger public health and the environment if discharged without adequate treatment.

Heavy metals are elements such as Cu (Copper), Cd (Cadmium), Ni (Nickel), Pb (Lead), Zn (Zinc), Ag (Silver), Cr (III) (Chromium), Hg (Mercury), Fe (Iron), Co (Cobalt), As (Arsenic) which are usually associated with toxicity and natural components of the Earth's crust. They cannot be degraded or destroyed. To a small extent they enter our bodies via food, drinking water and air. As trace elements, some heavy metals (e.g. copper, selenium, zinc) are essential to maintain the metabolism of the human body. However, at higher concentrations they can lead to poisoning. Heavy metal poisoning could result, for instance, from drinking-water contamination (e.g. lead

pipes), high ambient air concentrations near emission sources, or intake via the food chain. Among them only Cu, Pb, Cd, and Ni were studied in this thesis.

Table 1.1. Ranking of risks associated with various metals.
(Source: WEB_1 2007)

Relative Priority	Environmental Risk
High	Cd
	Pb
	Hg
Medium	Cr
	Co
	Cu
	Ni
	Zn
Low	Al
	Fe

Copper is widely distributed in nature as the free metal and more commonly, as compounds in various ores such as cuprite (Cu_2O), chalcopyrite ($CuS{\cdot}FeS$), azurite ($Cu(OH)_2{\cdot}2CuCO_3$) and malachite $Cu_2CO_3(OH)_2$. There are also deposits of cupric chloride and cupric arsenide.

Copper is used mainly in the production of alloys with zinc, nickel and tin, as a catalyst in the chemical industry, in the electrochemical industry where it is used in wires, generators, transformers and heat exchangers, and of course in the production of piping for water supply. Copper salts are used as pigments and fungicides, and also biocides for controlling slime and in human and animal waste.

Copper can exist in four valence states — the native element Cu^0 and the ions $^{1+}$, $^{2+}$, and $^{3+}$. The most common form is as Cu^{2+}. Cu^+ salts exist but are rapidly oxidized to Cu^{2+}. In water, most cupric Cu^{2+} salts readily dissolve to form an aquo complex $Cu(H_2O)_4^{2+}$, and the water molecules can then be replaced by a variety of ligands to form different complexes. Some of these organic complexes are essential to life, principally haemocyanin. Copper complexes found in water $[CuCO_{3(aq)}]^0$, $[Cu(CO_3)_2]^{2-}$, $[CuOH]^+$, $[Cu(OH)_3]^-$ and $[Cu(OH)_4]^{2-}$ forms (Dojlido and Best 1993).

Table 1.2. Copper (Cu^{2+}) ion properties.

(Source: Trivedi et al. 2001)

Mol. wt. (g/mol)	**Group**	**Pauling Electronegativity**	**Polarizability (10^{-24} cm^3)**	**log K_{MOH}**
63.55	IB	1.90	6.10	6.00
R_{ionic} (Å)	**$R_{covalent}$ (Å)**	**N**	**$R_{hydrated}$ (Å)**	**N/R_H ($Å^{1-}$)**
0.71	1.38	6.0	2.07	2.90

Lead is rarely found as the free metal in nature, but it is present in several minerals, principally in galena (PbS) the main source for lead production. It is also found as anglesite ($PbSO_4$) and cerrusite ($PbSO_3$).

Lead is one of the most commonly used non-ferrous metals. It has many applications; its largest use is in making storage batteries, most of which are recycled. As a result of its resistance to corrosion and its malleability, it finds use in building constructions, storage tank lining and corrosive liquid containers. Other uses of the metal are for radiation shielding, ammunition, solder, cable sheathing and pipework. Lead compounds are used as pigments in paints and ceramics, catalysers, antibacterial substances and wood preservatives. A major use is the production of anti-knock compounds for addition to petrol, particularly tetraethyl lead, $Pb(C_2H_5)_4$. The exhausts from vehicles are a major source of the environmental contamination by lead. Lead is present in exhaust gases mainly as lead halides and oxides, but incomplete combustion results in about 10% of alkyl lead compounds also being present. Other source of lead emissions are copper and nickel smelters, iron and steel production. Estimates vary as to the importance of vehicle emissions as the source of the lead contamination.

Lead exist in the oxidation states Pb^{2+} and Pb^{4+}, with the divalent form being the more stable in most aquatic environments. The speciation of lead compounds in water is complicated and depends upon a number of factors, principally pH, dissolved oxygen and the concentration of other organic and inorganic compounds. In surface waters, lead is presents as hydrated Pb^{2+}, or $[PbCO_{3(aq)}]^0$ in the pH range 7-9. At pH 6, Pb^{2+} and $Pb(OH)^+$ are in equal concentration, whereas at higher pH values there is an incrase in Pb in form of $Pb(CO_3)_2^{2-}$, $Pb(OH)^+$ and concentration of lead in waters is usually limited

by the solubility of $PbCO_3$, and by its adsorption onto particulate matter (Dojlido and Best 1993).

Table 1.3. Lead (Pb^{2+}) ion properties.
(Source: Trivedi et al. 2001)

Mol. wt. (g/mol)	**Group**	**Pauling Electronegativity**	**Polarizability (10^{-24} cm^3)**	**log K_{MOH}**
207.20	IVA	2.33	6.80	5.20
R_{ionic} (Å)	**$R_{covalent}$ (Å)**	**N**	**$R_{hydrated}$ (Å)**	**N/R_H (Å^{1-})**
1.33	1.47	4.0	2.74	1.46

Cadmium does not exist in nature as the native metal but principally as the sulphide ore greenockite (CdS), which is strongly associated with zinc sulphide ore sphalerite. Cadmium enters the environment in the waste waters of industries using cadmium, but also in discharge from the iron and steel industry.

Various soluble forms of cadmium exist in water. It exist mainly as Cd^{2+}, but also as $[CdCO_{3\ (aq)}]^0$, $[CdCl]^+$, $[Cd(OH)]^+$ and $[CdSO_{4(aq)}]$. Free Cd^{2+} ion occurs at pH levels below 8. At higher pH values, $[Cd(OH)]^+$ is formed and in very alkaline solutions $[Cd(OH)_3]^-$ and $[Cd(OH)_4]^{2-}$ are formed (Dojlido and Best 1993).

Table 1.4. Cadmium (Cd^{2+}) ion properties.
(Source: Trivedi et al. 2001)

Mol. wt. (g/mol)	**Group**	**Pauling Electronegativity**	**Polarizability (10^{-24} cm^3)**	**log K_{MOH}**
105.00	IIB	1.69	7.20	3.92
R_{ionic} (Å)	**$R_{covalent}$ (Å)**	**N**	**$R_{hydrated}$ (Å)**	**N/R_H (Å^{1-})**
0.97	1.48	6.0	2.28	2.63

The average concentration of nickel in earth's crust is about 75 mg/kg and it constitutes about 0.016% of the total mass. Its principal ores are pentlandite ($(FeNi)_9S_8$), millerite (NiS) and garnierite ($(NiMg)_6Si_4O_{10}(OH)_8$). It occurs as the natural metal only

in meteorites. It is used in the production of alloys, nickel plating for corrosion resistance and in the manufacture of batteries (e.g. nickel-cadmium batteries). The metal or its compounds are also used as catalysts, dyes, fungicides and pigments.

Nickel is present in crude oil in varying concentrations and burning of petroleum products, either in combustions processes or in vehicle fuel, introduces the metal into the environment. It also enters surface water by the natural weathering and leaching processes of minerals and rocks.

Nickel can exist in the oxidation states ranging from -1 to +4, but its aqueous chemistry is dominated by the +2 (nickelous) state. This ion forms stable complexes with both organic and inorganic ligands and is also adsorbed onto particular matter. The commonest inorganic ligands are halides, sulphate, phosphates, carbonate and carbonyls, whilst the organic ones are those containing oxygen or sulphur in their structure (Dojlido and Best 1993).

Table 1.5. Nickel (Ni^{2+}) ion properties.
(Source: Trivedi et al. 2001)

Mol. wt. (g/mol)	**Group**	**Pauling Electronegativity**	**Polarizability (10^{-24} cm^3)**	**log K_{MOH}**
58.69	VIII	1.91	6.80	4.14
R_{ionic} (Å)	**$R_{covalent}$ (Å)**	**N**	**$R_{hydrated}$ (Å)**	**N/R_H ($Å^{1-}$)**
0.83	1.21	6.6	2.06	3.20

In order to reduce the pollution problem in environment that is caused by these heavy metals, their concentrations must be reduced before discharging to obey the wastewater standards listed in Table 1.6. So, an effective treatment process must be applied.

Table 1.6. Wastewater standarts
(Source: WEB_2 2007)

Metal Ion	**Maximum Allowable Value(mg/L)**
Cadmium	2
Copper	1
Lead	3
Nickel	5

1.2. Health Effects of Heavy Metals

Heavy metals are dangerous because they tend to *bioaccumulate.* Bioaccumulation means an increase in the concentration of a chemical in a biological organism over time, compared to the chemical's concentration in the environment. Compounds accumulate in living things any time they are taken up and stored faster than they are broken down (metabolized) or excreted. Heavy metals can enter a water supply by industrial and consumer waste, or even from acidic rain breaking down soils and releasing heavy metals into streams, lakes, rivers, and groundwater.

Heavy metals are released into the environment by activities of people and high levels of these metals constitute a great risk for the aquatic ecosystem and human. Health effects of Cu, Pb, Cd and Ni were given in Table 1.7

Table 1.7. Health effects of heavy metals.
(Source: Kurniawan et al.2006)

Heavy Metal	Toxicities
Cu(II)	Liver Damage, Wilson disease, insomnia
Pb(II)	Depression, lethargy, neurologic signs, increased thirst
Cd(II)	Kidney damage, renal disorder, Itai-Itai, probable carcinogen
Ni(II)	Dermatitis, nausea, chronic asthma, coughing, human carcinogen

1.3. Common Methods Used to Remove Heavy Metals from Industrial Wastewater

Different treatment techniques for wastewater laden with heavy metals have been developed in recent years both to decrease the amount of wastewater produced and to improve the quality of the treated effluent. Although various treatments such as chemical precipitation, coagulation–flocculation, reverse osmosis, ultra-filtration, electro-dialysis flotation and ion exchange can be employed to remove heavy metals

from contaminated wastewater, they have their inherent advantages and limitations in application. The summary of these methods will be given in the following paragraphs.

1.3.1. Chemical Precipitation

Chemical precipitation involves the addition of chemicals to alter the physical state of dissolved and suspended solids and facilitate their removal by sedimentation. Chemical precipitation is employed for most of the metals. Common precipitants include hydroxide $(OH)^-$ and sulfide $(S)^{2-}$ Metals are precipitated commonly as metal hydroxides through the addition of lime or caustic to a pH of minimum solubility. The conceptual mechanism of heavy metal removal by chemical precipitation is;

$$M^{2+} + 2(OH)^- \leftrightarrow M(OH)_2 \downarrow$$

In practice, the minimum achievable residual metal concentrations are also dependent on the nature and concentration of the organic matter in the wastewater as well as the temperature. However, this method is inappropriate for large solution volumes with very low concentrations of metal ions. Precipitating hydrous oxides of the metals with lime and soda (NaOH) is used in removal of heavy metals.

In spite of its advantages, chemical precipitation requires a large amount of chemicals to reduce metals to an acceptable level for discharge (Jüttner et al.2000). Other drawbacks are its excessive sludge production that requires further treatment, the increasing cost of sludge disposal, slow metal precipitation, poor settling, the aggregation of metal precipitates, and the long-term environmental impacts of sludge disposal (Yang et al. 2001, Bose et al.2002, Wingenfelder et al. 2005).

1.3.2. Coagulation–Flocculation

Coagulation–flocculation can be employed to treat wastewater laden with heavy metals. Principally, the coagulation process destabilizes colloidal particles by adding a coagulant and results in sedimentation (Shammas et al. 2004). To increase the particle size, coagulation is followed by the flocculation of the unstable particles into bulky floccules (Semerjian and Ayoub 2003). The general approach for this technique

includes pH adjustment and involves the addition of ferric/alum salts as the coagulant to overcome the repulsive forces between particles (Licskó et al. 1997).

In spite of its advantages, coagulation–flocculation has limitations such as high operational cost due to chemical consumption. The increased volume of sludge generated from coagulation–flocculation may hinder its adoption as a global strategy for wastewater treatment. This can be attributed to the fact that the toxic sludge must be converted into a stabilized product to prevent heavy metals from leaking into the environment (Ayoub et al. 2001)**.** To overcome such problems, electro-coagulation may be a better alternative than the conventional coagulation, as it can remove the smallest colloidal particles and produce just a small amount of sludge (Vik 1984, Elimelech and O'Melia 1990). However, this technique also creates a floc of metallic hydroxides, which requires further purification, making the recovery of valuable heavy metals impossible (Persin and Rumeau 1989).

1.3.3. Reverse Osmosis

Reverse osmosis is used for the removal of dissolved constituents from wastewater remaining after advanced treatment. When two solutions having different solute concentrations are separated by a semipermeable membrane, a difference in chemical potential will exist across the membrane. Water will tend to diffuse through the membrane from the lower concentration side to the higher concentration side. In a system having a finite volume, flow continues until the pressure difference balances the chemical potential difference. This balancing pressure difference is termed the osmotic pressure and is a function of the solute characteristics and concentration and temperature. If a pressure gradient opposite in direction and greater than the osmotic pressure is imposed across the membrane, flow from the more concentrated to the less concentrated region will occur and is termed reverse osmosis (Metcalf and Eddy 2003). Reverse osmosis has been proposed for treatment for recovery of heavy metals. To protect the reverse osmosis membranes, feed solution pH must be adjusted. Reverse-osmosis alone will not achieve complete recovery and reuse of the solutions. Pretreatment required prior to the reverse osmosis unit includes equalization, media filtration, pH adjustment and anti-precipitant additions.

1.3.4. Ultrafiltration

Ultrafiltration technologies can be used in a variety of ways in wastewater treatment and water reuse systems. Ultrafiltration can reduce the amount of treatment chemicals, has smaller space requirements, and reduce labor requirements. On the contrary in this method uses more electricity, may need pretreatment, requires replacement of membranes (Eckenfelder et al. 2000).

1.3.5. Electrodialysis

In the elecrodialysis process, ionic components of a solution are separated through the use of semipermeable ion-selective membranes. This process may be operated in either a continuous or a batch mode. Problems associated with the electrodialysis process for wastewater renovation include chemical precipitation of salts with low solubility on the membrane surface. To reduce the membrane fouling, activated carbon pretreatment, possibly preceded by chemical precipitation and some form of multimedia filtration may be necessary (Metcalf and Edddy 2003). The electrolytic process has not been widely utilized in full-scale treatment of metal wastes.

1.3.6. Flotation

Flotation is employed to separate solids or dispersed liquids from a liquid phase using bubble attachment (Wang et al. 2004). The attached particles are separated from the suspension of heavy metal by the bubble rise. Flotation can be classified as: (i) dispersed-air flotation, (ii) dissolved-air flotation (DAF), (iii) vacuum air flotation, (iv) electro-flotation, and (v) biological flotation. Among the various types of flotation, DAF is the most commonly used for the treatment of metal-contaminated wastewater (Zabel et al. 1984). Adsorptive bubble separation employs foaming to separate the metal impurities. The target floated substances are separated from bulk water in a foaming phase.

Although it is only a kind of physical separation process, heavy metal removal by flotation has the potential for industrial application (Jokela and Keskitalo 1999). Low

cost materials such as zeolite and chabazite have been found to be effective collectors with removal efficiency of higher than 95% for an initial metal concentration ranging from 60 to 500 mg/L . Flotation can be employed to treat inorganic effluent with a metal concentration of less than 50 mg/L or higher than 150 mg/L. Other advantages such as a better removal of small particles, shorter hydraulic retention times and low cost make flotation one of the most promising alternatives for the treatment of metal-contaminated wastewater (Matis et al. 2003).

1.3.7. Ion Exchange

Ion exchange is a unit process in which ions of a given species are displaced from an insoluble exchange material by ions of a different species in solution. Materials used for the exchange of metals include zeolites, weak and strong anion and cation resins, chelating resins. Ion exchange processes are highly pH-dependent. Solution pH has a significant impact on the metal species present and the interaction between exchanging ions and the resin (Eckenfelder 2000).

1.4. Scope of the Study

Adsorption has become one of the alternative treatment techniques for wastewater laden with heavy metals. Basically, adsorption is a mass transfer process by which a substance is transferred from the liquid phase to the surface of a solid, and becomes bound by physical and/or chemical interactions (Kurniawan et al.2006).

The aim of this study is the characterization of chitin biopolymer, preparation and characterization of chitosan biopolymer from chitin biopolymer in controlled experimental condition to use these biopolymers as adsorbent materials and investigate the uptake performance for heavy metal ions (Cu^{2+}, Pb^{2+}, Cd^{2+} and Ni^{2+}).

Characterization of chitin and chitosan biopolymers was carried out with Viscosity Measurements, Particle Size Distribution Analysis, Surface Area Analysis, X-Ray Diffraction (XRD), Zeta Potential Analysis, IR Spectroscopy , Elemental Analysis, Scanning Electron Microscopy (SEM) and Thermal Gravimetric Analysis (TGA/DTA).

Batch experiments were carried out for the adsorption of heavy metal ions Cu^{2+}, Pb^{2+}, Cd^{2+}, and Ni^{2+} onto chitin and chitosan biopolymers. The primary parameters

investigated include solid liquid ratio (S/L), pH, contact time, concentration and temperature. Moreover the best fitting adsorption isotherm models are examined using the most widely applied isotherm models. Adsorption isotherms are helpful in demonstrating the extent of homogeneity of the adsorption sites and the affinity of these sites towards the adsorbed cations. The thermodynamic parameters, ΔH^{o}, ΔG^{o} and ΔS^{o} are also calculated, the thing that can help in testing whether or not electrostatic binding forces are involved in adsorption. Characterization of the liquid phase was carried out using Flame Atomic Absorption/Emission Spectroscopy (AAS/EES).

CHAPTER 2

PROPERTIES, CHARACTERIZATION AND APPLICATION AREAS OF CHITIN AND CHITOSAN BIOPOLYMERS

2.1. Chitin and Chitosan

Chitin, a naturally abundant mucopolysaccharide, and the supporting material of crustaceans, insects, etc., is well known to consist of 2-acetamido-2-deoxy-β-D-glucose through a β (1→4) linkage. It is a highly insoluble material resembling cellulose in its solubility and low chemical reactivity. It may be regarded as cellulose with hydroxyl at position C-2 replaced by an acetamido group. Like cellulose, it functions naturally as a structural polysaccharide. Chitin is a white, hard, inelastic, nitrogenous polysaccharide and the major source of surface pollution in coastal areas.

Chitosan is the *N*-deacetylated derivative of chitin, although this *N*-deacetylation is most never complete. A sharp nomenclature with respect to the degree of *N*-deacetylation has not been defined between chitin and chitosan. The structures of chitin, chitosan and cellulose are shown in Figure 2.1.

Chitin and chitosan are of commercial interest due to their high percentage of nitrogen (7.21%) compared to synthetically substituted cellulose (1.25%) (Muzzarelli et al. 1973). As most of the present-day polymers are synthetic materials, their biocompatibility and biodegradability are much more limited than those of natural polymers such as cellulose, chitin, chitosan and their derivatives. However, these naturally abundant materials also exhibit a limitation in their reactivity and process ability (Illum 1998, Mass 1998). In this respect, chitin and chitosan are yield recommended as suitable functional materials, because these natural polymers have excellent properties such as biocompatibility, biodegradability, non toxicity, chelating properties, etc.

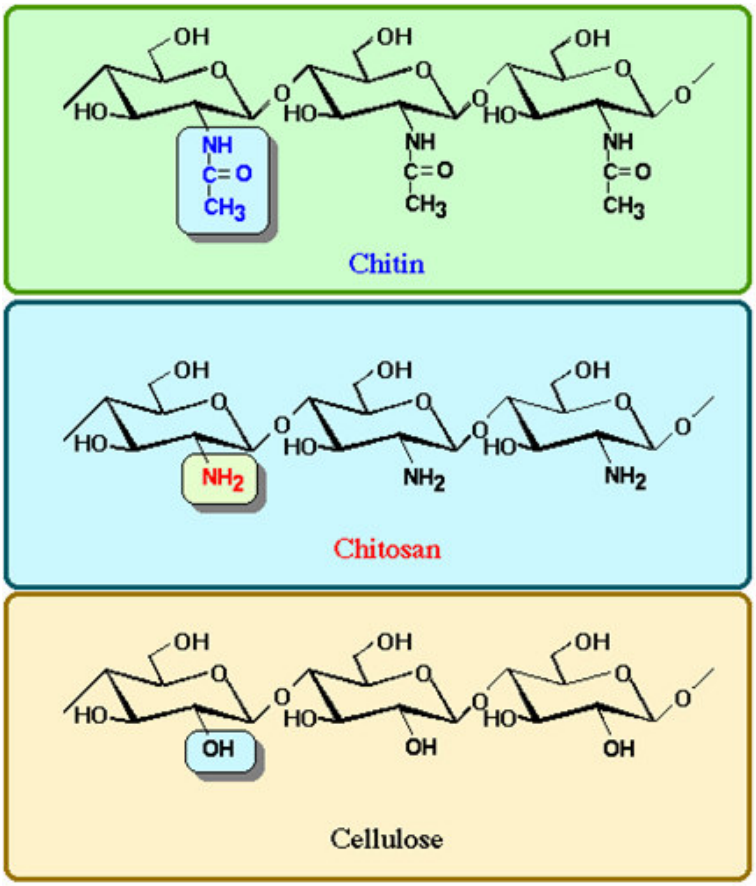

Figure 2.1. Chemical structures of chitin, chitosan and cellulose.
(Source:WEB_4 2007)

2.2. Processing of Chitin and Chitosan Production

Chitin is easily obtained from crab or shrimp shells and fungal *mycelia*. In the first case, chitin production is associated with food industries such as shrimp canning. In the second case, the production of chitosan-glucan complexes is associated with fermentation processes, similar to those for the production of citric acid from *Aspergillus niger*, *Mucor rouxii*, and *Streptomyces*, which involves alkali treatment yielding chitosan-glucan complexes. The alkali removes the protein and deacetylates chitin simultaneously. Depending on the alkali concentration, some soluble glycans are removed (Madhavan et al. 1992). The processing of crustacean shells mainly involves the removal of proteins and the dissolution of calcium carbonate which is present in crab shells in high concentrations. The resulting chitin is deacetylated in 40% sodium hydroxide at 120^{o}C for 1-3 h. This treatment produces 70% deacetylated chitosan.

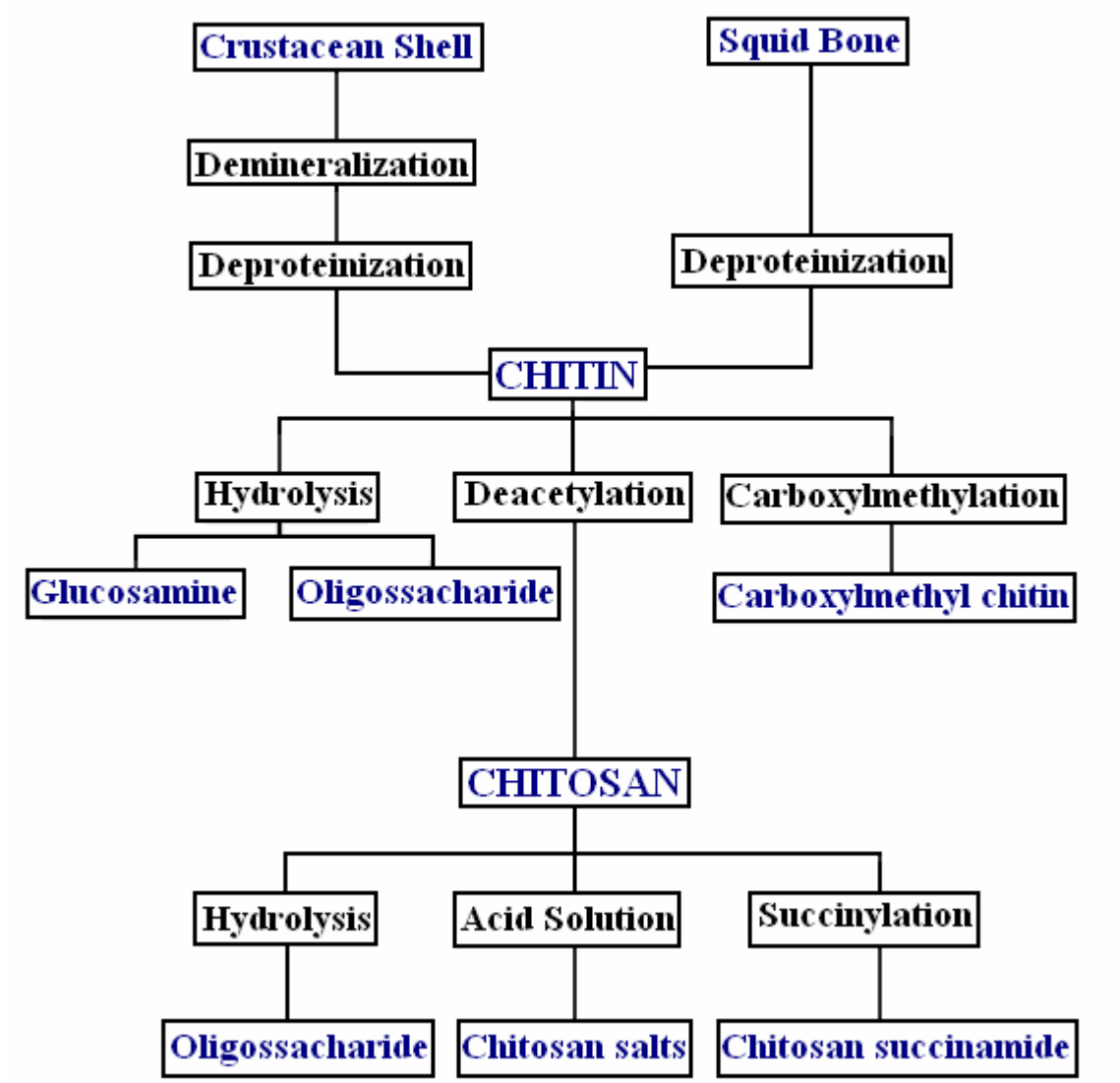

Figure 2.2. Manufacturing process of chitin, chitosan and their derivatives.

2.3. Economic Aspects

The production of chitin and chitosan is currently based on crab and shrimp shells discarded by the canning industries in Oregon, Washington, Virginia and Japan and by various fleets in the Antarctic. Several countries possess large unexploited crustacean resources, e.g. Norway, Mexico and Chile (Muzzarelli et al. 1984). The production of chitosan from crustacean shells obtained as a food industry waste is economically feasible, especially if it includes the recovery of carotenoids. The shells contain considerable quantities of astaxanthin, a carotenoid that has so far not been synthesized, and which is marketed as a fish food additive in aquaculture, especially for

salmon. To produce 1 kg of 70% deacetylated chitosan from shrimp shells, 6.3 kg of HCl and 1.8 kg of NaOH are required in addition to nitrogen, process water (0.5 t) and cooling water (0.9 t). Important items for estimating the production cost include transportation, which varies depending on labor and location. Chitin and chitosan are now produced commercially in India, Japan, Poland, Norway and Australia (Madhavan et al. 1974).

2.4. Properties of Chitin and Chitosan

Most of the naturally occurring polysaccharides, e.g. cellulose, dextran, pectin, alginic acid, agar, agarose and carragenans, are neutral or acidic in nature, whereas chitin and chitosan are examples of highly basic polysaccharides. Their unique properties include polyoxysalt formation, ability to form films, chelate ions and optical structural characteristics (Larry et al. 1998).

Like cellulose, chitin functions naturally structural polysaccharide, but differs from lose in its properties. Chitin is highly hydrophobic and is insoluble in water and organic solvents. It is soluble in hexafluoroisopropanol, hexafluoroacetone, chloroalcohols in conjugation with aqueous solutions of mineral acids and dimethylacetamide containing 5% lithium chloride (Madhavan et al. 1992). Chitosan, the deacetylated product of chitin, is soluble in dilute acids such as acetic acid, formic acid, etc. (Dutta 1997, Dutta 1999, Ravi Kumar 1999).

The nitrogen content of chitin varies from 5 to 8% depending on the extent of deacetylation, whereas the nitrogen in chitosan is mostly in the form of primary aliphatic amino groups. Chitosan, therefore, undergoes reactions typical of amines, of which *N*-acylation and Schiff reaction are the most important. Chitosan derivatives are easily obtained under mild conditions and can be considered as substituted glucans (Nishi 1979, Kaifu 1981).

2.4.1. Physical and Chemical Characterization of Chitin and Chitosan

The structural details of cellulose, chitin and chitosan are shown in Figure 1. Cellulose is a homopolymer, while chitin and chitosan are heteropolymers. Neither random nor block orientation is meant to be implied for chitin and chitosan. The

properties of chitin and chitosan such as the origin of the material (discussed in the previous section), structures in solid state, the degree of *N*-deacetylation, molecular weights and solvent and solution properties will be discussed in following passages.

2.4.2. Structures in the Solid State

Depending on its source, chitin occurs as two allomorphs, namely the α and β forms which can be differentiated by infrared and solid-state NMR spectroscopy together with X-ray diffraction. A third allomorph γ-chitin has also been described but from the detailed analysis, it seems that it is just a variant of the α family (Rudall 1973, Rudall 1969, Atkins 1985). α-chitin is by far the most abundant; it occurs in fungal and yeast cell walls, in krill, in lobster and crab tendons and shells, and in shrimp shells, as well as in insect cuticle. It is also found in or produced by varios marine living organism. In this respect, one can cite the harpoons of cone snails the oral grasping spine of *Sagitta* etc. and the filaments ejected by the seawed *Phaeocystis* etc. (Olivera 1995, Atkins 1979, Saito 1995, Chanzy 1998, Chrétiennot-Dinet 1997). These exotic α-chitins have proved particularly interesting for structural studies since, in comparison with the abundant arthopod chitin, some of them present remarkably high crystalinity together with high purity and they are synthesized in the absence of pigment, protein, or calcite (Rudall et al. 1976). In additon to the native chitin, α-chitin systematically results from re-crystallization from solution in vitro biosynthesis or enzymatic polymerization (Person 1990, Helbert 1998, Ruiz-Herrara 1975, Bartnicki-Garcia 1994, Sakamoto 2000).

The rarer β-chitin is found in association with proteins in squid pens and in the tubes synthesized by pogonophoron and vestimelfran (Blackwell 1965, Gaill 1992). It occurs also in aphrodite chaetae as well as in the lorica built by some seaweeds of protozoa (Herth 1977, Herth 1986). A particulary pure form of β-chitin is found in the monocrystalline sipnes excreted by the diatom *Thalasssiossa fluviatilis* (Revol et al. 1986). As of today, it has been possible to obtain β-chitin either from solution or by in vitro biosynthesis.

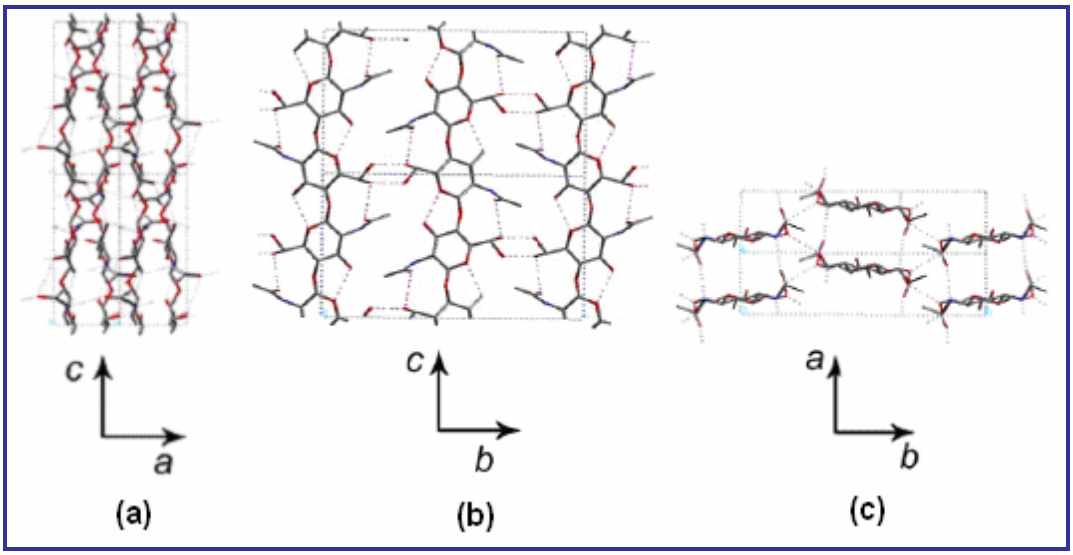

Figure 2.3. Solid state structure of α-chitin: (a) ac projection; (b) bc projection; (c) ab projection. The sturucture contains a statistical mixture of 2 conformations of the $–CH_2OH$ groups (Source: Rinaudo et al. 2005)

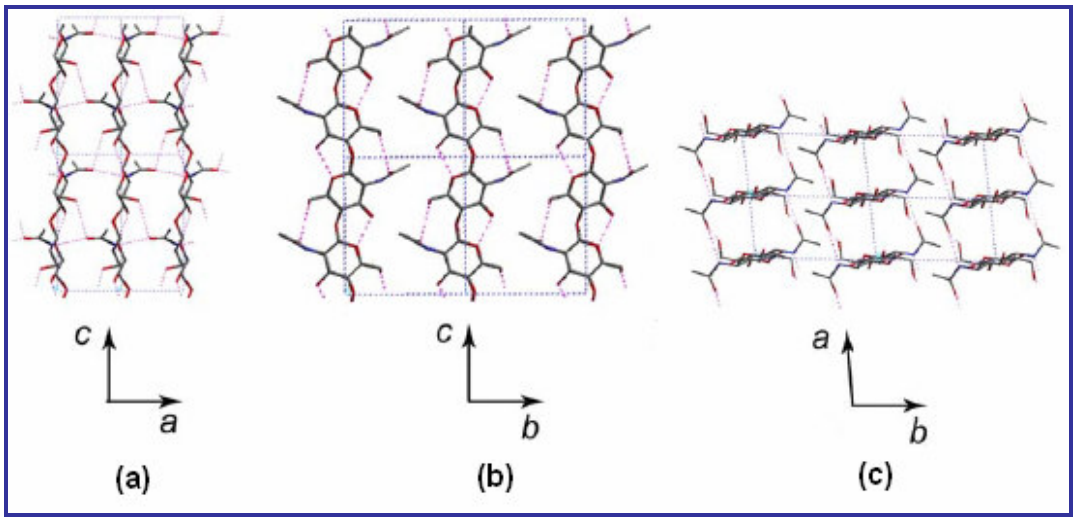

Figure 2.4. Solid state structure of β-chitin: (a) ac projection; (b) bc projection; (c) ab projection (Source: Rinaudo et al. 2005)

In the solid state, chitosan is semicrystalline polymer. Its morphology has been investigated, and many polymorphs are mentioned using fully deacetylated chitin of low molecular weight (Cartier et al. 1990). The electron diffraction diagram can be indexed in an orthorhombic unit cell ($P2_12_12_1$) with a= 0.807 nm, b= 0.844 nm, c= 1.034 nm; the

unit cell contains two parallel chitosan chains, but no water molecules. The influence of experimental conditions on the crytallinity has also been described (Ogawa 1991, Ogawa 1992).

2.4.3. Determination of Degree of Deacetylation

An important parameter to examine closely is the degree of deacetylation in chitin, i.e. the ratio of 2-acetamido-2-deoxy-D-glucopyranose to 2-amino-2-deoxy-D glucopyranose structural units. Chitosan is the universally accepted nontoxic deacetylated derivative of chitin, where chitin is deacetylated to such an extent that it becomes soluble in dilute aqueous acetic and formic acids. In chitin, the acetylated units prevail (degree of acetylation typically 0.90). Chitosan is the fully or partially deacetylated derivative of chitin with a typical degree of acetylation of less than 0.35. Many analytical methods are used to define this ratio. Table 2.1. shows these analytical methods in literature

Table 2.1. Analytical methods to determine degree of N-deacetylation

Analytical Method	Reference
IR spectroscopy	(Baxter et al. 1992)
Gel permeation chromatography	(Domard et al. 1986)
UV spectroscopy	(Domard et al.1987)
^{1}H-NMR spectroscopy	(Wei and Hudson 1993)
^{13}C solid state NMR	(Sashiwa et al. 1991)
Potentiometric Titration	(Tolaimate et al. 2000)
Acid hydrolysis	(Niola et al. 1983)
HPLC	(Pangburn et al. 1984)
Elemental analysis	(Kasaai et al. 2000)

2.4.3.1. Infrared Spectroscopic Analysis

The degree of deacetylation (DD) of the chitin and chitosan samples can be determined by infrared spectroscopic analysis using the two different equations. The computation equations are given below:

$$DD = 100 - \left[\frac{(A_{1655} / A_{3450}) x 100}{1.33} \right] \quad (2.1)$$

where A_{1655} and A_{3450} were the absorbance at 1655 cm^{-1} of the amide-I band as a measure of the N-acetyl group content and 3450 cm^{-1} of the hydroxyl band as an internal standard to correct for film thickness or for differences in chitosan concentration powder form. The factor "1.33" denoted the value of the ratio of A_{1655} /A_{3450} for fully N-acetylated chitosan. It was assumed that the value of this ratio was zero for fully deacetylated chitosan and there was a rectilinear relationship between the N-acetyl group content and the absorbance of the amide-I band (Domzy and Roberts 1985).

The second equation was proposed by (Baxter et al.1989) was modified from the method reported by (Domszy and Roberts 1985).

$$DD = 100 - \left(\frac{A_{1655}}{A_{3450}} \right) x115 \quad (2.2)$$

2.4.3.2. Elemental Analysis

The degree of deacetylation (DD) of the chitosan can be determined by elemental analysis using the following equation; (Kasaai et al. 2000)

$$DD = \left(1 - \frac{C/N - 5.145}{6.186 - 5.145} \right) x100 \quad (2.3)$$

where C : Mass of Carbon in Chitosan Sample

N : Mass of Nitrogen in Chitosan Sample

2.4.3.3. Potentiometric Titration

The deacetylation degree of chitosan can be determined by the potentiometric titration. Chitosan is dissolved in a known excess of acid. From the titration of this solution with base solution, a curve with two inflection points are obtained. The difference between the volumes of these two inflection points corresponded to the acid consumption for the salification of amine groups and permitted the determination of chitosan's deacetylation degree, through (Tolaimate et al. 2000).

$$\%NH_2 = 16.1(V_2 - V_1)x\frac{M_b}{W} \tag{2.4}$$

where V_1 : Base volume for the first inflexion point (mL)

V_2 : Base volume for the second infexion point (mL)

M_b : Base molarity (g/mol)

W : Weight of the chitosan sample

2.4.4. Solubility and Molecular Weight of Chitin and Chitosan

Chitin occurs naturally partially deacetylated (with a low content of glucosamine units), depending on the source (Table 2.2) nevertheless, both α and β forms are insoluble in all the usual solvents, despite natural variations in crystallinity. The insolubility is a major problem that confronts the development of processing and uses of chitin (Saito 1997, Mathur and Narank 1990). In addition, β -chitin is more reactive than the α form, an important property in regard to enzymatic and chemical transformations of chitin (Kurita et al. 1993).

Table 2.2. Sources of chitin and chitosan.

(Source: Rinaudo et al. 2006)

Sea animals	Insects	Microorganisms
Annelida	Scorpions	Green algae
Mollusca	Spiders	Yeast (β-type)
Crustaceans:	Ants	Mycelia Penicillium
Lobster	Cockroaches	Brown algae
Crab	Beetles	Spores
Shrimp		Chytridiaceae
Prawn		Ascomydes

Because of the solubility problem, only limited information is available on the physical properties of chitin in solution. The first well-developed study was by Austin who introduced the solubility parameters for chitin in various solvents. He obtained a complex between chitin and LiCl (which is coordinated with the acetyl carbonyl group). The complex is soluble in dimethylacetamide and in N-methyl-2-pyrrolidone. In addition, Austin also used formic, dichloroacetic and trichloroacetic acids for dissolution of chitin chains. Experimental values of parameters K and a relating intrinsic viscosity $[\eta]$ and molecular weight M for chitin in several solvents according to the well-known Mark–Houwink equation. Mark-Houwink parameters for chitin in various solvents are given in Table 2.3.

$$[\eta] = KM^{a} \tag{2.5}$$

Table 2.3. Mark–Houwink parameters for chitin in various solvents.

Solvent	K (mL/g)	a	T (°C)	Reference
2.77 M NaOH	0.1	0.68	20	(Einbu et al. 2004)
DMAc/LiCl 5%	7.6×10^{-3}	0.95	30	(Poirier and Charlet 2002)
DMAc/LiCl 5%	2.1×10^{-4}	0.88	25	(Terbojevich et al. 1988)

For a long time the most widely used solvent for chitin was a DMAc/LiCl mixture, though $CaCl_2 \cdot 2H_2O$-saturated methanol was also employed, as well as hexafluoroisopropyl alcohol and hexafluoracetone (Tamura et al. 2003). (Vincenton et al. 1994) dissolved chitin in concentrated phosphoric acid at room temperature. In this solvent, decreases of the viscosity and of the molar mass were observed with time with no change in the degree of acetylation. The same author also dissolved chitin in a fresh saturated solution of lithium thiocyanate and got the NMR spectra at 90 °C. A few papers discuss preparation of alkali chitin by dissolution of chitin at low temperature in NaOH solution. The chitin is first dispersed in concentrated NaOH and allowed to stand at 25°C for 3 h or more; the alkali chitin obtained is dissolved in crushed ice around 0°C. This procedure allowed the authors to cast transparent chitin film with good mechanical properties (Einbu 2004, Sannan 1975, Sannan 1976). The resulting chitin is amorphous and, under some conditions, it can be dissolved in water, while chitosan with a lower degree of acetylation (DA) and ordinary chitin are insoluble. The authors interpreted this phenomenon as related both to the decrease of molecular weight under alkaline conditions and to some deacetylation; they confirmed that to get water solubility, the DA has to be around 50% and, probably, that the acetyl groups must be regularly dispersed along the chain to prevent packing of chains resulting from the disruption of the secondary structure in the strong alkaline medium (Sannan 1976, Kubota 1997).

Recently, an interesting study, utilizing techniques such as rheology, turbidimetry and fluorescence, demonstrated that alkali chitin solubilized in cold (~0°C) aqueous NaOH (16% w/w) forms an LCST solution with a critical temperature around 30°C (Argüelles-Monal et al. 2003). A chitin gel, obtained from the solution by washing to extract NaOH, was found to be temperature and pH-sensitive (Goycoolea et.al 2006). These authors demonstrated a volume phase transition at ~21°C as the result of the influence of temperature on polymer–polymer and polymer–water interactions such as hydrogen bonding and hydrophobic interactions. This transition is observed only within a narrow range of pH (7.3–7.6) and modifies the mechanical shear modulus as a function of oscillating variation in temperature.

The rheology of chitin in solution is that of a semi-rigid polysaccharide for which the conformational analysis has been developed in comparison with chitosan.

The solution properties of a chitosan depend not only on its average DA but also on the distribution of the acetyl groups along the main chain in addition of the

molecular weight (Kuboto and Eguchi 1997, Aiba 1991, Rinaudo 1989). The deacetylation, usually done in the solid state, gives an irregular structure due the semicrystalline character of the initial polymer. Examination of the role of the protonation of chitosan in the presence of acetic acid and hydrochloric acid on solubility showed that the degree of ionization depends on the pH and the pK of the acid. Solubilization of chitosan with a low DA occurs for an average degree of ionization α of chitosan around 0.5; in HCl, α= 0.5 corresponds to a pH of 4.5–5. Solubility also depends on the ionic concentration, and a salting-out effect was observed in excess of HCl (1 M HCl), making it possible to prepare the chlorhydrate form of chitosan. When the chlorhydrate and acetate forms of chitosan are isolated, they are directly soluble in water giving an acidic solution with pK_0=6±0.1 in agreement with previous and corresponding to the extrapolation of pK for a degree of protonation α=0. Thus, chitosan is soluble at pH below 6.

The solubility of chitosan is usually tested in acetic acid by dissolving it in 1% or 0.1 M acetic acid. (Rinaudo et al. 1999). demonstrated that the amount of acid needed depends on the quantity of chitosan to be dissolved. The concentration of protons needed is at least equal to the concentration of $-NH_2$ units involved.

In fact, the solubility is a very difficult parameter to control: it is related to the DA, the ionic concentration, the pH, the nature of the acid used for protonation, and the distribution of acetyl groups along the chain, as well as the conditions of isolation and drying of the polysaccharide. It is important also to consider the intra-chain H bonds involving the hydroxyl groups. The role of the microstructure of the polymer is clearly shown when a fully deacetylated chitin is reacetylated in solution; the critical value of chitosan DA to achieve insolubility in acidic media is then greater than 60%. In addition, solubility at neutral pH has also been claimed for chitosan with DA around 50% (Aiba et al. 1991).

Another important characteristic to consider for these polymers is the molecular weight and its distribution. The first difficulty encountered in this respect concerns the solubility of the samples and dissociation of aggregates often present in polysaccharide solutions (Philippova et al. 2001). As to choice a solvent for chitosan characterization, various systems have been proposed, including an acid at a given concentration for protonation together with a salt to screen the electrostatic interaction.

The solvent is important also when molecular weight has to be calculated from intrinsic viscosity using the Mark–Houwink relation, Equation (2.5) above, with known

values of the parameters *K* and *a.* One solvent first proposed (0.1 M AcOH/0.2 M NaCl) for molecular weight characterization was shown to promote aggregation and to overestimate the values of molecular weights calculated**.** Some values of the Mark–Houwink parameters for chitosan solutions are given in Table 2.4. It was demonstrated that the aggregates perturb not only the molecular weight determination by light scattering but also the viscosity determination. To avoid these artifacts, (Rinaudo et al. 1993) proposed to use 0.3 M acetic acid/0.2 M sodium acetate (pH= 4.5) as a solvent since had no evidence for aggregation in this mixture. Absolute M values were obtained from size exclusion chromatography (SEC) with on-line viscometer and light scattering detectors to allow determination of the Mark–Houwink parameters, and also the relation between the molecular radius of gyration R_g and molecular weight. This analysis also required determination of the refractive index increment d*n*/d*c* (where *c* is the polymer concentration).

Table 2.4. Mark–Houwink parameters for chitosan in various solvents

Solvent	K (mL/g)	*a*	T (°C)	Reference
0.1 M AcOH/0.2 M NaCl	1.81×10^{-3}	0.93	25	(Roberts et al. 1982)
0.1 M AcOH/0.02 M NaCl	3.04×10^{-3}	1.26	25	(Roberts et al. 1982)
0.2 M AcOH/0.1 M AcONa/ 4 M urea	8.93×10^{-2}	0.71	25	(Lee et al. 1974)
0.3 M AcOH/0.2 M AcONa	8.2×10^{-2}	0.76	25	(Rinaudo et al. 1993)
0.3 M AcOH/0.2 M AcONa	7.9×10^{-2}	0.79	25	(Brugnerotto et al. 2001)

2.5. Applications

The great potential for application of chitin and chitosan is reflected by the coexistence of approximately 3500 patents or patent applications, in addition to a much higher number of scientific articles which have appeared in the literature during the past decate. Many of the claims suggest uses for chitin and chitosan where these biopolymers actually replace existing synthetic or natural polymers, irrespective of economical aspects (Lang 1995, Peter 1995, Daly and Macossay 1997, Kurita 1997,

Kumar 2000). The most frequently cited advantages of chitosan are seen in the unique physico-chemical and biological properties of the polymer, including antimicrobial activity and biodegradability. The commercial exploration of chitosan has been particularly successful in cosmetics, the manufacture of textile and dietary health food productions.

2.5.1. Photography

Chitosan has important applications in photography due to its resistance to abrasion, its optical characteristics, and film forming ability. Silver complexes are not appreciably retained by chitosan and therefore can easily be penetrated from one layer to another of a film by diffusion (Muzzarelli et al. 1997).

2.5.2. Cosmetics

For cosmetic applications, organic acids are usually good solvents, chitin and chitosan have fungicidal and fungistatic properties. Chitosan is the only natural cationic gum that becomes viscous on being neutralized with acid. These materials are used in creams, lotions and permanent waving lotions and several derivatives have also been reported as nail lacquers (Mark et al. 1985).

2.5.3. Chitosan as an Artificial Skin

Individuals who have suffered extensive losses of skin, commonly in fires, are actually ill and in danger of succumbing either to massive infection or to severe fluid loss. Patients must often cope with problems of rehabilitation arising from deep, disfiguring scars and crippling contractures. (Malettas et al. 1986) studied the effect of treatment with chitosan and saline solution on healing and fibroplasia of wounds made by scalpel insertions in skin and subcutaneous tissue in the abdominal surface of dogs. (Yannas et al. 1982) proposed a design for artificial skin, applicable to long-term chronic use, focusing on a nonantigenic membrane, which performs as a biodegradable template for synthesis of neodermal tissue. It appears that chitosan, having structural

characteristics similar to glycosamino glycans, could be considered for developing such substratum for skin replacement (Le 1996, Olsen 1989, Sandford and Stinnes 1991).

2.5.4. Chitin and Chitosan Based Dressings

Chitin and chitosan have many distinctive biomedical properties. However, chitin-based wound healing products are still at the early stages of research (Le et al. 1997).

(Sparkes and Murray 1986) developed a surgical dressing made of a chitosan–gelatin complex. The procedure involves dissolving the chitosan in water in the presence of a suitable acid, maintaining the pH of the solution at about 2–3, followed by adding the gelatin dissolved in water. The ratio of chitosan and gelatin is 3:1 to 1:3. To reduce the stiffness of the resulting dressing a certain amount of plasticizers such as glycerol and sorbitol could be added to the mixture. Dressing film was cast from this solution on a flat plate and dried at room temperature. It was claimed that, in contrast to conventional biological dressings, this experimental dressing displayed excellent adhesion to subcutaneous fat.

(Nara et al. 1987) patented a wound dressing comprising a nonwoven fabric composed of chitin fibres made by the wet spinning technique. In one of the examples, chitin powder was ground to 100 mesh and treated in 1 M HCl for 1 h at 4°C. It was then heated to 90°C where it was treated for 3 h in a 0.3% NaOH solution to remove calcium and protein in the chitin powder, and rinsed repeatedly followed by drying. The resultant chitin was dissolved in a dimethylacetamide solution containing 7 wt% lithium chloride to form a 7% dope. After filtering and allowing defoaming to occur, the dope was extruded through a nozzle of diameter 0.06 mm and 200 holes into butanol at 60°C at a rate of 2.2 g/min. The chitin was coagulated and collected at a speed of 10 m/min. The resultant strand was rinsed with water and dried to obtain a filament of 0.74 dtex with a strength of 2.8 g/den. The filaments were then cut into staple fibres. Using poly(vinyl alcohol) as a fibrous binder, non-woven dressings were made.

2.5.5. Food and Nutrition

The *N*-acetylglucosamine (NAG) moiety present in human milk promotes the growth of bifido bacteria, which block other types of microorganism and generate the

lactase required for digestion of milk lactose. Cow's milk contains only a limited amount of the NAG moiety, hence some infants fed cow's milk may have indigestion. Many animals and some humans (including the elderly) have similar lactose intolerances (Knorr 1991, Nicol 1991).

Animal nutritional studies have shown that the utilization of them may be improved if the diet contains small amounts of chitinous material. This improvement is attributed to the change in the intestinal microflora brought about by the chitinous supplement (Austin et al. 1989). Chickens fed a commercial broiler diet containing 20% dried whey and 2 or 0.5% chitin had significantly improved weight again compared to controls (Spreen 1984, Zikakis 1982).

2.5.6. Opthalmology

Chitosan possesses all the characteristics required for making an ideal contact lens: optical clarity, mechanical stability, sufficient optical correction, gas permeability, particularly towards oxygen, wettability and immunological compatibility. Contact lenses are made from partially depolymerized and purified squid pen chitosan by spin casting technology and these contact lenses are clear, tough and possess other required physical properties such as modulus, tensile strength, tear strength, elongation, water content and oxygen permeability. The antimicrobial and wound healing properties of chitosan along with an excellent film capability make chitosan suitable for development of ocular bandage lenses (Markey et al. 1989).

2.5.7. Paper Finishing

Chitosan has been reported to impart wet strength to paper. Hydroxymethyl chitin and other water-soluble derivatives are useful end additives in paper making. This polymer, although potentially available in large quantities, never became a commercially significant product. The entrepreneur in paper making can utilize this polymer for better finish paper properties (Kumar et al. 2000).

2.5.8. Solid-State Batteries

Chitosan is insoluble in water. This poses a problem in the fabrication of solid-state proton-conducting batteries because there will not be any water present in the chitosan which can act as a source of hydrogen ions. In other words, the proton-conducting polymer needed for solid-state battery application cannot be obtained from chitosan alone. Chitosan is a biopolymer which can provide ionic conductivity when dissolved in acetic acid. The conductivity is due to the presence of protons from the acetic acid solution. The transport of these protons is thought to occur through many microvoids in the polymer since the dielectric constants from piezoelectric studies are small. The choice of a more suitable electrode material may produce a better battery system (Arof et al. 1995).

2.5.9. Drug Delivery Systems

Controlled-release technology emerged during the 1980s as a commercially sound methodology. The achievement of predictable and reproducible release of an agent into a specific environment over an extended period of time has much significant merit. It creates a desired environment with optimal response, minimum side-effects and prolonged efficacy. Controlled-release dosage forms enhance the safety, efficacy and reliability of drug therapy. They regulate the drug release rate and reduce the frequency of drug administration to encourage patients to comply with dosing instructions. Conventional dosage forms often lead to wide swings in serum drug concentrations. Most of the drug content is released soon after administration, causing drug levels in the body to rise rapidly, peak and then decline sharply. For drugs whose actions correlate with their serum drug concentration, the sharp fluctuations often cause unacceptable side-effects at the peaks, followed by inadequate therapy at the troughs. A new dimension is the incorporation of biodegradability into the system. A number of degradable polymers are potentially useful for this purpose, including synthetic as well as natural substances. The release of drugs, absorbed or encapsulated by polymers, involves their slow and controllable diffusion from/through polymeric materials. Production of slow release (SR) drugs by the pharmaceutical industry is now a matter of routine. Drugs covalently attached to biodegradable polymers or dispersed in a

polymeric matrix of such macromolecules may be released by erosion/degradation of the polymer. Therapeutic molecules, complexed by polymers, may also be released from gels by diffusion.

Chitosan is non-toxic and easily bioabsorbable with gel-forming ability at low pH. Moreover, chitosan has antacid and antiulcer activities which prevent or weaken drug irritation in the stomach. Also, chitosan matrix formulations appear to float and gradually swell in an acid medium. All these interesting properties of chitosan make this natural polymer an ideal candidate for controlled drug release formulations. Many excellent reviews and books deal with the properties, chemistry, biochemistry and applications of chitin, chitosan and their derivatives (Kumar et al. 2000).

2.6. Chitin and Chitosan as Alternative Heavy Metal Adsorbent Materials

In recent years, consideration of public health, environmental and economic pressure have made it desirable to reconsider the methods employed for treatment and disposal of toxic wastes. This is true, especially for waste waters containing toxic, since the metals cannot be destroyed; certainly their fate is to abnormally increase the metal content of the environment where they are deposited.

Certain metals, like mercury and cadmium, present special hazards because they are accumulated biologically, but metals like copper, nickel, chromium and zinc , widely used in metal finishing, are also of concern because their discharge in waste waters may contaminate sewage sludge to the extent it becomes unsuitable for farm land, reduce the efficiency of sewage-treatment processes and harm aquatic life.

Since its first introduction for heavy metal removal, activated carbon has undoubtedly been the most popular and widely used adsorbent in wastewater treatment applications throughout the world. In spite of its prolific use, activated carbon remains an expensive material since higher the quality of activated carbon, the greater its cost. Activated carbon also requires complexing agents to improve its removal performance for inorganic matters. Therefore, this situation makes it no longer attractive to be widely used in small-scale industries because of cost inefficiency.

Due to the problems mentioned previously, research interest into the production of alternative adsorbents to replace the costly activated carbon has intensified in recent

years. Attention has been focused on the various adsorbents, which have metal-binding capacities and are able to remove unwanted heavy metals from contaminated water at low cost. Because of their low cost and local availability, natural materials such as, zeolites, clay, or certain waste products from industrial operations such as fly ash, coal, and oxides are classified as low-cost adsorbents.

As alternative to traditional treatment processes, chitin and chitosan biopolymers can be an answer for the prevention of water pollution by mercury, copper and many other elements.

2.7. Adsorption Process and Heavy Metal Adsorption on Different Substances

2.7.1. Adsorption Process

Adsorption is the process of accumulating substances that are in solution on a suitable interface. Adsorption is a mass transfer operation in that a constituent in the liquid phase is transferred to the solid phase. The *adsorbate* is the substance that is being removed from the liquid phase at the interface. The *adsorbent* is the solid, liquid or gas phase onto which the adsorbate accumulates. Although adsorption is used at the air-liquid interface, only the case of adsorption at the liquid-solid interface will be discussed in this study.

The term adsorption is used also to describe two kinds of forces of interaction between the adsorbate and the adsorbent. These interaction forces are broadly described as *physisorption* (physical adsorption) and *chemisorption* (chemical adsorption) (Rouquerol 1999). The basic characteristics of them are given below in Table 2.5.

Physical adsorption (physisorption) is relatively non-specific and is due to the operation of weak forces between molecules. In this process, the adsorbed molecule is not affixed to a particular site on the solid surface; it is free to move over the surface (Sawyer et.al. 1994). The physical interactions among molecules, based on electrostatic forces, include dipole-dipole interactions, dispersion interactions and hydrogen bonding. When there is a net separation of positive and negative charges within a molecule, it is said to have a dipole moment. Molecules such as H_2O and N_2 have permanent dipoles because of the configuration of atoms and electrons within them. Hydrogen bonding is a

special case of dipole-dipole interaction and hydrogen atom in a molecule has a partial positive charge. Positively charged hydrogen atom attracts an atom on another molecule which has a partial negative charge. When two neutral molecules which have no permanent dipoles approach each other, a weak polarization is induced because of interactions between the molecules, known as the dispersion interaction (Montgomery 1985).

Table 2.5. Properties of physisorption and chemisorption.
(Source: Atkins 1994)

Physisorption	**Chemisorption**
Multilayer adsorption	Monolayer adsorption
Low degree of specificity	Depends on the reactivity of adsorbent and adsorbable substance
Desorption is possible (adsorbed molecule keeps its identity)	Desorption is impossible (adsorbed molecule loses its identity)
Always exothermic (energy involved is <~40kJ/mole)	Exothermic or endothermic, chemical bond forms (energy involved can reach several hundreds of kJ/mole)
System generally reaches thermodynamic equilibrium rapidly	Activation energy is involved and at low temperatures, system may not reach equilibrium

Chemical adsorption, (chemisorption) is also based on electrostatic forces, but much stronger forces act a major role on this process (Sawyer et al. 1994). In chemisorption, the attraction between adsorbent and adsorbate is a covalent or electrostatic chemical bond between atoms, with shorter bond length and higher bond energy (Montgomery 1985).

The enthalpy of chemisorption is very much greater than that for physisorption, and typical values are in the region of 200 kJ/mol, whereas this value for physisorption is about 20 kJ/mol. Except in special cases, chemisorption is exothermic. A spontaneous process requires a negative free energy (ΔG) value. Because, the translational freedom of the adsorbate is reduced when it is adsorbed, entropy (ΔS) is usually negative. Therefore, in order for $\Delta G = \Delta H - T\Delta S$ to be negative, ΔH is expected to be negative, and

the process is exothermic. If the enthalpy values less negative than -25 kJ/mole, system is physisorption and if the values more negative than -40 kJ/mole it is signified as chemisorption (Atkins 1994).

Table 2.6. The bond energies of various mechanisms for adsorption.
(Source: Atkins 1994)

Interaction between adsorbent and adsorbate	**Enthalpy (kJ/mol)**		**Adsorption Tye**
	-ΔH	**+ΔH**	
Electrostatic chemical bonding	> 40	> 200	chemisorption
Dispersion interactions and hydrogen bonding	8 - 40		physisorption
Dipole-dipole interaction	< 8	< 20	physisorption

2.7.2. The Liquid – Solid Interface

The interaction of ions in the hydrosphere with solid components is subject to various types of factors. These factors are related with the properties of groundwater (temperature, pH, E_h), the speciation of these cations and their concentrations, the structural characteristics of the solid components like porosity, surface area, swelling, grain size, in addition to them, factors that include period of contact, degree of mixing and solid/liquid ratio.

The adsorption process, as illustrated on Figure. 2.5. takes place in four more or less definable steps: (1) bulk solution transport, (2) film diffusion transport, (3) pore transport and, (4) adsorption. *Bulk solution transport* involves the movement of the material to be adsorbed through the bulk liquid to the boundary layer of fixed film of liquid surrounding the adsorbent, typically by advection and dispersion. *Film diffusion transport,* involves the transport by diffusion of the material through the stagnant liquid film to the entrance of the pores of the adsorbent. *Pore transport* involves the transport of the material to be adsorbed through the pores by a combination of molecular diffusion through the pore liquid and/or by diffusion along the surface of the adsorbent.

Adsorption involves the attachment of adsorbate to adsorbent at an available adsorption site (Metcalf and Eddy 2003).

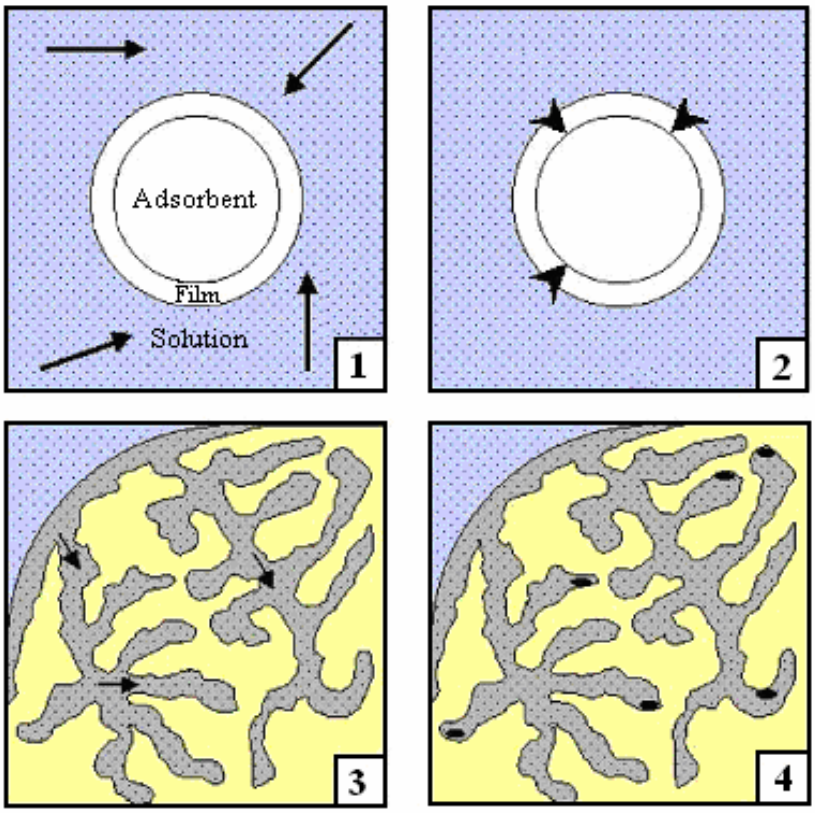

Figure 2.5. Schematic illustration of adsorption steps.

Adsorption can occur on the outer surface of the adsorbent and in the macropores, mesopores, micropores, and submicropores, but the surface area of the macro and mesopores is small compared with the surface area of the micropores and submicropores and the amount of material adsorbed there is usually considered negligible.

The type of diffusion in an ion exchange process is affected by soil particle size and nuclide concentration. Film diffusion occurs usually with a low concentration and small-sized particles. Soil mineral composition affects the amount of exchanging cations. Also many factors such as ion exchange, soil particle radius, and organic constituents affect the rate of ion exchange on soils. Usually the rate of ion exchange declines with increasing charge of the exchanging species (Liu et al. 1995).

2.7.3. Adsorption Isotherms

The relation between amount adsorbed and concentration is known as the adsorption isotherm. Adsorption equilibrium data are typically plotted in the form of an adsorption isotherm with the mass adsorbed on the y-axis and the mass in the fluid on the x-axis at constant temperature.

Adsorption isotherms are mathematical models that describe the distribution of the adsorbate specie among liquid and solid phases, based on a set of assumptions that are related to the heterogeneity/homogeneity of the solid surface, the type of coverage, and the possibility of interaction between the adsorbate specie.

Freundlich Isotherm: A brief empirical equation often used to represent adsorption data is called the Freundlich equation. The Freundlich isotherm describes physical adsorption from liquids.

The empirically derived Freundlich isotherm is defined as follows;

$$q_e = K_f C_e^{1/n} \tag{2.6}$$

where; q_e : Amount adsorbed per unit weight of adsorbent at equilibrium (mg/g), (mol/g)

C_e : Equilibrium concentration of adsorbate in solution after adsorption (mg/g), (mol/L)

K_f : Empirical Freundlich constant or capacity factor (mg/g), (mol/g)

1/n : Freundlich exponent

The exponent $\frac{1}{n}$ is an index of the diversity of free energies associated with the adsorption of the solute by multiple components of a heterogeneous adsorbent. When $\frac{1}{n}=1$, the isotherm is linear and system has a constant free energy at all adsorbate concentrations. When $\frac{1}{n}<1$, the isotherm is concave and sorbates are bound with weaker and weaker free energies, finally, when $\frac{1}{n}>1$, the isotherm is convex and more

adsorbate presence in the adsorbent enhance the free energies of further adsorption (Schwarzenbach 2003).

The good fit of Freundlich isotherm to an adsorption system means there is almost no limit to the amount adsorbed and there is a multilayer adsorption. The applicability of the Freundlich equation to a particular case is tested by plotting $\log q_e$ against $\log C_e$ from the logarithmic form of Equation 2.6.

$$\log q_e = \log K_f + \frac{1}{n} \log C_e \tag{2.7}$$

such a plot should yield a straight line with intercept equal to $\log K_f$ and slope equal to $\frac{1}{n}$.

Langmuir Isotherm: An alternative equation was derived by Langmuir on the basis of a definite case of the nature of the process of adsorption from solution. The Langmuir adsorption isotherm was developed assuming that;

- A fixed number of accessible sites are available on the adsorbent surface, all of which have the same energy.
- Adsorption is reversible.
- Monolayer adsorption occurs.
- There are no lateral interactions among the adsorbates.

The Langmuir adsorption isotherm is defined as

$$q_e = \frac{q_0 K_L C_e}{1 + K_L C_e} \tag{2.8}$$

where; q_e : Amount adsorbed per unit weight of adsorbent at equilibrium (mg/g), (mol/g)

C_e : Equilibrium concentration of adsorbate in solution after adsorption (mg/g), (mol/L)

q_0 : Empirical Langmuir constant which represents maximum adsorption capacity (mg/g), (mol/g)

K_L : Empirical Langmuir constant (L/mg), (L/mol) (Fingueneisel 1998)

The q_0 represents the total number of surface sites per mass of adsorbent. In the ideal case, q_0 would be equal for all adsorbates. However, q_0 may vary somewhat between different compounds because of differences in adsorbate sizes. Therefore, it usually represents the maximum achievable surface concentration of a given compound. The constant K_L which is commonly referred to as the Langmuir constant is defined as the equilibrium constant of the adsorption reaction. The K_L also implies a constant adsorbate affinity for all surface sites (Schwarzenbach 2003).

Assuming the above Equation (2.8) as Equation (2.9)

$$\frac{C_e}{q_e} = \frac{1}{q_0 K_L} + \frac{C_e}{q_0} \tag{2.9}$$

and plotting of $\frac{C_e}{q_e}$ vs C_e give a straight line with slope $\frac{1}{q_0}$ and intercept $\frac{1}{q_0 K_L}$.

The Langmuir isotherm is limited in its application to adsorption in monolayer. It applies well to chemical adsorption and to physical adsorption when saturation is approached (Brev 1958).

Temkin Isotherm: Temkin adsorption isotherm was developed assuming that;

- the heat of adsorption of all the molecules in the layer decreases linearly with coverage due to adsorbate–adsorbate interactions
- adsorption is characterized by a uniform distribution of binding energies, up to some maximum binding energy

The Temkin isotherm is represented by following equation:

$$q_e = \frac{RT}{b} \log(K_T C_e) \tag{2.10}$$

Equaton 2.10 can be expressed in its linear form as:

$$q_e = B_T \log K_T + B_T \log C_e \tag{2.11}$$

where B_T : $\frac{RT}{b}$ (Temkin constant related to the heat of adsorption(kJ/mol)

R : Gas constant (8.314 J/mol.K)

T : Temperature (K)

K_T : Emprical Temkin constant related to the equilibrium binding constant related to the maximum binding energy (L/mg), (L/mol)

The adsorption data can be analyzed according to the Equation (2.11). A plot of the q_e versus log C_e enables the determination of the isotherm constants K_T and B_T. (Sristeva et al. 2006)

2.7.4. Thermodynamic Parameters of Adsorption

For designing adsorption column or batch adsorption systems, the designer should be able to understand the following: what changes can be expected to occur and how fast will they take place. The fast of the reaction can be calculated from the knowledge of kinetic studies. But the change in reaction that can be expected during the process require the brief idea of thermodynamic parameters. The concept of thermodynamic assumes that in an isolated system where energy cannot be gained or lost, the entropy change is the driving force (Ho et al. 2003). The thermodynamic parameters that must be considered to determine the process, are enthalpy of adsorption (ΔH^o), free energy change (ΔG^o) and entropy change (ΔS^o) due to transfer of unit mole of solute from solution onto the solid–liquid interface. The important thermodynamic function ΔH^o is very useful whenever there is a differential change occurs in the system. Enthalpy is an additive property that is its value is additive. The negative value of ΔH^o indicates the exothermic process and positive value indicates the endothermic process. The other important thermodynamic parameter is the change in entropy ΔS^o. The parameter ΔS^o is used to identify the spontaneity in the adsorption process. The value of ΔH^o and ΔS^o were computed using the equation as follows: (Vadivelan and Kumar 2005)

$$\ln K_d = \frac{\Delta S^o}{R} - \frac{\Delta H^o}{RT} \tag{2.12}$$

where R : Universal gas constant (8.314 J/mol.K)

T : Absolute solution temperature (K)

K_d : Distribution coefficient

K_d (distribution coefficient) can be calculated by following equation

$$K_d = \frac{q_e}{C_e} \tag{2.13}$$

where q_e : Amount adsorbed per unit weight of solid (mg/g), (mol/g)

C_e : Equilibrium concentration of solute in solution (mg/g), (mol/g)

The value of ΔS^o and ΔH^o can be calculated from the slope from and intercept of plot between ln K_d versus $1/T$

Another most important thermodynamic parameter involved in the adsorption process is the free energy change and can be calculated using the relation:

$$\Delta G^o = -RT \ln K_d \tag{2.14}$$

where ΔG^o : Gibbs Free energy change

R : Universal gas constant (8.314 J/mol.K)

T : Temperature (K)

2.7.5. Adsorption Kinetics

The prediction of batch adsorption kinetics is necessary for the design of industrial adsorption columns. The nature of the adsorption process will depend on physical or chemical characteristics of the adsorbent system and also on the system conditions. Previously several researchers used different kinetic models, such as

Lagergren's pseudo first order, pseudo second order, Elovich kinetic equation, and parabolic diffusion model, in order to predict the mechanism involved in the adsorption process. From these models the adsorption kinetics was usually described by the Lagergren pseudo first order model (Inbaraj 2002, Mall and Upadhyay 1998, Khare 1987). Currently the pseudo second order model has been widely used for adsorption systems due to its good representation of the experimental data for most of the adsorbent adsorbate systems.

2.7.5.1. Lagergren's Pseudo First Order Kinetics

The pseudo first order kinetic model has been widely used to predict the metal adsorption kinetics. The metal adsorption kinetics following the pseudo first order model is given by (Ho and McKay 1998, Sivaraj 2001)

$$\frac{dq}{dt} = k_1(q_e - q) \tag{2.15}$$

where q : Amount of metal adsorbed at any time (mg/g), (mol/g)

q_e : Amount of metal adsorbed at equilibrium time (mg/g), (mol/g)

k_1 : Pseudo first order rate constant (min^{-1})

Integrating Equation (2.15) with respect to boundary conditions $q = 0$ at $t = 0$ and $q = q$ at $t = t$, then Equation (2.15) becomes

$$\ln\left(\frac{q_e}{q_e - q}\right) = k_1 T \tag{2.16}$$

Thus the rate constant $k_1(min^{-1})$ can be calculated from the plot of $\ln\left(\frac{q_e}{q_e - q}\right)$ versus time

2.7.5.2. Ho Pseudo Second Order Kinetics

The adsorption kinetic data can be further analyzed using Ho's pseudo second order kinetics, which is represented by (Ho et al. 2003)

$$\frac{dq}{dt} = k_2 (q_e - q)^2 \tag{2.17}$$

where q : Amount of metal adsorbed at any time (mg/g), (mol/g)

q_e : Amount of metal adsorbed at equilibrium time (mg/g), (mol/g)

k_2 : Pseudo second order rate constant (g/mg.min), (g/mol.min)

Separating the variables in Equation (2.17) gives;

$$\frac{dq}{(q_e - q)^2} = k_2 dt \tag{2.18}$$

Integrating Equation (2.18) for the boundary conditions $t = 0$ to $t = t$ and $q = 0$ and $q = q_e$ gives

$$\frac{t}{q} = \frac{1}{k_2 q_e^2} + \frac{1}{q_e} t \tag{2.19}$$

A plot between $\frac{t}{q}$ versus t gives the value of the constants k_2 (g/mg h), (g/mole h) and also q_e (mg/g),(mole/g) can be calculated.

The constant k_2 is used to calculate the initial adsorption rate h, at $t \rightarrow 0$, as follows:

$$h = k_2 q_e^2 \tag{2.20}$$

Thus the rate constant k_2, initial adsorption rate h, and predicted q_e can be calculated from the plot of $\frac{t}{q}$ versus time t using Equation (2.19) and (2.20)

2.7.5.3. Intraparticle Diffusion Model

The most commonly used technique for identifying the mechanism involved in the adsorption process is by fitting the experimental data in an intraparticle diffusion plot. Previous studies by various researchers showed that the plot of q_t versus $t^{0.5}$ represents multi-linearity, which characterizes the two or more steps involved in the adsorption process (Sun and Yang 2003). According to (Weber and Morris 1963), an intra-particle diffusion coefficient K_i is defined by the equation:

$$K_i = q_t / t^{0.5} + C \tag{2.21}$$

where q_t : Amount of metal adsorbed at any time (mg/g), (mol/g)

K_i : Intraparticle diffusion rate constant (mg(min)$^{0.5}$/g, (mol(min)$^{0.5}$/g

C : Gives information about the boundary layer thickness

Upon fitting data to the above equation, If the linear correlation value is close to unity, then intra-particle diffusion process is effective. Also if the relation between log (% removal) and log(time) values give linear correlation, this revels the presence of intraparticle diffusion process (Kannan and Sundaram 2001).

2.7.5.4. Activation Energy

Activation energy refers to the minimum kinetic energy that must be supplied to the system in order for a chemical process to take place. In adsorption processes, the activation energy can be obtained using Arrhenius equation; (Levine 1988)

$$\ln \frac{k(T_2)}{k(T_1)} = -\frac{E_a}{R}\left(\frac{1}{T_2} - \frac{1}{T_1}\right) \tag{2.22}$$

where k : Apperant rate constant

E_a : Activation energy

R : Universal gas constant (8.314 J/mol.K)

T : Temperature (K)

If adsorption is carried out at two different temperatures, for each the rate constant k is known, then the activation energy can be calculated using this equation 2.22

2.7.6. Heavy Metal Adsorption by Different Low-Cost Adsorbents

2.7.6.1. Zeolites

In recent years, the search for low-cost adsorbents that have metal-binding capacities has intensified. Materials locally available in large quantities such as natural materials, agricultural waste or industrial by-products can be utilized as low-cost zeolites gained a significant interest among scientists due to their ion-exchange capability to preferentially remove unwanted heavy metals such as strontium and cesium (Grant et al.1987). This unique property makes zeolites favorable for wastewater treatment.

Basically zeolites are a naturally occurring crystalline aluminosilicates consisting of a framework of tetrahedral molecules, linked with each other by shared oxygen atoms. During 1970s, natural zeolites gained a significant interest among scientists due to their ion-exchange capability to preferentially remove unwanted heavy metals such as strontium and cesium (Grant et al.1987). This unique property makes zeolites favorable for wastewater treatment.

Zeolites consist of a wide variety of species such as clinoptilolite and chabazite. Clinoptilolite is most abundant in nature and is readily available from more than 40 natural zeolites species (Vaca-Mier et al. 2001). Among the most frequently studied natural zeolites, clinoptilolite was shown to have high selectivity for certain heavy metal ions such as Pb^{2+}, Cd^{2+}, Zn^{2+}, and Cu^{2+}. Table 2.7 shows that adsorption capacities of zeolites for some heavy metals in literature.

Table 2.7. Adsorption capacities (mg/g) of zeolites for some heavy metals.

Material	Cd^{2+}	Co^{2+}	Ni^{2+}	Zn^{2+}	Cu^{2+}	Pb^{2+}	Reference
Clinoptilolite	2.40	1.42	0.48	0.50	1.64	1.60	(Zamzow and Eichbaum 1990)
	1.20					1.40	(Malliou et al. 1992)
	70.0					62.0	(Ouki et al.1993)
	3.70	1.50	0.90	2.70	3.80	6.00	(Ouki and Kavanagh 1997)
Chabazite	137					175	(Ouki et al.1993)
	6.70	5.8	4.50	5.50	5.10	6.00	(Ouki and Kavanagh 1997)
Chabazite-phillipsite			0.56	0.04	0.37		(Ibrahim et al. 2002)

2.7.6.2. Clay

It is widely known that there are three basic species of clay: smectites (such as montmorillonite), kaolinite, and micas; out of which montmorillonite has the highest cation exchange capacity and that its current market price is considered to be 20 times cheaper than that of activated carbon. Therefore, a number of studies have been conducted using clays, mainly montmorillonite, to show their effectiveness for removing metal ions and Table 2.8 shows that adsorption capacities of clay for some heavy metals in literature.

2.7.6.3. Peat moss

Peat moss, a complex soil material containing lignin and cellulose as major constituents, is a natural substance widely available and abundant, not only in Europe (British and Ireland), but also in the US. Peat moss has a large surface area (>200 m^2/g) and is highly porous so that it can be used to bind heavy metals. In 1986, the use of peat to remove heavy metals was investigated (Gosset et al.1986). Table 2.9. shows that heavy metals adsorption capacity of peat moss in literature.

Table 2.8. Adsorption capacities (mg/g) of clay for some heavy metals.

Material	Pb^{2+}	Cd^{2+}	Zn^{2+}	Cr^{6+}	Sr^{+2}	Reference
Montmorillonite	0.68	0.72				(Srivastava et al. 1989)
		4.78	4.98			(Undaybeytia et al. 1996)
Kaolinite			1.25			(Singh et al. 1988)
	0.12	0.32				(Srivastava et al 1989)
	1.41					(Chantawong et al. 2001)
Bentonite		11.41	4.54			(Panday et al. 1989)
				0.57		(Khan et al. 1995)
					32.94	(Khan et al. 1995)
			52.91			(Mellah et al.1997)
Illite	4.29					(Chantawong et al. 2001)

Table 2.9. Adsorption capacities (mg/g) of peat moss for some heavy metals.

Material	Cu^{2+}	Cr^{6+}	Cd^{2+}	Zn^{2+}	Ni^{2+}	Reference
Eutrophic peat	12.07		20.23	11.12	11.15	(Gosset et al 1986)
	19.56					(Chen et al. 1990)
Oligotrophic peat	12.07		22.48	13.08	11.74	(Gosset et al 1986)
	6.41					(Chen et al. 1990)
Sphagnum peat moss		132				(Sharma and Forster 1993)

2.7.6.4. Fly Ash

Fly ash, an industrial solid waste of thermal power plants, is one of the cheapest adsorbents having excellent removal capabilities for heavy metals. The adsorption capacity of fly ash for some metals in literature shown in Table 2.10.

Table 2.10. Adsorption capacities (mg/g) of fly ash for some heavy metals.

Material	Cu^{2+}	Cr^{6+}	Hg^{2+}	Reference
Fly ash	1.39			(Panday et al. 1985)
			2.82	(Sen and Arnab 1987)
Fly ash-wollastonite	1.18	2.92		(Panday et al. 1984)
Fly ash-China clay		0.31		(Panday et al. 1984)

2.7.6.5. Natural Oxide

In 1985, a study on the use of aluminium oxide to remove Cr^{6+} from aqueous waste was conducted (Gupta and Tiwari 1985). It was reported that the ultimate adsorption capacity of 11.7 mg of Cr^{6+}/g alumina was observed at pH of 4.0. It is important to note that the adsorption capacity of alumina significantly reduced in the presence of CN^- anions. It can be explained due to the fact that cyanide has a strong anionic influence upon the sorption characteristics of alumina. Therefore, CN^- anions are competitively adsorbed covering the surface sites of alumina, which in turn prevent the Cr^{6+} to be adsorbed on the internal surface of adsorbent.

The removal of Pb^{2+} and Cd^{2+} from aqueous solutions using aluminium oxide and goethite, an iron oxide was also explored (Srivastava et al. 1988). It was found that goethite exhibits a better sorption capacity for both ions than alumunium oxide and that the uptake of Pb^{2+} is higher than that of Cd^{2+} (Table 2.11) The adsorption capacity of Natural oxides for some metals in literature shown in Table 2.11.

Table 2.11. Adsorption capacities (mg/g) of natural oxides for some heavy metals.

Material	Cd^{2+}	Pb^{2+}	Cr^{6+}	Reference
Aluminium oxide			11.7	(Gupta and Tiwari 1985)
	31	33		(Srivastava et al. 1988)
Ferric Oxide	72	230		(Srivastava et al. 1988)

2.7.6.6. Chitin and Chitosan

Among various biosorbents, chitin is the second most abundant natural biopolymers after cellulose. However, more important than chitin is chitosan, which has a molecular structure similar to cellulose. Presently, chitosan is attracting an increasing amount of research interest, as it is an effective scavenger for heavy metals. The adsorption capacity of chitosan for some metals in literature shown in Table 2.12.

Table 2.12. Adsorption capacities (mg/g) of chitosan for some heavy metals.

Material	Cu^{2+}	Cr^{6+}	Cd^{2+}	Pb^{2+}	Ni^{2+}	Reference
Chitosan			5.93			(Jha et al. 1988)
	222					(Mckay et al. 1989)
		273				(Udaybhaskar et al. 1990)
	16.8		8.54	16.36	2.40	(Huang et al. 1996)
Chitosan beads			250			(Hsien et al. 1992)

CHAPTER 3

MATERIALS AND METHODS

3.1. Materials

Solid, powder and α-form of chitin from crushed crab shells (Sigma Chemicals Co.) was used in this study. The chitin sample was dry-sieved and particle size of chitin used in our study was d < 150 μm. For removing the impurity of chitin which was poured in deionized water and boiled for 30 min. Then it was washed several times with deionized water and dried in a vacuum oven for 3 days at 60 °C. All dried samples were kept in desiccator. Only the prufied chitin sample was used for all experiments.

Viscosity and molecular weight determination of chitin biopolmer performed with Dimethyl Acetamide-DMAc (Sigma Chemicals Co.)/ Lithium Chloride-LiCl (Sigma Chemical Co.) solvent system with Ubbelohde capillary viscometerer. Viscosity and molecular weight determination of chitosan biopolymer performed with Acetic Acid (Sigma Chemical. Co.) and Sodium chloride (Sigma Chemical Co.) solvent system.

Standard heavy metal stock solutions (1000 mg/L) were prepared by dissolving 2.952 g $Cu(NO_3)_2$, 2.032 g $CdCl_2.5/2H_2O$, 1.578 g $Pb(NO_3)$ (Sigma Chemicals Co.) and 4.478 g $NiSO_4.6H_2O$ (Fluka) in ultra pure water which was passed through Barnstead Easypure UV- Compact ultra pure water system (18.3 ohm) then diluted to 1000 ml. pH adjustment of solutions were made using dilute or concentrated NaOH (Sigma Chemicals Co.) and HCl (Sigma Chemicals Co.) solutions using Orion 420 A pH meter.

Double distilled water was used to prepare all solutions. All reagents were analytical grade and stored in polyethylene-polypropylene containers. Plastics were cleaned in dilute HNO_3 (10% v/v) and dried at 60˚C after rinsing with deionized water.

3.2. Methods

3.2.1. Preparation of Chitosan from Chitin

Chitosan sample was prepared from reaction of purified chitin with %50 NaOH (12.5 mL NaOH/g of chitin) at 120^{o}C under nitrogen atmosphere. The reaction times of purified chitin was changed from 15 minutes to 1 day. The chitosan samples were washed with several times and soaked in double distilled water untill neutral pH. Later the chitosan samples were dried in oven and degree of N-deacetylation values were determined with elemental analysis. At a constant N-deacetylation time was choosen to prepare chitosan from chitin to use adsorption and characterization experiments (Chang et al. 1997).

3.2.2. Characterization of Chitin and Chitosan

Characterization of chitin and chitosan biopolymers carried out by viscosity measurements, particle size distribution analysis, surface area and pore size analysis, X-ray diffraction, zeta potential analysis, IR spectroscopy, elemental analysis, scanning electron microscopy (SEM) and thermal gravimetric analysis (TGA/DTA)

3.2.2.1. Viscosity Measurements

In order to evalute the molecular weight of polymeric chains, various methods can be used. Widespread are viscosity and gel permeation chromatographic techniques.

Viscometry is commonly selected as it is one of the simplest and most rapid methods for determining these molecular weights.

A well established correlation between viscosity and molecular weight is given by the Mark-Houwink equation and this equation was explained in chapter 2, given by,

$$[\eta] = KM^{a} \tag{2.5}$$

where η : Intrinsic viscosity

K : Viscometric parameter

M : Molecular weight

a : Viscometric parameter

Measurements of a solution viscosity is made by comparing the time taken, *t,* for the solution flow through a capillary tube t_o the time taken, t_o, for the solvent used. From *t*, t_o, and solute concentration c, the followig can be derived.

Specific Viscosity ;

$$\eta_{sp} = \left(\frac{\eta}{\eta_0} - 1 \right) \tag{3.1}$$

where η : Intrinsic viscosity

η_0 : Viscosity of pure solvent

η_{sp} : Specific viscosity

Inherent Viscosity;

If the $\left(\frac{\eta}{\eta_0} \right)$ is expanded as an infinite series and the higher terms neglected then;

$$[\eta] = \left(\frac{1}{c} \ln \left(\frac{\eta}{\eta_0} \right) \right)_{c \to 0} \tag{3.2}$$

where c : Concentration (g of solute per 100 ml of solvent)

Intrinsic Viscosity;

$$[\eta] = \left(\frac{\eta_{sp}}{c} \right)_{c \to 0} \tag{3.3}$$

Combining Equations 3.1, 3.2 and 3.4 yields

$$\frac{n_{sp}}{c} = KM^{a} \tag{3.4}$$

Therefore plotting a graph of $\left(\frac{1}{c}\ln\left(\frac{\eta}{\eta_0}\right)\right)$ and $\left(\frac{\eta_{sp}}{c}\right)$ versus c and extrapolating back to zero to determine a mean value for intrinsic viscosity of the polymer solution. Using this value and the correct constants for *K* and *a* in equation 2.5 yields the molecular weight of the polymer (Flory 1953, Tanford 1961).

PETROTEST kinematic viscosity apparatus was used to determine the molecular weights of chitin and chitosan biopolymers. In this case 0.25 g of chitin was added to 200 mL solvent which was N,N dimethylacetamide/Lithium chloride, (%5 DMAC/LiCl) to produce the required chitin concentration (0.125 w/v). Then chitin was left to dissolve in the solvent for approximately 48 hours. This solution were placed into nine volumetric flasks before being diluted with the solvent to produce nine different concentration (w/v) of the chitin solution. Kinematic viscosity measurements of chitin solutions were carried out using to an Ubbelohde U-Tube capillar viscometer which is 0.004720 cSt/s^2 capillary constant in thermostated water bath at 25^{o}C. Same procedure was applied for chitosan with acetic acid/sodium chloride (0.2M NaCl/AcH(1%)) solvent system. Each biopolymer solution were filtered through a 0.45 μm Millipore filter to get rid of dusts and insoluble impurities. Each viscosity measurements were performed for three times and average values of these were used to determine intrinsic viscosities [η] and moleculer weights of chitin and chitosan biopolymers.

3.2.2.2. Particle Size Distribution Analysis

The purpose of the particle size distribution analysis is to measure the quantities of particles contained in each size class in a powder sample. Most particle size analysis techniques define particle sizes by reporting equivalent spherical diameters (ESD). Particles are grouped into many narrowly defined size classes that cover the whole range of sizes. Quantities of particles in each size class are usually reported as mass or volume percentages (Dinger 2005).

Particle size distribution of powder forms of chitin and chitosan biopolymers were analyzed with Malvern Mastersizer 2000 instrument. Approximately %10-15 (m/m) suspension of chitin and chitosan were prepared in ultra-purewater and then analyzed with Malvern Mastersizer 2000 apparatus at room temperature. This apparatus measure the particle size of sample with "Mie scattering" measurement principle. Detection system of this apparatus was red light for forward scattering , side scattering and back scattering. In addition Helium neon laser source is used for light source.

3.2.2.3. Surface Area Analysis

Surface area analyzers measure the total exposed surface area (m^2) present in powder samples. Surface area values are usually reported as either Specific Surface Area (SSA) which is the surface area in a fixed mass of particles (m^2/g) or as Volume specific Surface Area (VSA) which is the surface area in a fixed volume of particles (m^2/cm^3) (Dinger 2005).

When a gas is physically adsorbed (condensed) on the surface of a solid, the quantity adsorbed varies with pressure. The B.E.T. equation was to permit the measurement of V_m, the volume of gas necessary to form a monolayer of liquid across a solid surface. The equation is;

$$\frac{x}{V(1-x)} = \frac{1}{V_m} + \frac{(C-1)x}{V_m} \tag{3.5}$$

Where x is the relative pressure, P/P_0 , at which a gas volume V (m^3 at S.T.P.) is adsorbed, P is the pressure of the gas, and P_0 is the saturated vapor pressure at the temperature of the vessel holding the adsorbent.

V_m is the volume of gas required to form a monolayer on the adsorbent at the system temperature, and C is a constant. Therefore, a plot of [x/V(1-x)] against x should be linear, with slope $[(C-1)/V_m]$ and intercept (C-1). Determination of these values from the plot gives two simultaneous equations, enabling the calculation of V_m. Linear plots of [x/V(1-x)] against x are usually observed over the relative pressure range 0.05 P/P_0, although expections to this are known.

Equation 3.5 is a generalization of the Langmuir adsorption isotherm applied to multilayer adsorption. The theory is based on the establisment of an equilibrium between gas and adsorbed material involving the dynamic transfer of molecules between the gas phase and the surface.

The B.E.T. method yields a value for the volume of a monolayer of adsorbed gas on the solid surface. The surface area of one molecule of adsorbed gas (adsorbate) may be calculated from its density and molecular weight. Using this datun the total surface area of the solid may be calculated (McKay 1996).

The B.E.T. and Langmuir surface area, pore size and volume of chitin and chitosan biopolymers were determined by Micromeritics Gemini 2380 model surface area analyzer. The chitin and chitosan samples were degassed at 200 ± 1 °C in a vacuum and then the adsorption measurements of nitrogen were carried out at 77 ± 1 K. In this method, the average pore diameter of the composite adsorbents can be calculated from the surface area and the pore volume by assuming cylindrical pores.

3.2.2.4. X-Ray Diffraction (XRD)

X-ray diffraction is a versatile analytical technique for examining crystalline solids, which include ceramics, metals, electronic materials, geological materials, organics, and polymers. These materials may be powders, single crystals, multilayer thin films, sheets, fibers, or irregular shapes, depending on the desired measurement. X-Ray diffractometers fall broadly into two classes: single-crystal and powder. Single-crystal diffractometers are most often used to determine the molecular structure of new materials. Powder diffractometers are routinely used for phase identification and quantitative phase analysis but can be configured for many applications, including variable-temperature studies, texture and stress analysis, grazing incidence diffraction, and reflectometry. The theoretical basis of X-Ray diffraction stands on Bragg's equation given by;

$$n\lambda = 2d\sin\theta \tag{3.6}$$

where n is the order of reflection n =(1, 2, 3, ……), λ, the wavelength, d the distance between parallel lattice planes, and θ the angle the incident beam and a lattice plane,

known as the Bragg angle. When the path length in the crystal (*2dsin θ*) is a multiple of the wavelength, constructive interference occurs and diffracted intensity is obtained. In general, the d-spacing is a function of the lattice parameters (a,b,c) and angles (α, β, γ) defining the unit cell, and the Miller indices (h, k, l) denoting a particular reflection. As such, it is the geometry of the crystal lattice that determines the position of the peaks in an X-ray diffraction pattern. In general, the more symmetrical the material, the fewer peaks in its diffraction pattern. The diffracted intensities associated with those peaks are determined by the and arrangement of atoms wthin the crystal lattice.

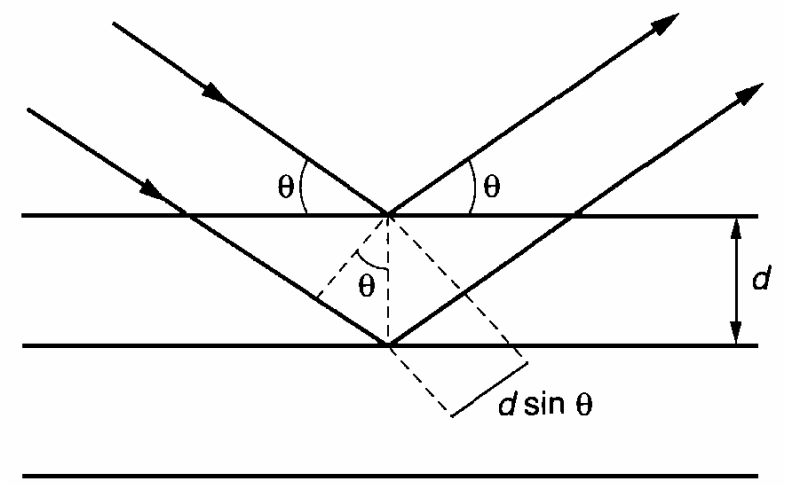

Figure 3.1. Illustration of Bragg's law

The radiation used in a typical diffraction measurement contains several wavelengths, denoted $K_{\alpha 1}$, $K_{\alpha 2}$, K_{β}, which are characteristic of the material producing the X rays (Settle 1997). Common anode materials and their specific wavelengths are showed in Table 3.1.

X-ray powder diffraction (XRD) data were colloected on a Philipps X'Pert Pro diffractometer using Cu $K_{\alpha 1}$ radiation (λ=0.154056nm) in 5-45 θ values. Chitin and chitosan samples were prepared by compresing in the cassette sample holder without any adhesive substances.

Table 3.1. X-Ray wavelengths (in Å) for common anode materials.
(Source: Settle 1997)

Anode	$K_{\alpha 1}$	$K_{\alpha 2}$	K_{β}
Chromium(Cr)	2.28970	2.29361	2.08487
Cobalt (Cu)	1.78897	1.79285	1.62079
Copper (Cu)	1.54056	1.54439	1.39222
Molybdenum (Mo)	0.70930	0.71359	0.63229

3.2.2.5. Zeta Potential Analysis

The development of a net charge at the particle surface affects the distribution of ions in the surrounding interfacial region, resulting in an increased concentration of counter ions (ions of opposite charge to that of the particle) close to the surface. Thus an "*electrical double layer"* exists around each particle. The liquid layer surrounding the particle exists as two parts; an inner region, called the *"Stern layer",* where the ions are strongly bound and an outer, diffuse, region where they are less firmly attached. Within the diffuse layer there is a notional boundary inside which the ions and particles form a stable entity. When a particle moves (e.g. due to gravity), ions within the boundary move with it, but any ions beyond the boundary do not travel with the particle. This boundary is called the surface of hydrodynamic shear or slipping plane. The potential that exists at this boundary is known as the *"Zeta potential"*.

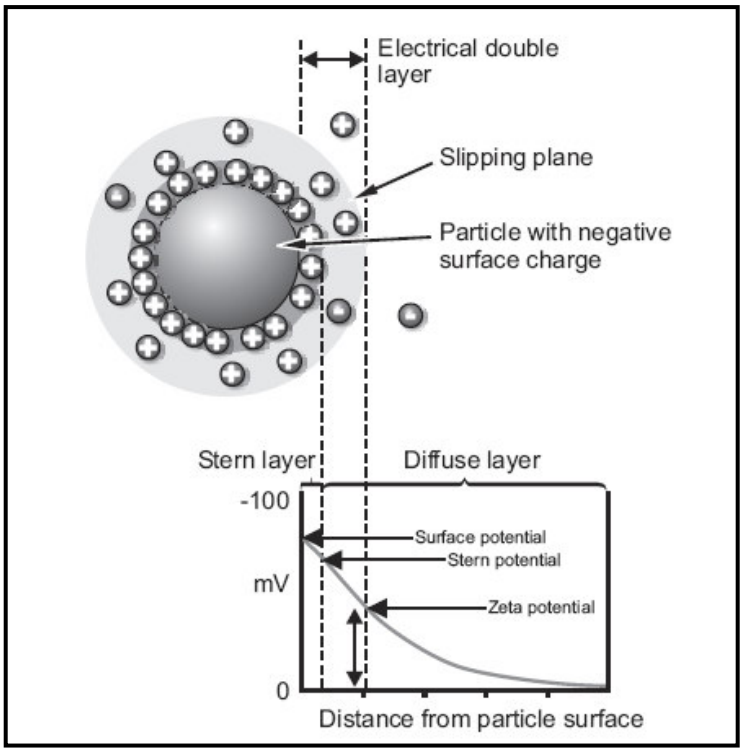

Figure 3.2. Schematic representation of zeta potential.

(Source:WEB_6 2007)

The magnitude of the zeta potential gives an indication of the potential stability of the colloidal system. A colloidal system is when one of the three states of matter: gas, liquid and solid, are finely dispersed in one of the others. For this technique we are interested in the two states of a solid dispersed in a liquid, and a liquid dispersed in a liquid, i.e. an emulsion. If all the particles in suspension have a large negative or positive zeta potential then they will tend to repel each other and there is no tendency to flocculate. However, if the particles have low zeta potential values then there is no force to prevent the particles coming together and flocculating. The general dividing line between stable and unstable suspensions is generally taken at either +30mV or -30mV. Particles with zeta potentials more positive than +30mV or more negative than -30mV are normally considered stable.

The point where the plot passes through zero zeta potential is called the "*Isoelectric point*" and is very important from a practical consideration. It is normally the point where the colloidal system is least stable (WEB_6 2007).

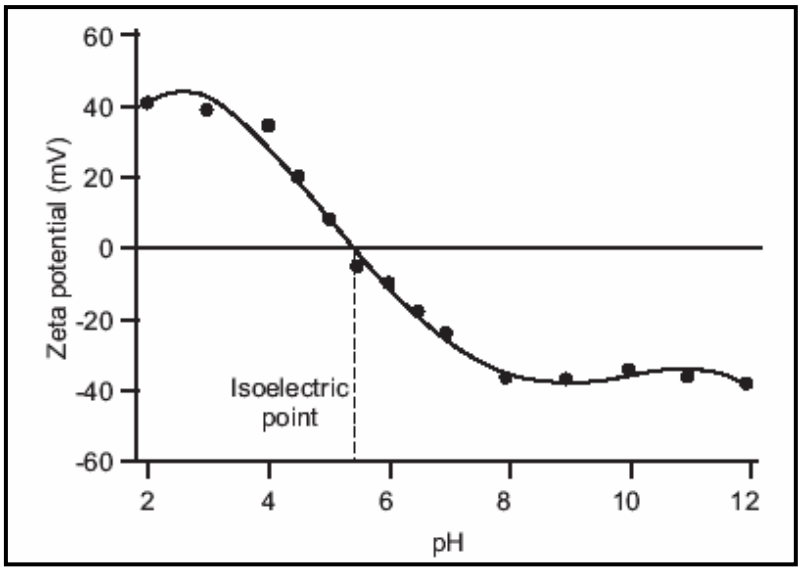

Figure 3.3. A typical plot of zeta potential versus pH.
(Source:WEB_6 2007)

Zeta potentials and isoelectric point (point of zero charge) determination of chitin and chitosan biopolmers performed using a Malvern Zetasizer Nano ZS model of zeta potential apparatus. A 0.1 wt % chitin and chitosan suspensions were prepared and pH adjustments made using HCl or NaOH. After the pH stabilized, required amount of these solutions transferred to the measuring cell and about 3 values of zeta potential were measured at room temperature.

3.2.2.6. IR Spectroscopy

Infrared (IR) spectroscopy measures the absorption of IR radiation by materials as the atoms vibrate about their bonds. It is primarily used to idenify bond types, structures and functional groups in organic and inorganic compounds. IR sensitive vibrations are associated with changes in dipole moments.

IR spectroscopy measures vibrational energy levels in molecules. It can be used for both qualitative and quantitative analysis, to identify molecules and compounds, and to determine the presence or absence of certain types of bonds and functional groups. For example, double and single bonds associated with carbon-hydrogen and carbon-oxygen bonding (=C-H,-C-H, C-O and C=O) can be distinguished by IR absorption. When functional groups can be bonded at different locations on molecules, IR

spectroscopy can frequently identify the positions at which the functional groups are atteched. The reason is that vibrational frequencies differ when functional groups are atteched at different sides in molecules.

When illuminated by IR radiation of the appropriate frequencies, atoms, ions, and functional groups in molecules will vibrate about their bonds and energy will be absorbed. Each bending and stretching vibrational mode of a molecule or functional group will absorb at a particular frequency. When exposed to appropriate IR frequencies, energy will be absorbed from the incident radiation as vibrational intensities increase. Many IR frequencies have no effect at all and will not be absorbed (Dinger 2005).

IR characterization of chitin and chitosan biopolymers were performed with Nicolet Magna 550 FT-IR instrument with a frequency range of 4000-400 cm^{-1}. Chitin and chitosan samples prepared in the forms of potassium bromide (KBr) disk. Approximately 40-60 mg of chitin or chitosan powder and 120 mg of KBr was blended and triturated with agate mortar and pestle for 10 min. Approximately 40 mg of the mixture were compacted using a IR hydraulic press at a pressure of 8 tons for 60 s. The disk was conditioned in a desiccator placed in an oven at 80°C for 16 hr before analysis. The spectra of chitin and chitosan samples (in the forms of KBr disk) were obtained with a frequency range of 4000-400 cm^{-1}

3.2.2.7. Elemental Analysis

For the chemical composition of the carbonaceous materials C, H, N analysis is used. The carbon, hydrogen and nitrogen contents of the samples are determined from the quantities of CO_2, H_2O and NO_2 produced by the combustion of the dried solid in oxygen (Dinger 2005).

LECO CHNS-932 elemental analysis apparatus was used to determine the amount of C, H, and N in chitin and chitosan biopolymers. In this case samples were heated to a temperature of 1000°C and approximately 2 mg of chitin or chitosan was placed inside a silver capsule and was dropped into the CHNS-932 furnace, where it was completely combusted. This instrument relies upon infrared detection to measure the weight percent of carbon, hydrogen, and sulfur, while nitrogen were measured using thermal conductivity detection.

3.2.2.8. Scanning Electrom Microscope (SEM) Analysis

Scanning Electron Microscope (SEM) are commonly used to study surfaces, structures, morphologies, and forms of materials.

The images viewed using SEM are created by detecting secondary electrons ejected from samples as they are bombarded by focused, high energy electron beams. Unlike optical microscopy, one does not look through lenses at the actual sample, but one observes images of the sample created by the instrument's electronics.

SEM can achieve higher magnifications than optical microscopes. When samples are probed with focused electron beams, a variety of signals can be collected and displayed on the view screen. In addition to secondary electron signals, X-rays characteristic of the elemental composition of the sample can be mapped to sample images, and back-scattered electrons can also be collected and displayed. When SEMs are fitted with appropriate detectors, one can not only see images of the samples (using secondary and back-scattered electron signals) but one can also see images which map the elemental compositions of the samples.

SEM analyses are conducted in vacuum environments. All non-conductive samples must be coated with electrically conductive coatings before they can be observed in SEM (Dinger 2005).

SEM characterization was carried out using a Philips XL-30S FEG type instruments in vacuum environment. Prior to analysis the chitin and chitosan samples were sprinkled onto Al or C tapes which are adhesive and supported on metallic disks and coated with Au. Images of the sample surfaces were recorded at different areas and magnifications.

3.2.2.9. Thermal Gravimetric Analysis (TGA/DTA)

Thermal Gravimetric Analysis (TGA) measures the masses of samples as they are heated and cooled through standard firing programs.

TGA analyses are very similar to DTA analyses. In the case of TGA analyses, the increase, decreases, or constancy of mass of samples at each temperature in the firing program indicates the presence or absence of reactions and the nature of each reaction that takes place. Foreaxample, phase changes occur without change of mass;

some decomposition reactions are accompanied by weight loses; and oxidation reactions are accompanied by weight gains.

TGA analyses require small samples (several grams) of dry powders or particulate suspensions. All such samples must be throughly dried before performing before performing the analyses. Similar to the DTA analysis technique TGA analyses are also routinely used to identify during body development. Some modern instruments smultaneously perform DTA and TGA analyses (Dinger 2005).

Chitin and chitosan biopolymers were analyzed with Perkin-Elmer Diamond TG/TDA apparatus under nitrogen atmosphere (20ml/min) in platin crose increasing the temperature 10 ^{o}C (10 ^{o}C/minute) between 50-400^{o}C.

3.2.3. Heavy Metal Adsorption Studies

In batch adsorption experiments known weights of chitin and chitosan samples (0.1 g) were added to polyethylene tubes containing 10 mL heavy metal solution with adjusted pH and shaked by a Nuve ST 402 temperature-controlled water bath at approximately 600 rpm (a speed rate at which the chitin and chitosan would not precipitate). The contact time was changed from 5 minutes to 24 hours.

The effect of adsorbent dosage on adsorption was examined by operating various dosages (0.0125, 0.025, 0.05 0.1 and 0.2 g) of chitin and chitosan were applied to 10 mL of the solution containing 100 mg/L heavy metals at 298.15 K in order to find out the effect of adsorbent dosage for heavy metal removal.

The effect of pH on adsorption was examined by operating various pH values (1, 2, 3, 4, 5, 6, 7 and 8) of chitin and chitosan were applied to 10 ml of the solution containing 100 mg/L heavy metals at 298.15 K in order to find out the effect of pH on heavy metal removal. Precipitation of the metal species were observed over the pH 8.

The effect of temperature on adsorption was examined by operating at various temperatures; 298.15 K and 313.15 K in a temperature-controlled water bath equipped with a shaker.

The effect of initial concentration of heavy metal ions was examined by studying different initial concentrations changing from 10 to 1000 mg/L. Initial concentration values were chosen as 10, 25, 50, 100, 250, 500, 750 and 1000 mg/L. At the end of each mixing period the liquid phases were separated from the solution by filtration.

All adsorption experiments were performed for two times and average values were used for all calculations.

3.2.4. Analysis of Aqueous Solutions

3.2.4.1 Atomic Absorption Spectrometry

Atomic absorption spectrometry (AAS) is a widely used and accepted technique capable of determining trace (μg/mL) and ultratrace (sub-μg/mL) levels of elements or metals in a wide variety of samples, including biological, clinical, environmental, food, and geological samples, with good accuracy and acceptable precision. It is arguably the predominant technique in elemental analysis, although it does have some limitations. (Settle 1997)

Atomic absorption spectrometry uses the absorption of radiation by free gaseous atoms in order to achieve qualitative detection and quantitative determination of elements (Welf and Sperling 1998). An atomic absorption spectrometer measures the absorbance which is the logarithm of the rate of incident light power (P_o) to transmitted light power (P)

$$A = \log \frac{P_0}{P} \tag{3.7}$$

There is relationship between P_o and P when a light beam is decreased by the medium throughy which it passes:

$$P = P_0 \exp(- kL) \tag{3.8}$$

where k : Absorption coefficient which is a function of wavelenght of light , number of atoms in the ground state per unit volume

L : Path length in medium

There are two main components in an atomic spectrometer: atom cell which creates atoms at the free gaseous ground state, optical system to measure the signal. Atom cell dissolvates the liquid sample and dissociates analyte elements into their free gaseous ground state form in which the atoms are available to absorb radiation coming from light source and create a measurable signal which is proportional to concentration (Tyson and Haswell). The atomizer, in which the analyte is atomized, is flame, graphite tube or quartz tube. In flame atomization fixed aliquot of measurement solution is converted into an aerosol in nebulizer and transported into the flame which must has enough energy both vaporize and atomize the sample. Properties of flame types are presented in Table 3.2 (Welz and Sperling 1998)

Table 3.2. Spectroscopic flames for AAS with their properties.
(Source: Tyson and Haswell 1991)

Oxidant	**Fuel Gas**	**Max.Flame Temperature (^oC)**	**Max.Burning Velocity (cm/s)**	**Remarks**
Air	Acetylene	2250	158	Most commonly used flame
Nitrous Oxide	Acetylene	2700	160	For difficulty volatilized and atomized substances
Air	Hydrogen	2050	310	Flame of high transparency; for easily ionized elements
Air	Propane /Butane	1920	82	Flame of ionized elements

The filtrate solutions obtained in the adsorption process were analyzed using flame AAS. The instrument applied was a Thermo Elemental SOLAAR M6 Series atomic absorption spectrometer. Element content of aqueous solutions was determined with hallow cathode lamps. Table 3.3 shows that specific wavelengths and analysis conditions for used metal ions in our study.

Table 3.3. Specific wavelengths and AAS analysis conditions for used metal ions.

Element	Wavelength (nm)	Flame Type	Hallow-Cathode Lamp
Copper (Cu^{2+})	324.8	Air/acetylene	Copper
Lead (Pb^{2+})	217.0	Air/acetylene	Lead
Cadmium (Cd^{2+})	228.8	Air/acetylene	Cadmium
Nickel (Ni^{2+})	232.0	Air/acetylene	Nickel

CHAPTER 4

RESULTS AND DISCUSSION

4.1. Preparation of Chitosan from Chitin

Elemental analysis is simple, suitable and rapid method to determine degree of deacetylation (DD) value of chitin using the following equation;(Kasaai et al. 2000).

$$DD = \left(1 - \frac{C/N - 5.145}{6.186 - 5.145}\right) x100 \qquad (2.3)$$

Figure 4.1. shows degree of deacetylation values of chitin biopolymer with reaction of 50% (m/m) NaOH (12.5 mL NaOH/gr of chitin) at 120°C under nitrogen atmosphere with various times. Figure 4.1. shows that chitin biopolymer is deacetylated gradually at 360 minutes and then there is no change after this time. In this case approximately a 6 hours period is enough to prepare nearly 82.95 % deacetylated chitin (chitosan) which was used later in characterization and adsorption experiments. Elemental analysis results and degree of deacetylation values of alkaline deacetylation of chitin at various times are shown in Table 4.1.

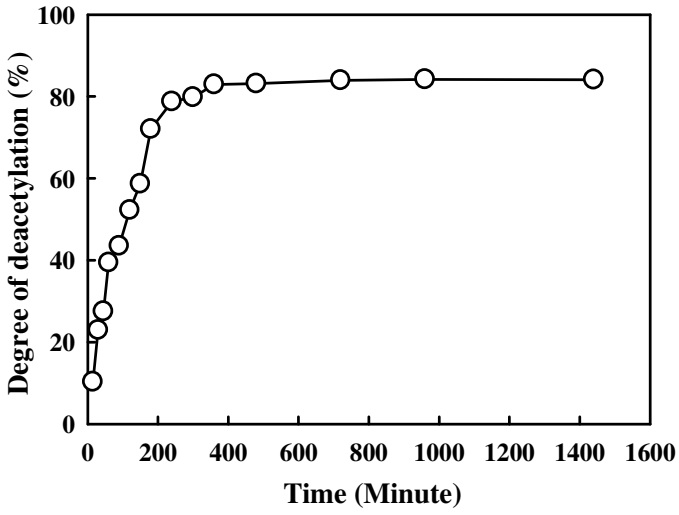

Figure 4.1. Time-course of alkaline deacetylation of chitin

Table 4.1. Elemental analysis results of time course of alkaline deacetylation of chitin.

Reaction Time (Minute)	Average Mass of Chitin (mg)	Average Carbon (%)	Average Hydrogen (%)	Average Nitrogen (%)	Average (DD) (%)
0	2.01	40.82	6.45	6.69	8.25
15	1.94	40.73	6.46	6.70	10.34
30	2.01	40.16	6.52	6.75	23.00
45	2.04	39.94	6.55	6.77	27.54
60	1.99	39.82	6.76	6.90	39.43
90	2.02	39.67	6.78	6.92	43.52
120	2.03	39.46	6.84	6.99	52.25
150	1.99	39.13	6.81	7.02	58.69
180	2.02	38.60	6.84	7.10	72.05
240	2.09	38.45	6.84	7.17	78.78
300	2.11	38.42	6.85	7.18	79.83
360	2.01	38.23	6.85	7.18	82.95
480	2.11	38.22	6.86	7.18	83.16
720	2.17	38.16	6.85	7.18	83.96
960	2.02	38.15	6.86	7.18	84.20
1440	2.04	38.17	6.87	7.19	84.12

4.2. Characterization of Chitin and Chitosan

4.2.1. Molecular Weight Determination of Chitin and Chitosan with Viscosity Measurements

The molecular weights of chitin and chitosan biopolymers were determined according to viscosity measurements using the Mark Houwink equation;

$$[\eta] = KM^{a} \tag{2.5}$$

Figure 4.2. shows that the intrinsic viscosity of chitin biopolymer sample used in this research was 5.36 mL/g at N,N dimethylacetamide/lithium chloride (%5 DMAC/LiCl) solvent system, whose molecular weight corresponds to approximately

$1.02x10^5$ (g/mole) on the basis of the Mark-Houwink equation. In addition Figure 4.2 shows that intrinsic viscosity of chitosan biopolymer sample used in this research was 8.96 mL/g at acetic acid/sodium chloride (0.2M NaCl/0.1M CH_3COOH) solvent system, whose molecular weight corresponds to approximately $9.44x10^3$ (g/mole) on the basis of the Mark-Houwink equation. The molecular weight results of chitin and chitosan biopolymers used in this study showed that molecular weight of chitin is nearly 10 times greater than molecular weight of 82.9 % deactylated chitin (chitosan). These results confirm the conversion of the acetamido groups of chitin to amino groups with reaction of hot and concentrated alkali solution. Table 4.2 gives the Mark-Houwink parameters, intrinsic viscosities, solvent systems and molecular weights of used chitin and chitosan biopolymers in this study at 25°C.

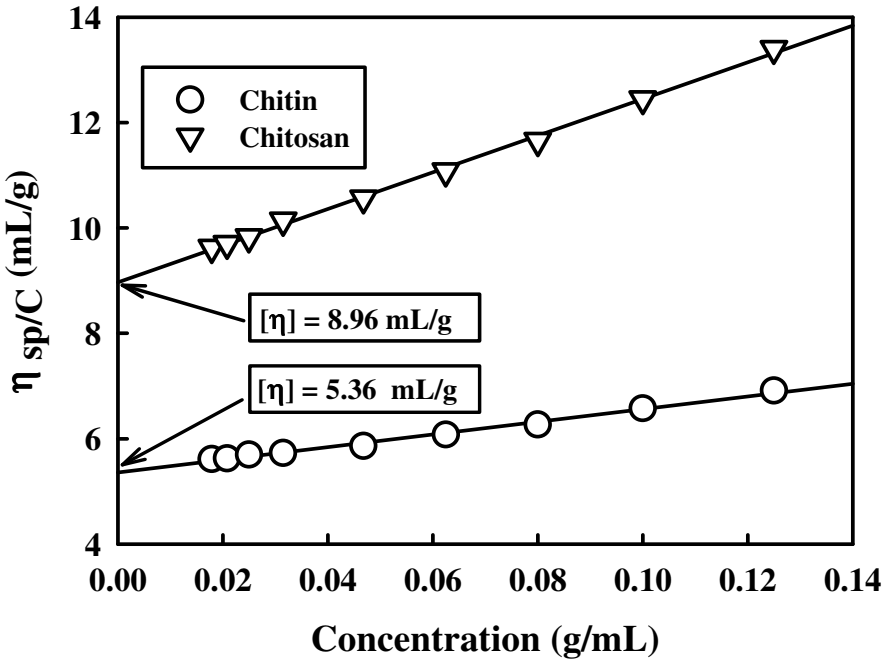

Figure 4.2. Determination of the intrinsic viscosities of used chitin and chitosan.

Table 4.2. Molecular weights, solvent system and Mark-Houwink parameters of used chitin and chitosan.

Biopolymer	Solvent System	α	K (mL/g)	η (mL/g)	Mol.Weight (g/mole)
Chitin	N-N, DMAc/LiCl 5%	0.88	2.1×10^{-4}	5.36	$1.02\text{x}10^{5}$
Chitosan	0.1 M AcH/0.2 M NaCl	0.93	1.81×10^{-3}	8.96	$9.44\text{x}10^{3}$

4.2.2. Particle Size Distribution Analysis

Figures. 4.3. and 4.4. show the particle size distribution of chitin and chitosan biopolymers. The maximum volume percentages corresponds to the particle sizes of approximatelly 120 μm and 100 μm for chitin and chitosan, respectively.

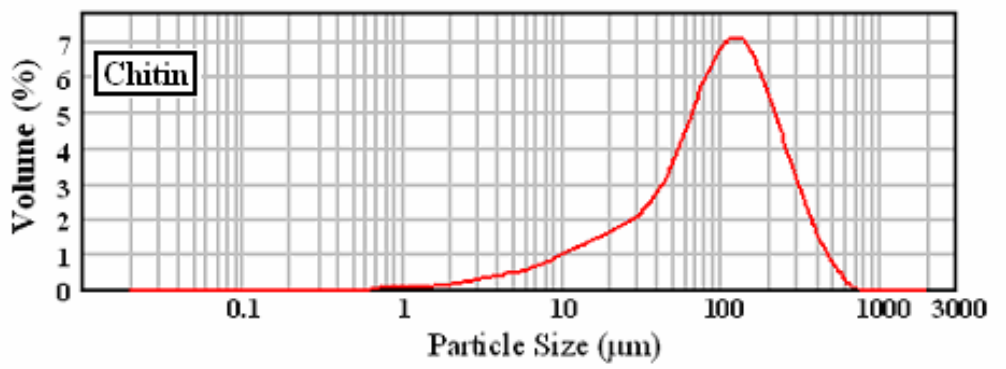

Figure 4.3. Particle size distribution of chitin used in this study.

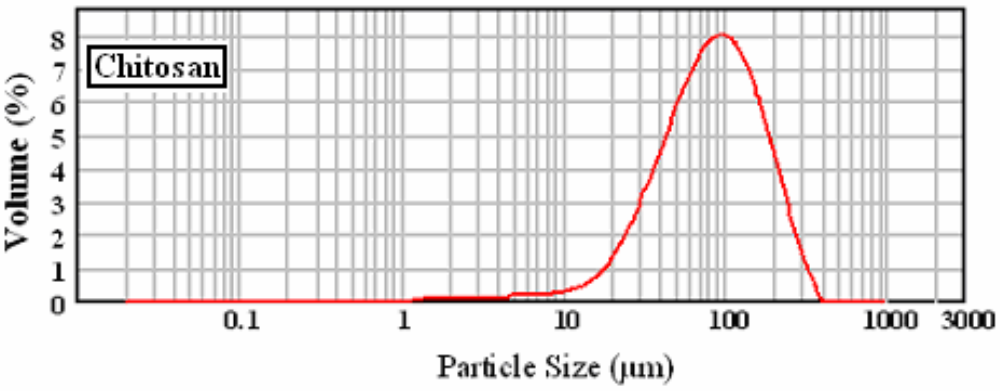

Figure 4.4. Particle size distribution used chitosan used in this study.

4.2.3. Surface Area Analysis

Table 4.3. shows B.E.T and Langmuir surface area, pore volume and average pore size analysis results of chitin and chitosan biopolymers in this study. The values of the corresponding to chitosan appear to be slightly larger than those of chitin. The pore volume, average pore size and B.E.T surface area for chitin to be 0.00308 cm^3/g, 28.96 Å and 4.32 m^2/g, respectively. Comparatively for chitosan, the corresponding values are 0.00332 cm^3/g, 29.87 Å and 4.45 m^2/g, respectively. Alkali deacetylation of chitin to produce chitosan may slightly change the pore size and pore volume of chitosan.

Table 4.3. Surface area, pore volume and average pore size of chitin and chitosan

Biopolymer	BET Surface Area (m^2/g)	Langmuir Surface Area (m^2/g)	Pore Volume (cm^3/g)	Average Pore Size (Å)
Chitin	4.32	16.70	0.00308	28.96
Chitosan	4.45	17.18	0.00332	29.87

4.2.4. Zeta Potential Analysis

The variation of the zeta potential of both chitin and chitosan biopolymers with respect to pH has been studied in order to determine the surface charge of these biopolymers. The results of the zeta potential variation as a function of pH are shown in Figure 4.5. The point of zero charge (PZC) increases from about 6.2 for chitin to 6.9 for chitosan thus confirming a successful modification of chitin to chitosan. Over a wide range of pH up to about 6.2 for chitin and up to 6.9 for chitosan; both biopolymers exhibits a net positive zeta potential attributed to the protonation of the acetamido and amino groups onto chitin and chitosan respectively. Above the PZC, both of chitin and chitosan demonstrate a net negative zeta potential due to the lack of protonation and attechment of OH- ions.

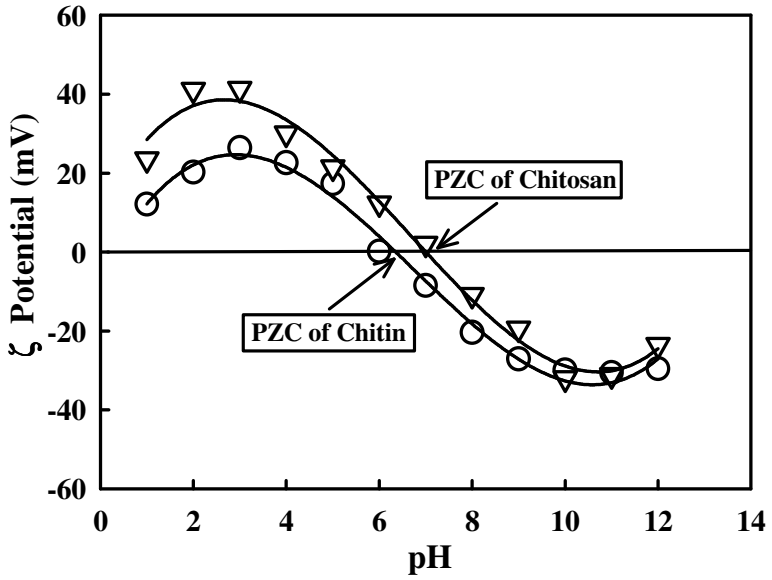

Figure 4.5. Variation of zeta potential versus pH for chitin and chitosan used in this study

4.2.5. X-Ray Diffraction (XRD)

Figure 4.6**.** shows the XRD patterns of used chitin and chitosan biopolymers in this study. Five crystalline reflections were observed in 2θ range of 5-50^{o}. They were indexed as 020, 110, 120, 101 and 130 from lower angle of chitin (Zhang et al. 2005).

$$CrI = \left(\frac{I_{\Theta M} - I_{\Theta A}}{I_{\Theta A}} \right) x100 \qquad (4.1)$$

The degree of crystallinity for chitin and chitosan biopolymers was investigated through X-ray diffractometry, in a process which refers to cellulose as a standard due to the fact that the studied materials did not present the crystallographic planes that could be characterized as crystallinity, but its use is related to natural structural features, which are very close to both biopolymers chitin and chitosan. In this process equation 4.1. was employed to determine the crystallinity index (*CrI*) for chitin and chitosan, and two important peaks due to the maximum intensity in the diffraction at 19^{o} and 9^{o} were considered as shown in Figure 4.6. The first one corresponds to the maximum intensity (I_{110}), and the second to the amorphous diffraction (I_{020}), gave the values 40.1

and 26.8% for chitin and chitosan respectively. These values suggested that when chitin is chemically treated with alkali solution to produce chitosan, a decrease in crystallinity is observed (Lima and Airoldi 2004).

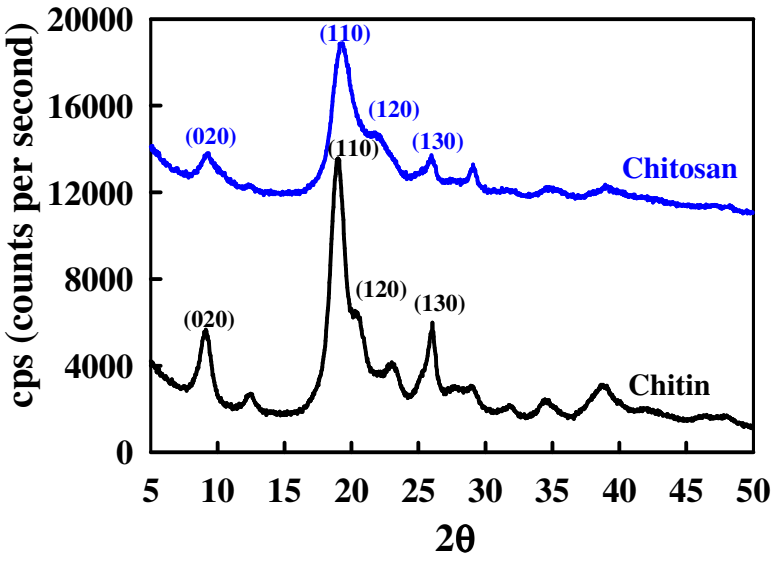

Figure 4.6. XRD diffractogram of used chitin and chitosan

4.2.6. FT-IR Analysis

The attached pendant N-acetyl group of natural chitin were partially removed using alkaline conditions to yield the more reactive derivative chitosan. The infrared spectra for chitin and chitosan biopolymers are shown in Figure 4.7. The common, large and intense bands located at 3700 and 3000 cm^{-1} can be attributed to axial OH and NH group deformations, which are more evident in the chitin spectrum. On the other hand, the absorption band at nearly 3480cm^{-1} can be assigned to the hydrogen bond between OH on carbon 5 of the biopolymer structure with the carbonyl acetamide, attributed to amide II in the 1700 cm^{-1} region (Lima and Airoldi 2004). The other absorption at 3260 and 3100 cm^{-1} are associated with the intermolecular hydrogen bond to acetamide vibration. The axial carbon-hydrogen bond that appears in the 3000-2800 cm^{-1} range is more intense for the chitin biopolymer. The symmetrical and asymmetrical carbon-oxygen-carbon ring gives rise to that bands located at 1051 and 1161 cm^{-1} respectively. Finally, it is important to mention the absorptions at 1420 and 1380 cm^{-1} that are

assigned as CH_2 and CH bending bands, respectively, which appear with low intensity, as shown in Figure. 4.7. (Lima and Airoldi 2004).

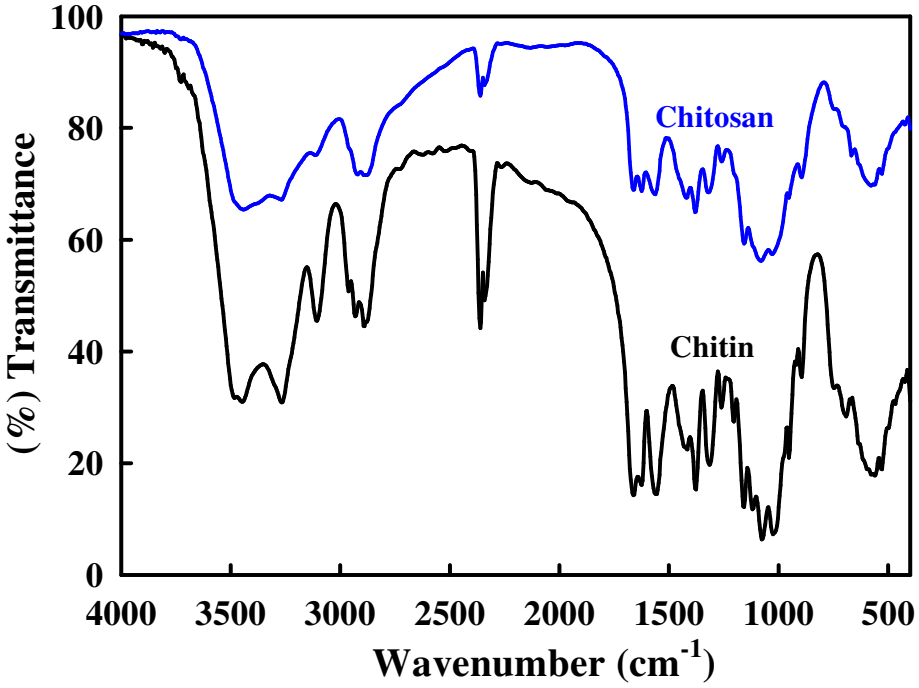

Figure 4.7. Infrared spectrum of used chitin and chitosan

4.2.7. Scanning Electrom Microscope (SEM) Analysis

The morphology of chitin and chitosan biopolymers were studied by Scanning Electron microscope (SEM). SEM images with different magnifications and different areas of chitin and chitosan biopolymers were shown in Figures 4.8. and 4.9. respectively. It was observed that chitin and chitosan biopolymers have porous and fibril structures.

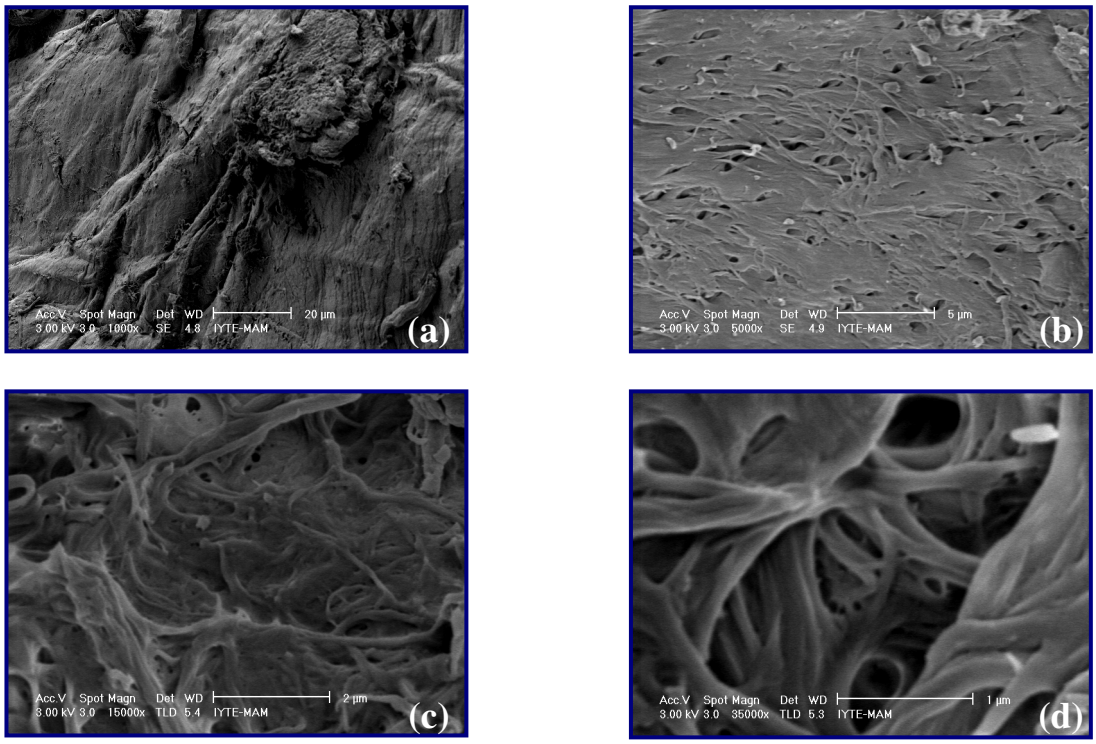

Figure 4.8. SEM images of chitin a) x1000 b) x5000 c) x15000 d) x35000

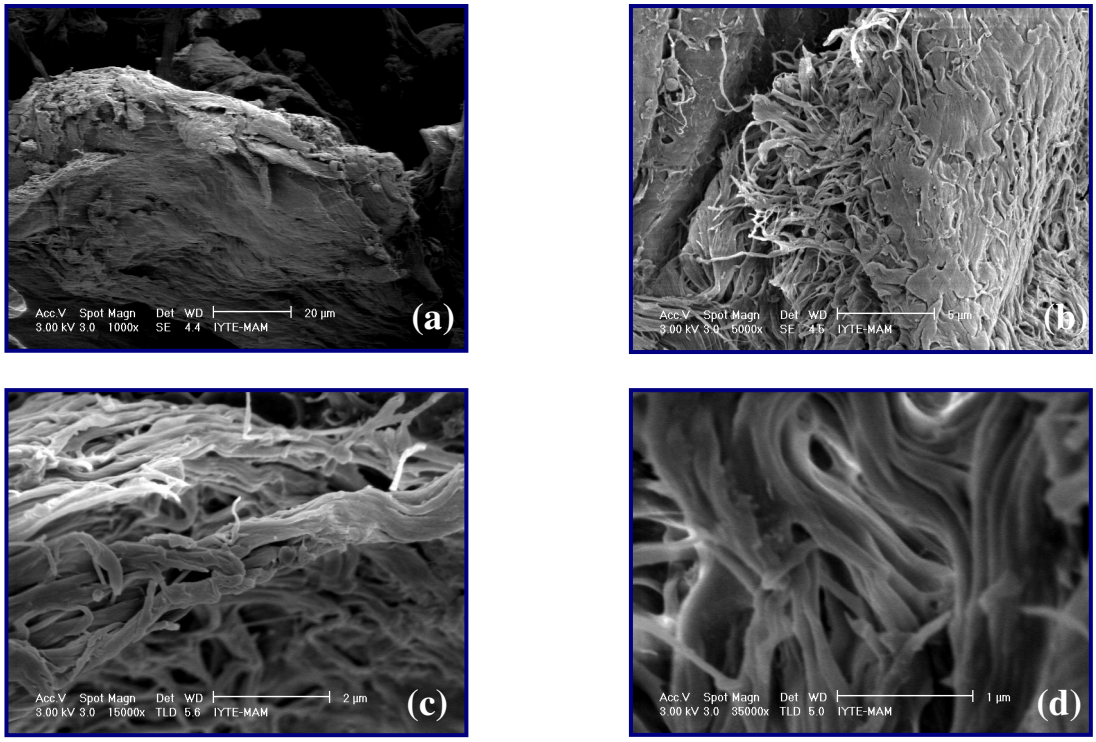

Figure 4.9. SEM images of chitosan a) x1000, b) x5000, c) x15000, d) x35000

4.2.8. Thermal Gravimetric Analysis (TGA/DTA)

Thermal Gravimetric Analysis (TGA/DTA) curves of chitin and chitosan biopolymers are shown in Figure 4.10. A single degradation stage was observed for both biopolymers. The degradation of these biopolymers begin at 288.32°C with 5.07 % weight loss and 261.54°C with 5.49 % chitin and chitosan respectively. Moreover it was observed that at 400°C chitin and chitosan lost about 83.08 and 76.30 % of their masses respectively, Hence it is seen that the thermal behavior of chitin and chitosan biopolymers used in this study are slightly different from each other.

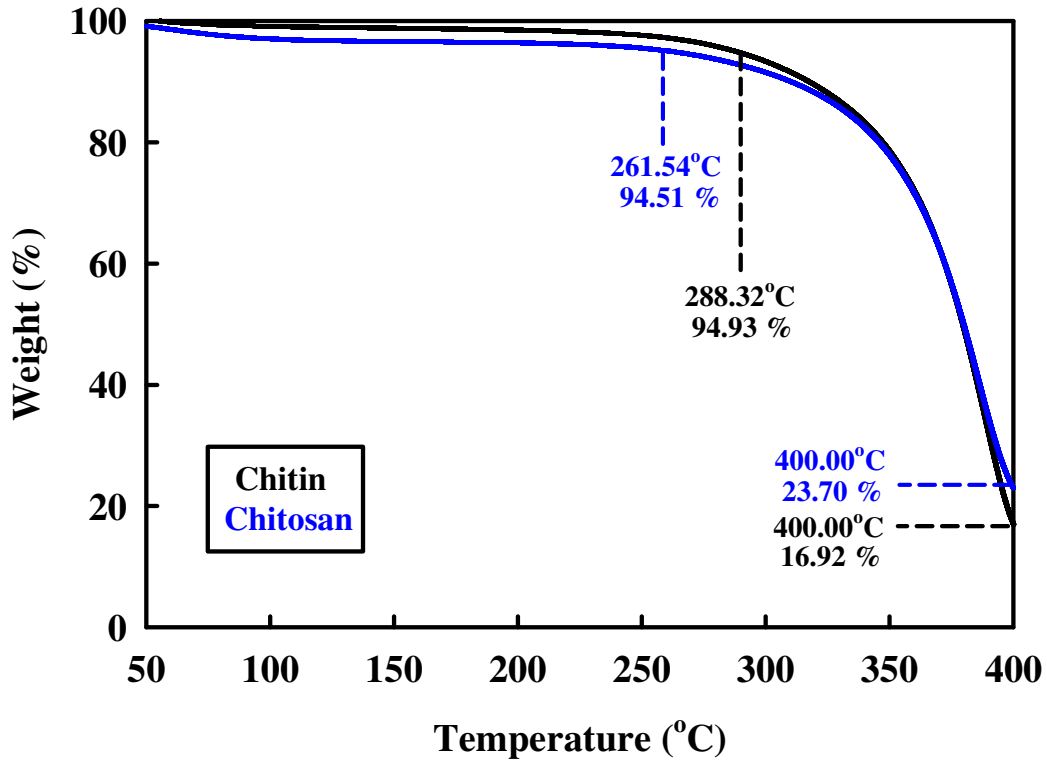

Figure 4.10. TGA curves of chitin and chitosan biopolymers used in this study

4.2.9. The Influence of Analytical Methods on the Determine of the Degree of Deacetylation Value of Chitosan

Various methods have been reported for the determination of degree of deacetylation of chitosan. From the literature, the degree of deacetylation values of chitosan appeared to be highly influenced by the employed analytical method. For this

purpose, three commonly used analytical methods, Infrared Spectroscopy, Elemental Analysis and Potentiometric Titration were employed.

The degree of deacetylation (DD) value of chitosan sample can be determined with elemental analysis using the following equation; (Tolaimate et al. 2000).

$$DD = \left(1 - \frac{C/N - 5.145}{6.186 - 5.145}\right) x100 \tag{2.3}$$

where C : Mass of carbon in chitosan sample

N : Mass of nitrogen in chitosan sample

Another method to determine the degree of decatylation value of chitosan is FT-IR analysis. The degree of deacetylation (DD) of the chitosan samples can be determined by infrared spectroscopic analysis using the following equation; (Baxter et al. 1992)

$$DD = 100 - \left[\frac{(A_{1655}/A_{3450})x100}{1.33}\right] \tag{2.1}$$

where A_{1655} : Absorbance of the amide-I band

A_{3450} : Absorbance of hydroxyl band

The deacetylation degree of chitosan can be also determined by potentiometric titration. Chitosan is dissolved in a known excess of hydrochloric acid. From the titration of this solution with sodium hydroxide solution, a curve with two inflection points are obtained. The diffeerence between the volumes of these two inflection points correspond to the acid consumption for the salification of amine groups and permitted the determination of chitosan's deacetylation degree using the following equation; (Tolaimate et al. 2000).

$$\%NH_2 = 16.1(V_2 - V_1)x\frac{M_b}{W} \tag{2.4}$$

where V_1 : Base volume for the first inflection point (mL)

V_2 : Base volume for the second infection point (mL)

Mb : Base molarity (g/mol)

W : Weight of the chitosan sample

The degree of deacetylation values determined with different instrumental and analytical methods for chitosan sample and results are shown in Table 4.4. The table shows that the degree of deacetylation value of chitosan sample is directly some what affected by instrumental and analytical technique. This table indicates that potentiometric titration method gives the highest degree of deacetylation while FT-IR analysis gives the lowest degree of deacetylation value for chitosan sample applied in this study.

Table 4.4. Degree of deacetylation (DD) values of chitosan biopolymer as determined by different analytical methods.

Analytical Method	**Degree of Deacetylation (%)**
IR Spectroscopy	79.6±1
Potentiometric Titration	84.3±2
Elemental Analysis	82.9 ±1

4.3. Metals

4.3.1. Speciation of Metal Ions in Water as a Function of pH

pH is a significant factor for determining the form of the metallic species in aqueous media. When determining various metal species, equilibrium models for many metals are constructed using the set of equations used for simple acid-base calculations. First, total concentrations of all components are stated, then all possible species are identified, and mass balances, charge balance and equilibrium equations are written.

However, it is time wasting to solve these equations manually. Alternatively, Visual Minteq Version 2.15. can be used. After obtaining the form of the metallic species, graphs were drawn for copper, lead, cadmium and nickel concentrations as a function of pH and given in Figures 4.11, 4.12, 4.13. and 4.14. respectively. The pH is one of the principal factors influencing the adsorption process of metal ions, as it determines the magnitude and sign of the charge on ions.

Figure 4.11. gives the distribution of copper species as a function of pH for 100 mg/L concentration. The dominant specie is Cu(II) below the pH of 6. It is seen that there are negatively and positively charged Cu species between pH: 4 and 12. For pH values between 4 and 11, copper and its species are positively charged, however, for pH values higher than 11 they are negatively charged.

Figure 4.12. gives the distribution of lead species as a function of pH for 100 mg/L concentration. In case of low pH(<6), positively charged lead (II) species are dominant. In case of high pH values (pH 6-14), however, there are several lead species with different charges.

Figure 4.13. gives the distribution of cadmium species as a function of pH for 100 mg/L concentration. According to this figure, the divalend form of Cd (II) is dominant for pH below 7. In case of high pH (pH 8-14), however, there are several cadmium species with different charges.

Figure 4.14. gives the distribution of nickel species as a function of pH for 100 mg/L concentration. In case of low pH (<8), positively charged , nickel (II) species are dominant. In case of high pH values(pH 8-14), however, there are several nickel species with different charges.

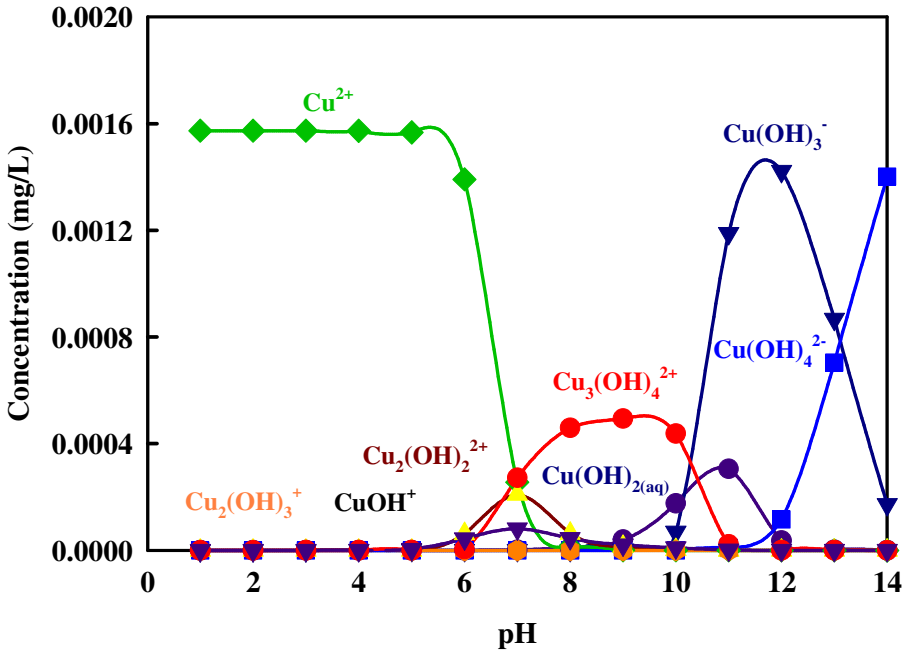

Figure 4.11. Chemical speciation of Copper (100 mg/L) in water as a function of pH.

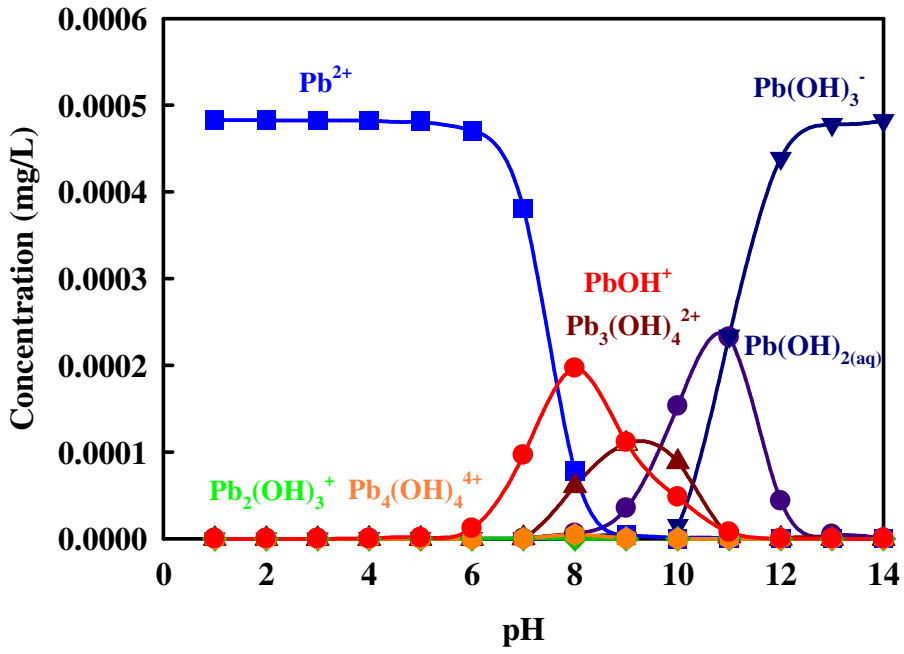

Figure 4.12. Chemical speciation of Lead (100 mg/L) in water as a function of pH.

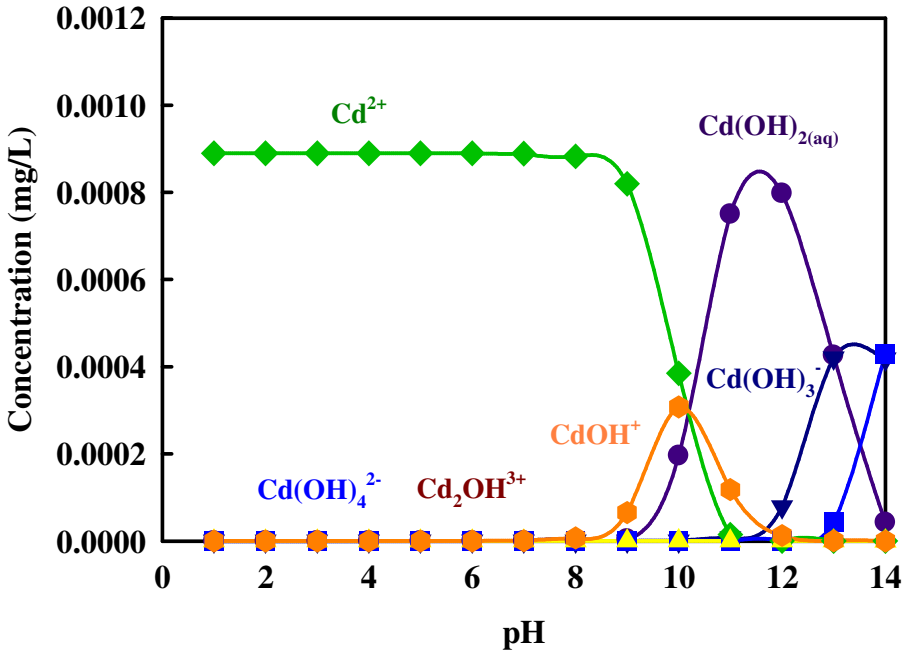

Figure 4.13. Chemical speciation of Cadmium (100 mg/L) in water as a function of pH.

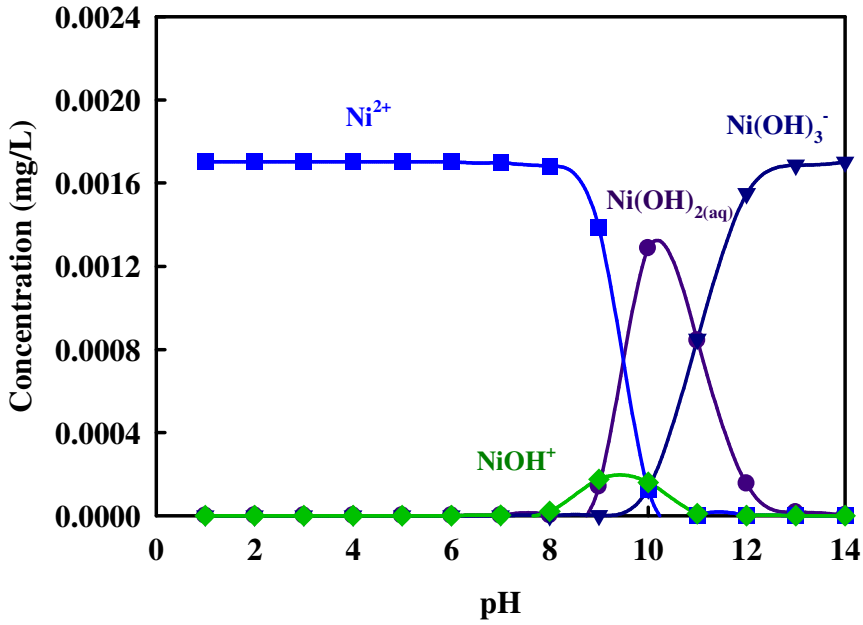

Figure 4.14. Chemical speciation of Nickel (100 mg/L) in water as a function of pH.

4.4. Adsorption Studies

Various operational parameters were tested to determine adsorption characteristics of chitin and chitosan biopolymers for heavy metal ions adsorption from aqueous solutions. These include solid/liquid ratio (S/L), pH, contact time, metal ion concentration and temperature.

4.4.1. Effect of Solid Liquid (S/L) Ratio

The effect of solid/liquid ratio for Cu^{2+}, Pb^{2+}, Cd^{2+} and Ni^{2+} ions adsorption on chitin and chitosan biopolymer were examined. In these experiments, operational parameters were kept constant (T= 298.15 K, C_o= 100 mg/L, pH= 6-7, time= 24 hours). The results are presented in Figures 4.15 and 4.16. Generally, it is observed that heavy metal ion removal increases with increasing solid/liquid ratios for chitin and chitosan biopolymers. Increasing solid/liquid ratio leads to an increase in the number of active sites available for adsorption and thus fixation of a large amount of solute ions as long as an enough number of these ions is available in solution in contact with solid.

Figures 4.15. and 4.16. show the difference between adsorption capacities of chitin and chitosan for all the metal ions (Cu^{2+}, Pb^{2+}, Cd^{2+}, Ni^{2+}) used. However the adsorption trend of metal ions seem to follow the order $Cu^{2+} > Pb^{2+} > Cd^{2+} > Ni^{2+}$, in both cases.

It is observed that the solid/liquid ratio at which all the metal ion species (100 mg/L) removed from aqueous solution is different for chitin and chitosan biopolymers. While it is 0.06 g/mL for chitin, it is only 0.02 mg/L for chitosan. This might be due to the presence of larger amount of amino groups instead of acetamido groups.

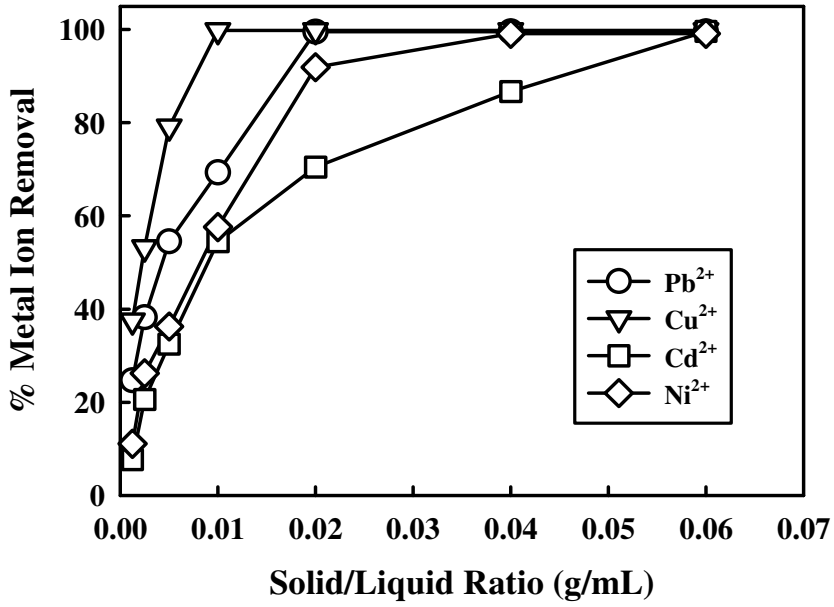

Figure 4.15. Effect of S/L ratio on adsorption of heavy metal ions for chitin (C_o= 100 mg/L, pH= natural, temperature= 298.15 K, agitation rate= 600 rpm, agitation time= 24h).

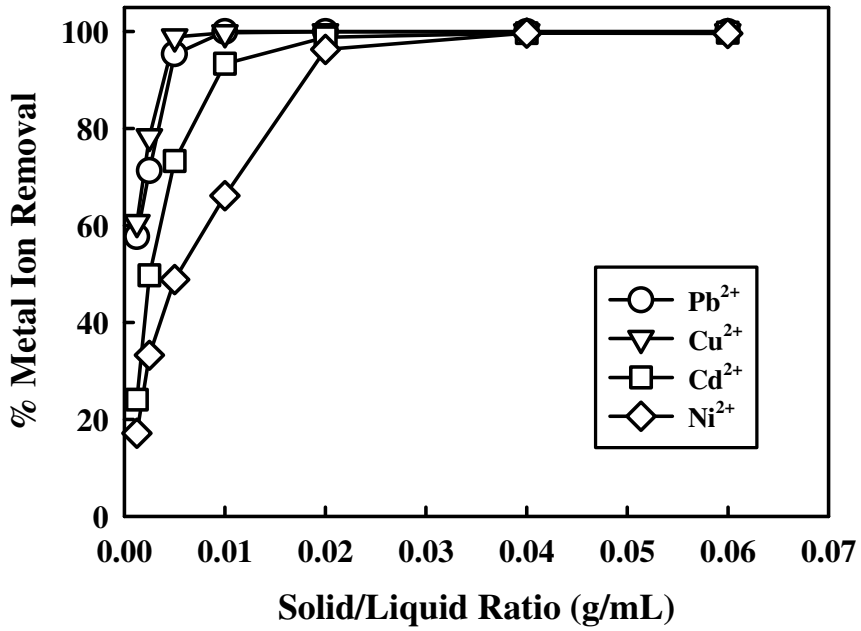

Figure 4.16. Effect of S/L ratio on adsorption of heavy metal ions for chitosan (C_o= 100 mg/L, pH= natural, temperature= 298.15 K, agitation rate= 600 rpm, agitation time= 24h).

4.4.2. Effect of pH

The effect of pH on metal ion adsorption by chitin and chitosan biopolymers was investigated and the results are presented in Figures 4.17. and 4.18. The initial pH of the metal ion solutions were changed between 2 and 7. As discussed previously, the PZC of chitin and chitosan was obtained to be 6.2 and 6.7, respectively. As seen from Figures 4.17. and 4.18. adsorption of metal ions increases with an increase in pH where the charge of surface decreases also within the studied pH range, the best adsorption was obtained at pH values close to PZC.

At low pH values adsorption is low where surfaces have strong positive charge similar to that of the ions. However there is still adsorption eventhough there is an repulsion between surfaces and metal ions. This might indicate a limited contribution of chemical adsorption that is caused by the unpaired electrons of nitrogens at acetamido and amino functional groups of chitin and chitosan.

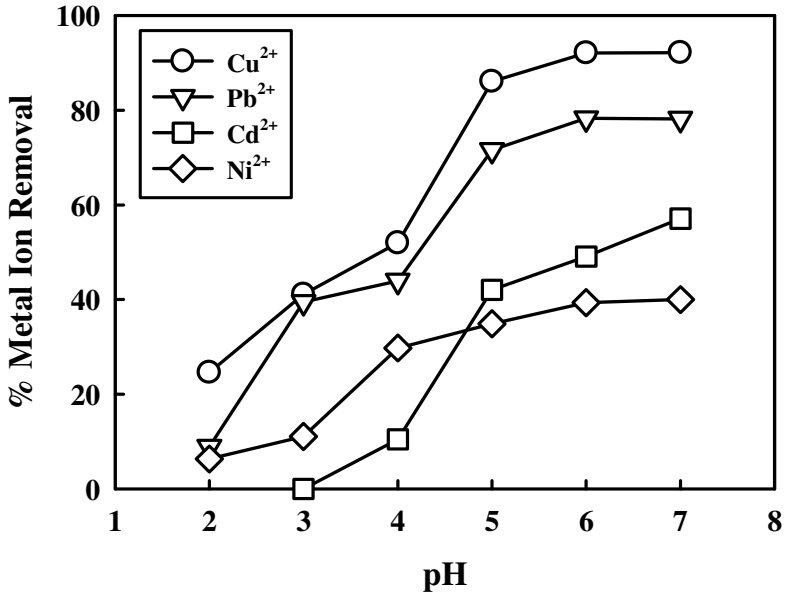

Figure 4.17. Effect of initial pH on adsorption of heavy metal ions for chitin (C_o= 100 mg/L, S/L= 0.01 g/mL, temperature= 298.15 K, agitation rate= 600 rpm, agitation time= 24h).

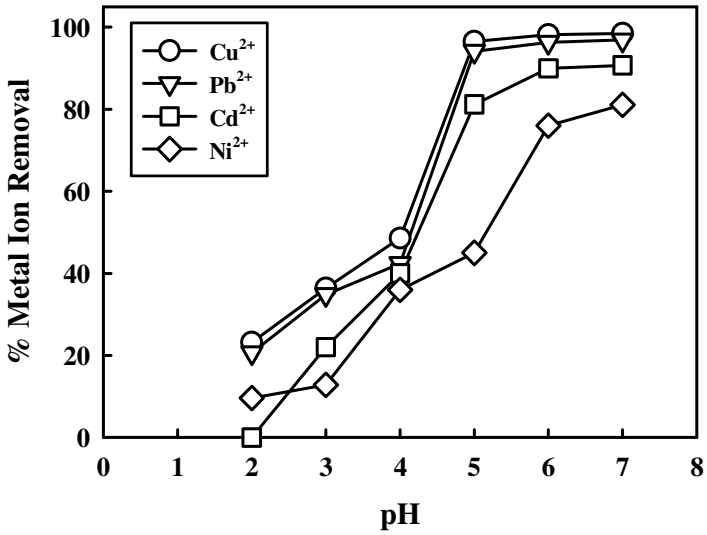

Figure 4.18. Effect of initial pH on adsorption of heavy metal ions for chitosan (C_o= 100 mg/L, S/L= 0.01 g/mL, temperature= 298.15 K, agitation rate= 600 rpm, agitation time= 24h).

4.3.3. Effect of Contact Time

Contact time is an important parameter because this factor determines the adsorption kinetics of an adsorbate at a given initial concentration of the adsorbate. The effect of contact time on the heavy metal ions adsorption by chitin and chitosan biopolymers was investigated for 24 hours. The kinetic studies were carried out for different initial concentrations 100, 500 and 1000 mg/L for Cu^{2+}, Pb^{2+}, Cd^{2+} and Ni^{2+} ions on chitin and chitosan biopolymers at 298.15 K and 328.15 K.

4.4.3.1. Copper (Cu^{2+})

Figures 4.19. a-b and 4.20. a-b show the amount of Cu^{2+} ion adsorbed on chitin and chitosan biopolymers as a function of time and concentration at 298.15 and 328.15 K respectively.

In Figure 4.19. a-b it was observed that the uptake amount of Cu^{2+} ions on chitin increases rapidly with increasing of the contact time 0 to 180 minute and then reaches the equilibrium after 480 minutes. A similar trend was observed for the remaining the initial Cu^{2+} concentrations (500 and 1000 mg/L) studied and at 328.15 K. The initial rapid phase is due to the presence of large number of vacant sites and , as a

result there exist increased the concentration gradient between adsorbate in solution and adsorbate in the adsorbent surface. As time proceeds, this concentration is reduced due to the accumulation of Cu^{2+} ions on the vacant sites, leading to decrease in gradient the adsorption rate after 180 to 480 minute.

In Figure 4.20. a-b it was observed again that the uptake of Cu^{2+} ions increases with increasing of the contact time 0 to 180 minute and then reaches equilibrium after 240 minutes for chitosan biopolymer at 298.15 K. A similar trend is observed for the initial Cu^{2+} ion concentrations of 500 and 100 mg/L studied at 328.15 K. Figures 4.19. a-b and 4.20. a-b show that the uptake of Cu^{2+} ion on chitosan biopolymer is greater in magnitude than chitin biopolymer at all concentrations and temperatures.

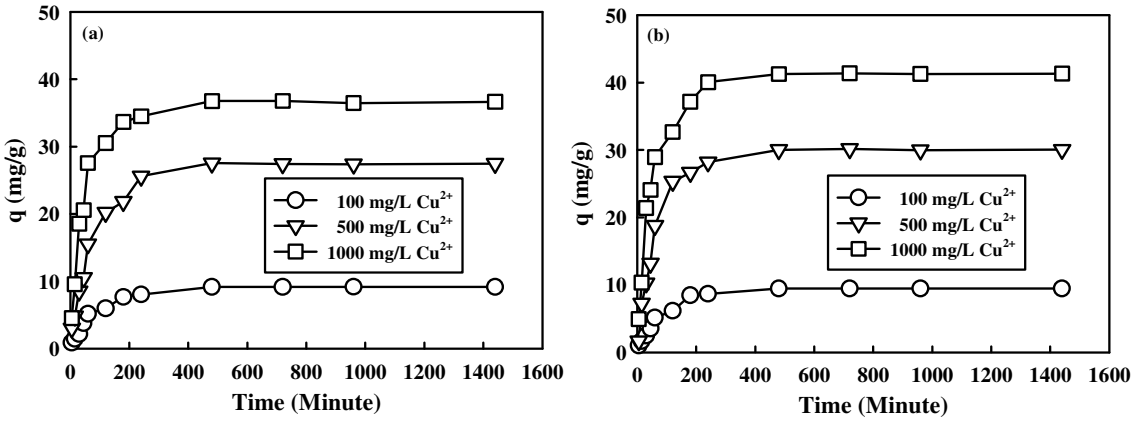

Figure 4.19. Effect of contact time on adsorption of Cu^{2+} ion for chitin a) 298.15 K b) 328.15 K (pH= 6, S/L= 0.01 g/mL, agitation rate= 600 rpm).

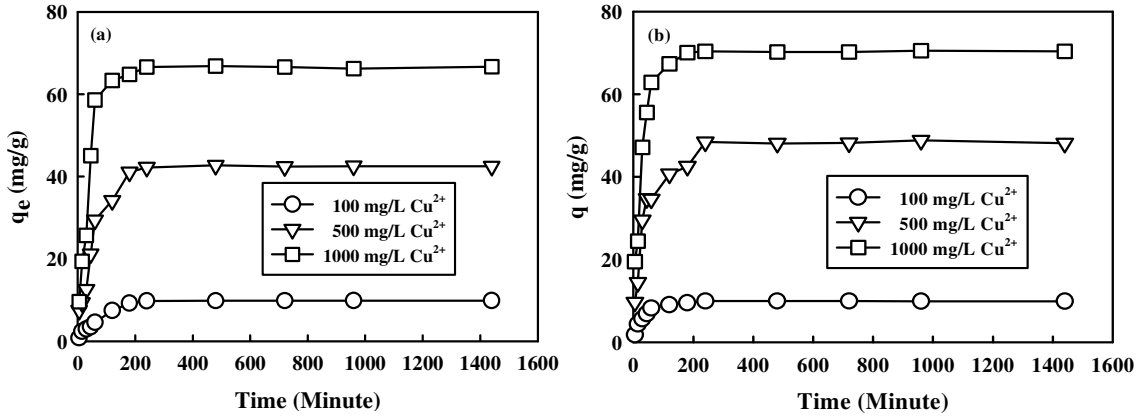

Figure 4.20. Effect of contact time on adsorption of Cu^{2+} ion for chitosan a) 298.15 K b) 328.15 K (pH= 6, S/L= 0.01 g/mL, agitation rate= 600 rpm).

4.4.3.2. Lead (Pb^{2+})

Figures 4.2. a-b and 4.22. a-b show the effect of contact time, concentration and temperature on adsorption of Pb^{2+} ions on chitin and chitosan biopolymers, respectively.

In Figures 4.21. a-b it was observed that Pb^{2+} ions is gradually adsorbed and nearly 480 and 360 minutes are enough to reach equilibrium for chitin and chitosan at 298.15 and 328.15 K respectively. The uptake of Pb^{2+} is increasing with temperature and concentration for chitin biopolymer. Increasing the uptake amount of Pb^{2+} with temperature show the endothermic nature of adsorption process.

As shown in Figures 4.22. a-b Pb^{2+} ions are adsorbed by chitosan gradually and this trend is similar to that on chitin. Moreover, the uptake extent of Pb^{2+} on chitosan is greater than chitin and increases with increase in concentration and temperature.

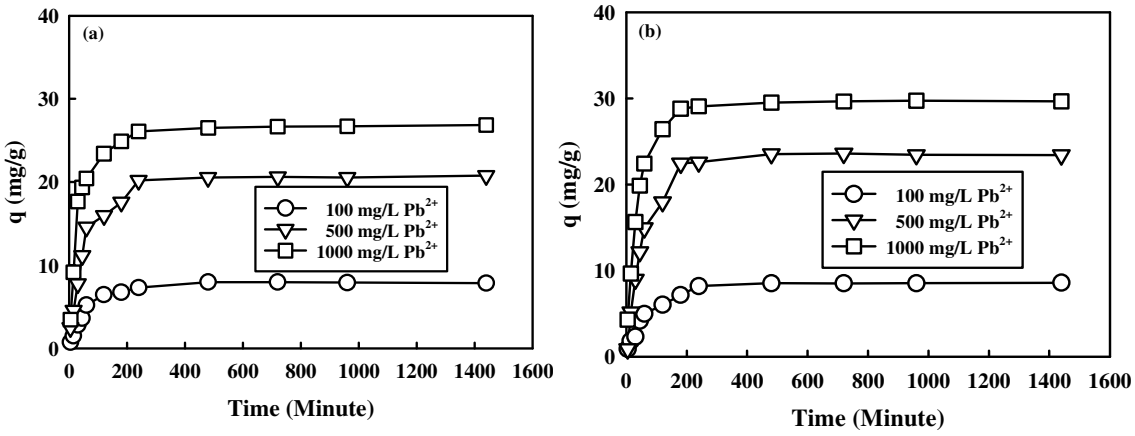

Figure 4.21. Effect of contact time on adsorption of Pb^{2+} ion for chitin a) 298.15 K b) 328.15 K (pH= 6, S/L= 0.01 g/mL, agitation rate= 600 rpm).

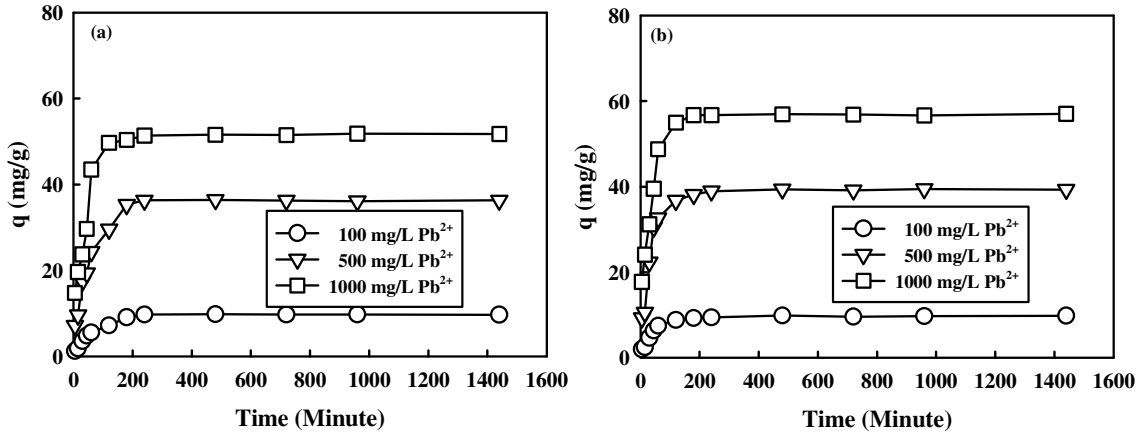

Figure 4.22. Effect of contact time on adsorption of Pb^{2+} ion for chitosan a) 298.15 K b) 328.15 K (pH= 6, S/L= 0.01 g/mL, agitation rate= 600 rpm).

4.4.3.3. Cadmium (Cd^{2+})

The effect of contact time on adsorption of Cd^{2+} ion by chitin and chitosan was investigated as a function of temperature and concentration. Figs. 4.23. a-b and 4.24. a-b show the results of the relevant experiments.

As demonstrated in Figure 4.23. a-b, Cd^{2+} ions are gradually adsorbed by chitin nearly 480 minutes required reach equilibrium at 298.15 and 328.15 K. According to Fig. 4.23. a-b it is observed that Cd^{2+} ions are also adsorbed by chitosan gradually similar trend to that on chitin. Moreover, uptake amount of Cd^{2+} on chitosan is significantly greater than chitin, and approximately 240 minutes is enough for adsorption of Cd^{2+} ion to reach equilibrium.

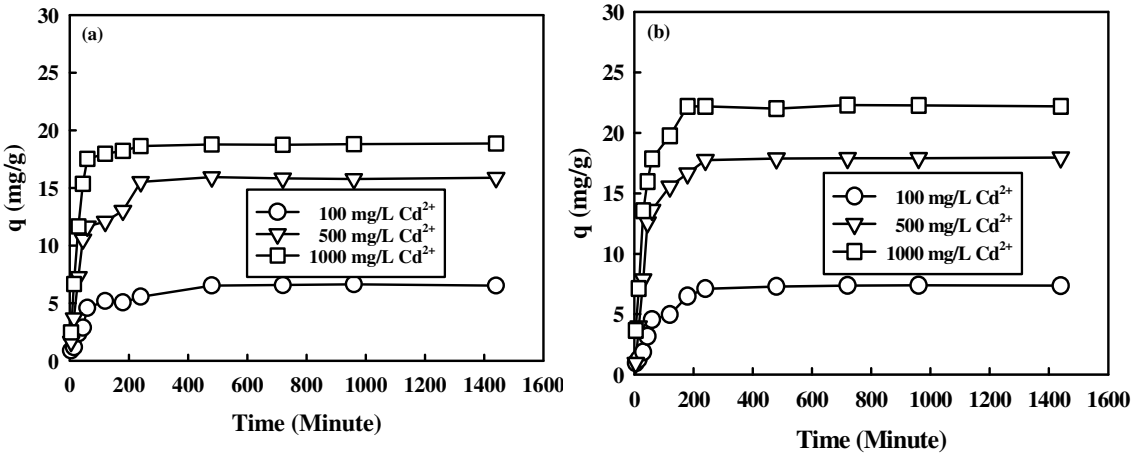

Figure 4.23. Effect of contact time on adsorption of Cd^{2+} ion for chitin a) 298.15 K b) 328.15 K (pH= 7, S/L= 0.01 g/mL, agitation rate= 600 rpm).

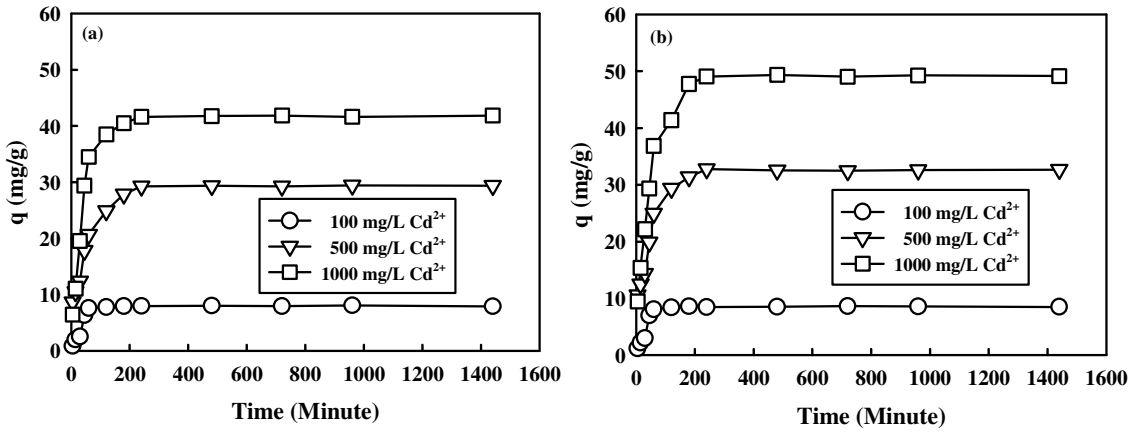

Figure 4.24. Effect of contact time on adsorption of Cd^{2+} ion for chitosan a) 298.15 K b) 328.15 K (pH= 7, S/L= 0.01 g/mL, agitation rate= 600 rpm).

4.4.3.4. Nickel (Ni^{2+})

Figures 4.25. a-b and 4.26. a-b show the effect of contact time on the extent of adsorption of Ni^{2+} ion at different concentrations and temperatures on chitin and chitosan biopolymers. In Figures 4.25. a-b and 4.26. a-b it is seen that Ni^{2+} ions are gradually adsorbed by chitin and chitosan biopolymer at 180 minutes and then adsorbed Ni^{2+} ions increased nearly 480 minutes on chitin and chitosan. Approximately 480 minute is enough for the adsorption of Ni^{2+} ions, to reach equilibrium on chitin and chitosan at 298.15 K and 328.15 K, respectively.

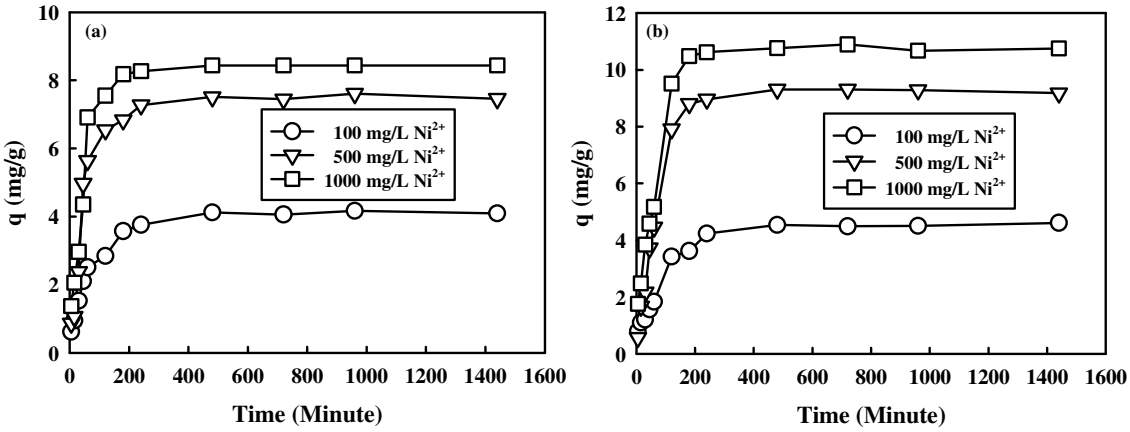

Figure 4.25. Effect of contact time on adsorption of Ni^{2+} ion for chitin a) 298.15 K b) 328.15 K (pH= 6, S/L= 0.01, agitation rate= 600 rpm).

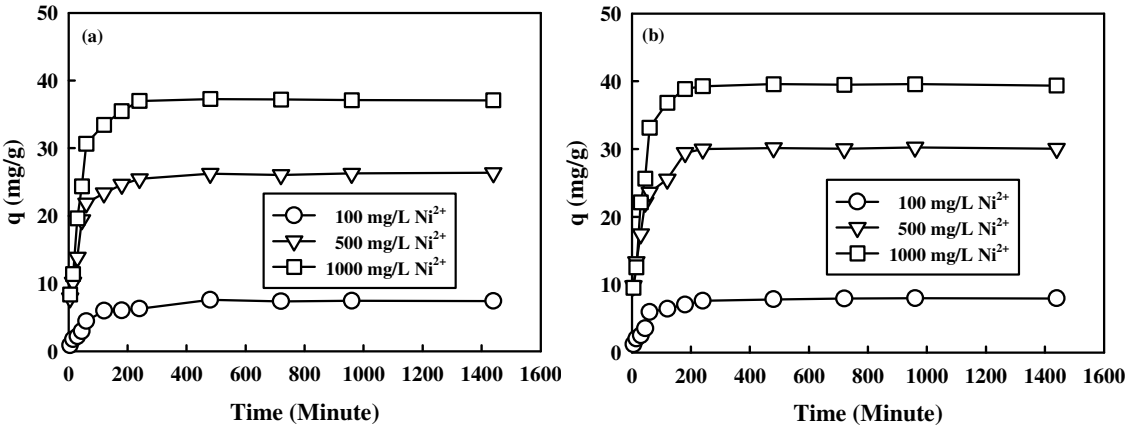

Figure 4.26. Effect of contact time on adsorption of Ni^{2+} ion for chitosan a) 298.15 K b) 328.15 K (pH= 6, S/L= 0.01 , agitation rate= 600 rpm).

4.4.3.5. Determination of Rate Parameters

The adsorption kinetic of Cu^{2+}, Pb^{2+}, Cd^{2+} and Ni^{2+} ions were modeled using the pseudo first order and pseudo second order equations. The first order rate equation of Lagergren is one of the most widely used for the adsorption of solute from a liquid solution. It is explained in Chapter 2 and represented as follows: (Ho and McKay 1998, Sivaraj 2001)

$$\ln\left(\frac{q_e}{q_e - q}\right) = k_1 T \tag{2.16}$$

Another important kinetic model is Ho pseudo second order kinetic model which is discussed in Chapter 2 and linear form of this model is given by following equation; (Ho et al. 2001).

$$\frac{t}{q} = \frac{1}{k_2 q_e^2} + \frac{1}{q_e} t \tag{2.19}$$

Thus the pseudo first order rate constants k_1 (min^{-1}) and pseudo second order rate constants k_2 ($g/mg^{1-}min^{1-}$) for heavy metal ions adsorption on chitin and chitosan biopolymers were calculated using the equation 2.16 and 2.19, and discussed in the following sections.

4.4.3.5.1. Copper (Cu^{2+})

Table 4.5. shows the pseudo first order and pseudo second order rate constants of Cu^{2+} ion adsorption by chitin and chitosan biopolymers respectively. As seen in the table, the linear correlation coefficients indicate that the pseudo second order model provides better description of the adsorption kinetics of Cu^{2+} ions on both biopolymers and rate constant is increased with temperature for each concentrations. The linear fits of pseudo first order and pseudo second order kinetics models for Cu^{2+} ion adsorption onto chitin and chitosan biopolymers are showed in Figures 4.27. a-b, 4.28. a-b, 4.29. a-b, and 4.30. a-b.

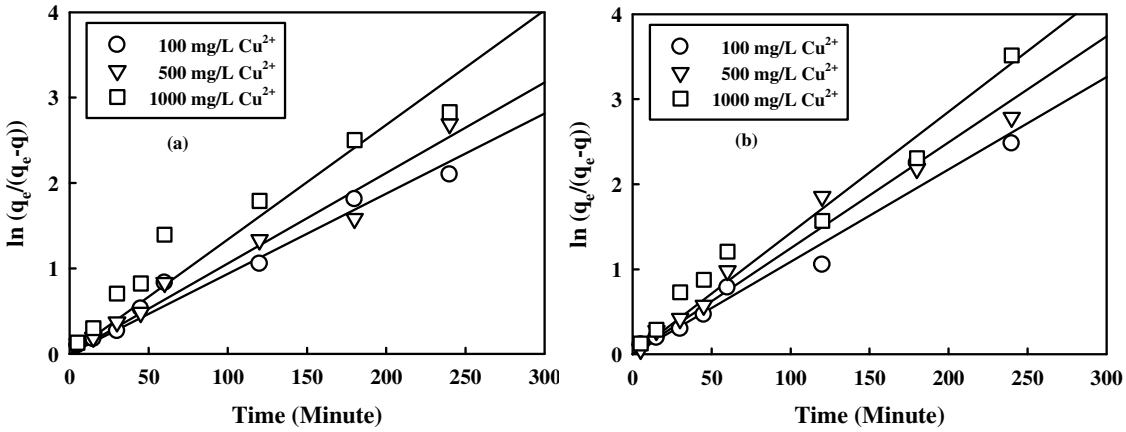

Figure 4.27. Pseudo first order kinetic plots for Cu^{2+} for chitin a) 298.15 K b) 328.15 K.

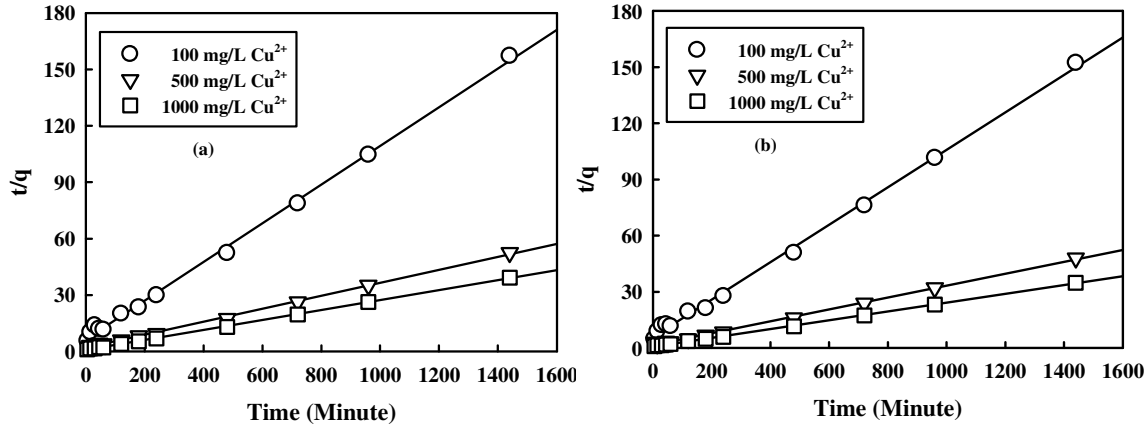

Figure 4.28. Pseudo second order kinetic plots of Cu^{2+} for chitin a) 298.15 K b) 328.15 K.

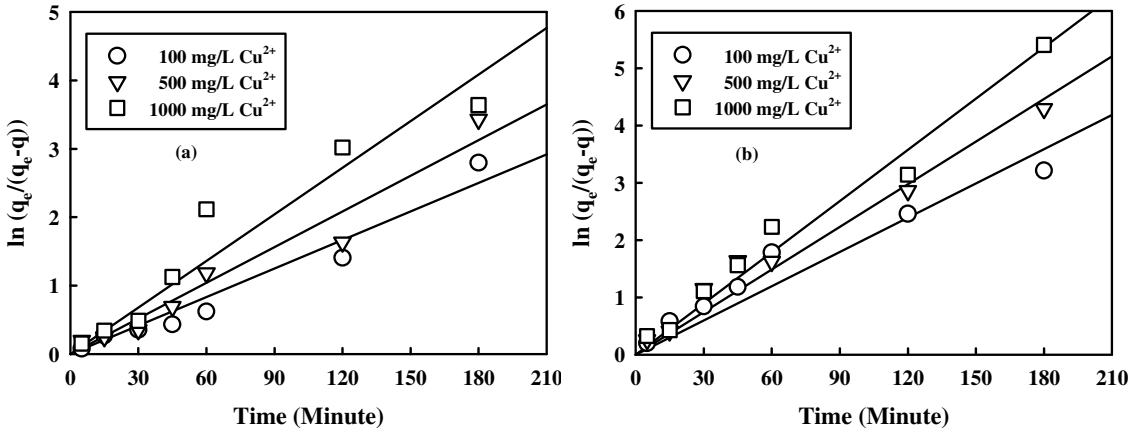

Figure 4.29. Pseudo first order kinetic plots of Cu^{2+} for chitosan a) 298.15 K b) 328.15 K.

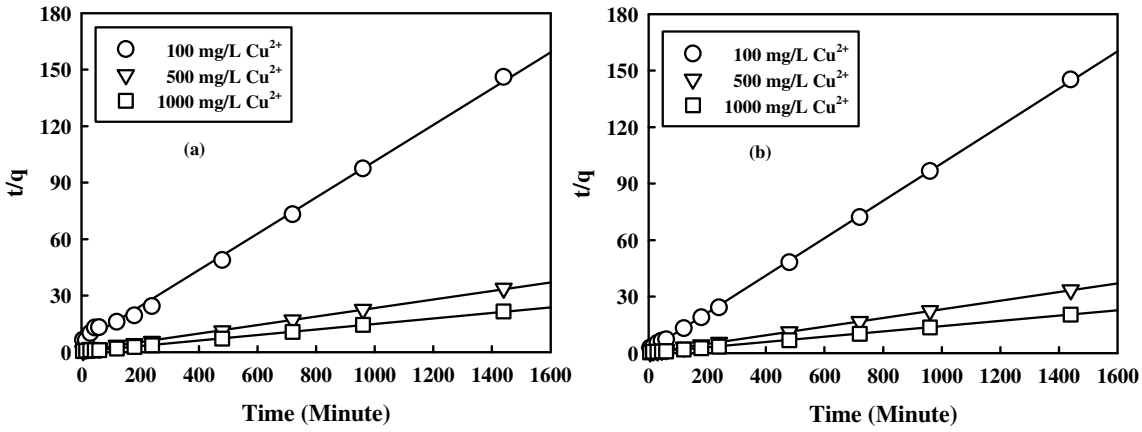

Figure 4.30. Pseudo second order kinetic plots of Cu^{2+} on chitosan a) 298.15 K b) 328.15 K.

Table 4.5. Pseudo first order and pseudo second order rate constants for the adsorption of Cu^{2+} on chitin and chitosan.

Adsorbent	**T (K)**	**C_o (mg/L)**	**k_1 (min^{1-})**	**R_1^2**	**k_2 ($g/mg^{1-}\ min^{1-}$)**	**R_2^2**
Chitin	298.15	100	0.0094	0.9672	$1.6431x10^{-3}$	0.9978
	328.15	100	0.0107	0.9686	$2.5961x10^{-3}$	0.9977
	298.15	500	0.0106	0.9670	$0.6441x10^{-3}$	0.9984
	328.15	500	0.0125	0.9664	$0.6762x10^{-3}$	0.9981
	298.15	1000	0.0134	0.9005	$0.7775x10^{-3}$	0.9995
	328.15	1000	0.0143	0.9578	$0.9307x10^{-3}$	0.9995
Chitosan	298.15	100	0.0139	0.9557	$0.6529x10^{-3}$	0.9972
	328.15	100	0.0199	0.8979	$1.8229x10^{-3}$	0.9998
	298.15	500	0.0174	0.9547	$0.5411x10^{-3}$	0.9982
	328.15	500	0.0248	0.9574	$1.8052x10^{-3}$	0.9997
	298.15	1000	0.0227	0.9218	$0.6973x10^{-3}$	0.9991
	328.15	1000	0.0298	0.9735	$1.2679x10^{-3}$	0.9998

4.4.3.5.2. Lead (Pb^{2+})

The values of pseudo first order and pseudo second order rate constants are given in Table 4.6 together with the linear correlation coefficients for Pb^{2+} ion adsorption on chitin and chitosan. Again better correlation is obtained using the pseudo second order model and rate constant of adsorption is increased with temperature for all concentrations..

The linear plots of pseudo first order and second order kinetics models for Pb^{2+} adsorption onto chitin and chitosan biopolymers are shown in Figures 4.31. a-b, 4.32. a-b, 4.33. a-b and 4.34. a-b.

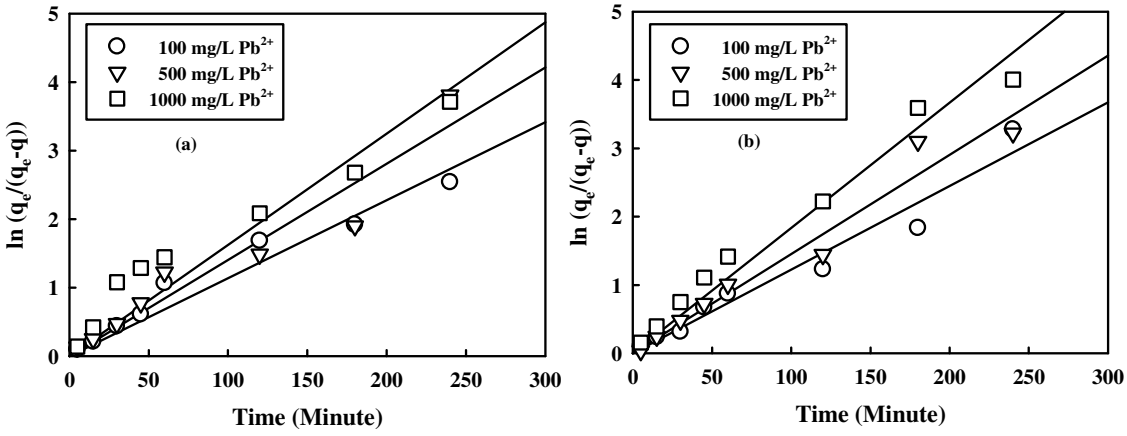

Figure 4.31. Pseudo first order kinetic plots of Pb^{2+} for chitin a) 298.15 K b) 328.15 K.

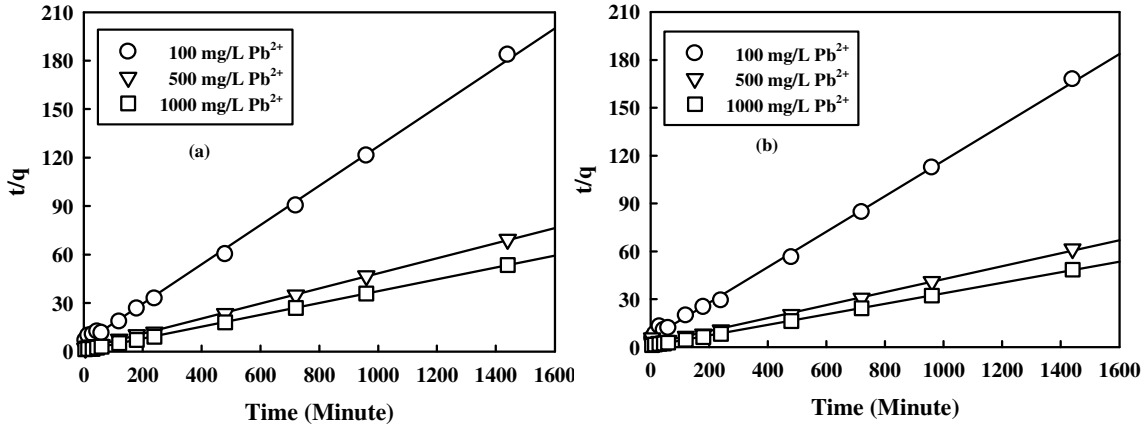

Figure 4.32. Pseudo second order kinetic plots of Pb^{2+} for chitin a) 298.15 K b) 328.15 K.

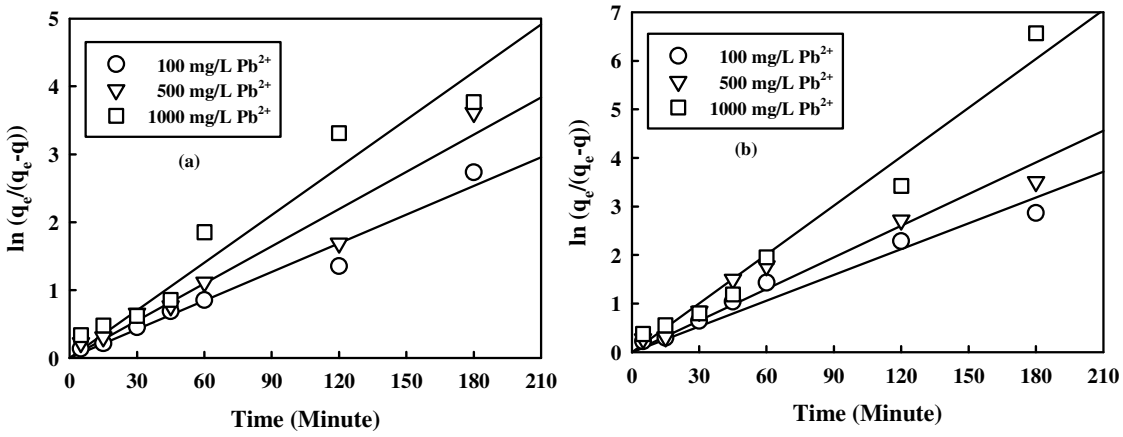

Figure 4.33. Pseudo first order kinetic plots of Pb^{2+} for chitosan a) 298.15 K b) 328.15 K.

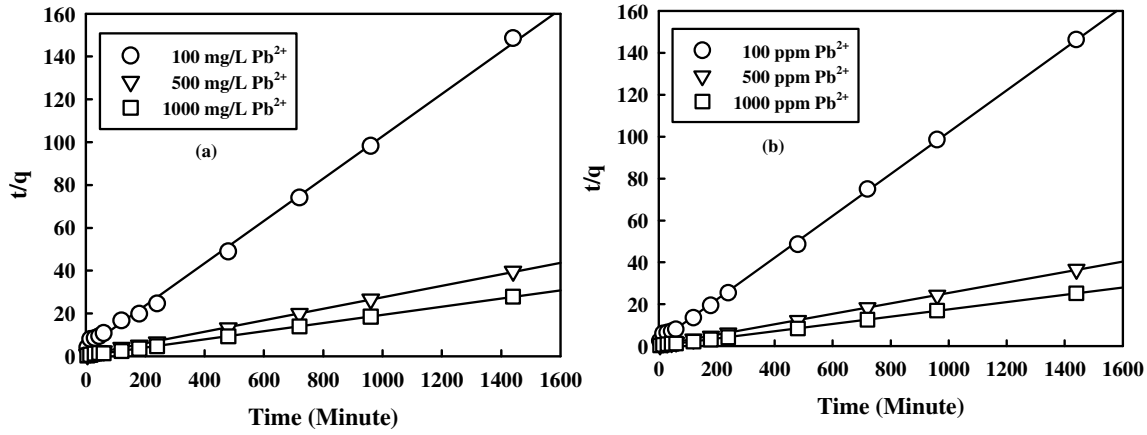

Figure 4.34. Pseudo second order kinetic plots of Pb^{2+} for chitosan a) 298.15 K b) 328.15 K.

Table 4.6. Pseudo first order and pseudo second order rate constants for the adsorption of Pb^{2+} on chitin and chitosan.

Adsorbent	T (K)	C_o (mg/L)	k_1 (min^{1-})	R_1^2	k_2 (g/mg^{1-} min^{1-})	R_2^2
Chitin	298.15	100	0.0114	0.9416	2.2298 x10^{-3}	0.9986
	328.15	100	0.0122	0.9553	2.8592 x10^{-3}	0.9986
	298.15	500	0.0140	0.9209	0.5409 x10^{-3}	0.9993
	328.15	500	0.0145	0.9607	2.7802 x10^{-3}	0.9952
	298.15	1000	0.0163	0.8950	0.9319 x10^{-3}	0.9998
	328.15	1000	0.0183	0.9670	1.1419 x10^{-3}	0.9997
Chitosan	298.15	100	0.0141	0.9664	2.5149 x10^{-3}	0.9983
	328.15	100	0.0177	0.9413	4.2760 x10^{-3}	0.9995
	298.15	500	0.0183	0.9527	1.0254 x10^{-3}	0.9992
	328.15	500	0.0217	0.9183	1.5310 x10^{-3}	0.9995
	298.15	1000	0.0234	0.9369	1.0849 x10^{-3}	0.9995
	328.15	1000	0.0310	0.9689	1.3804 x10^{-3}	0.9997

4.4.3.5.3. Cadmium (Cd^{2+})

The values of pseudo first order and second order rate constants of Cd^{2+} ion adsorption by chitin and chitosan are given in Table 4.7. Like in the cases of the Cu^{2+} and Pb^{2+}, the pseudo second order model is seem to provide better correlation with the adsorption data of Cd^{2+} and rate of adsorption increased with temperature for all concentrations. The corresponding linear fits are shown in Figures. 4.35. a-b, 4.36. a-b, 4.37. a-b and 4.38. a-b.

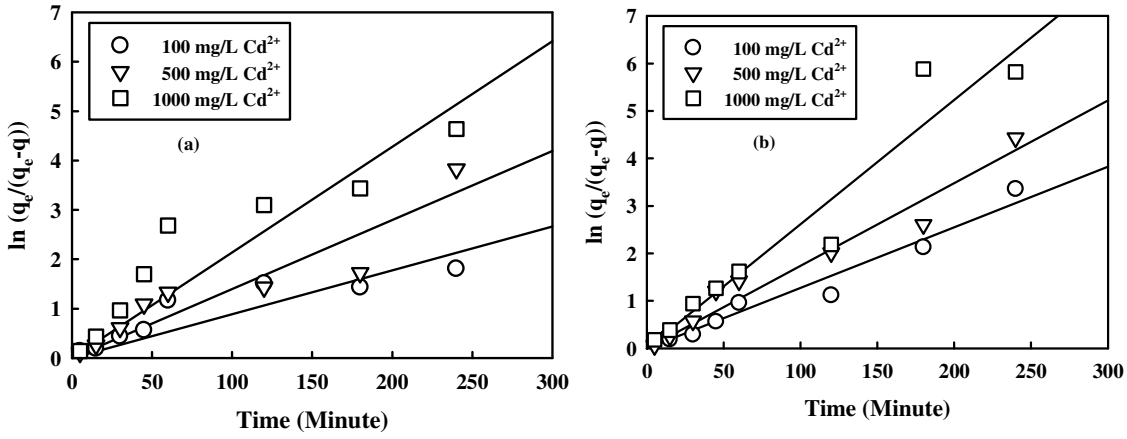

Figure 4.35. Pseudo first order kinetic plots of Pb^{2+} for chitin a) 298.15 K b) 328.15 K.

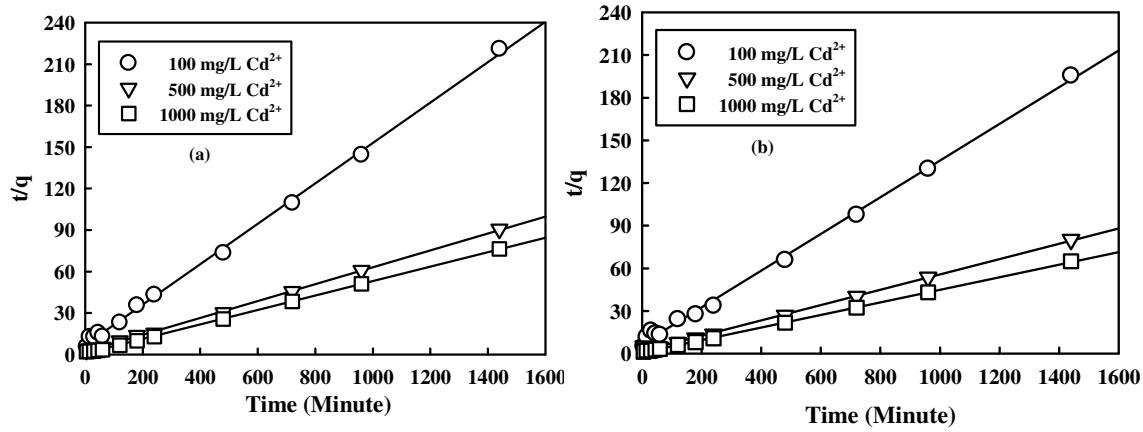

Figure 4.36. Pseudo second order kinetic plots of Cd^{2+} for chitin a) 298.15 K b) 328.15 K.

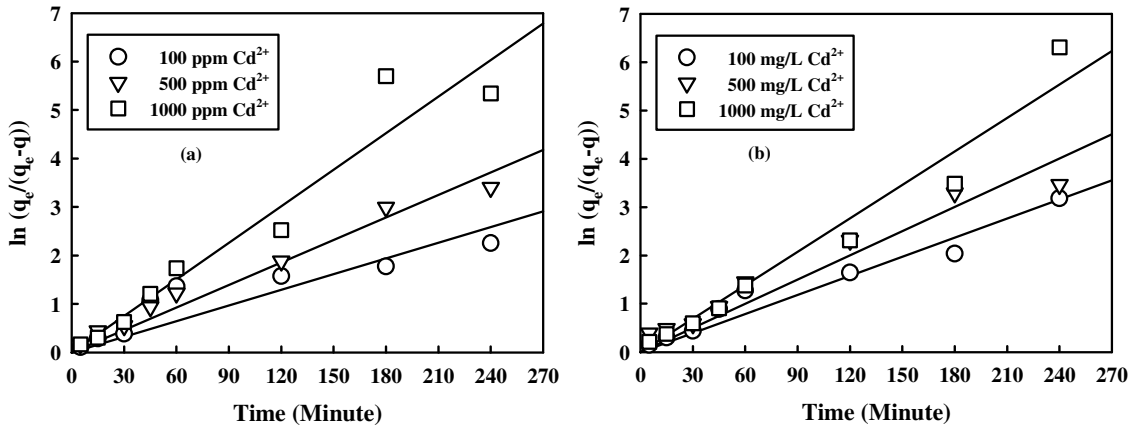

Figure 4.37. Pseudo first order kinetic plots of Cd^{2+} for chitosan a) 298.15 K b) 328.15 K.

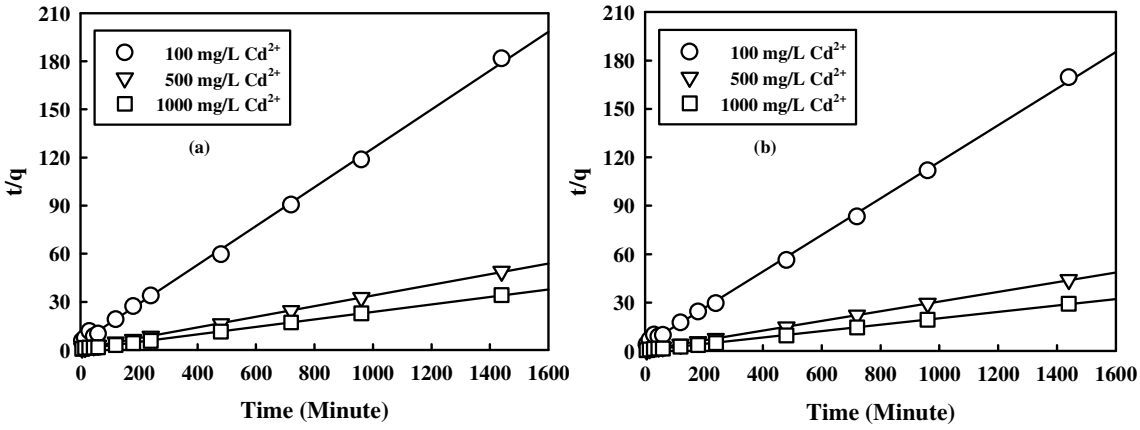

Figure 4.38. Pseudo second order kinetic plots of Cd^{2+} for chitosan a) 298.15 K b) 328.15 K.

Table 4.7. Pseudo first order and pseudo second order rate constants for the adsorption of Cd^{2+} on chitin and chitosan.

Adsorbent	**T (K)**	**C_o (mg/L)**	**k_1 (min^{1-})**	**R_1^2**	**k_2 ($g/mg^{1-}\ min^{1-}$)**	**R_2^2**
Chitin	298.15	100	0.0089	0.7278	2.4641 x10^{-3}	0.9984
	328.15	100	0.0130	0.9625	4.9914 x10^{-3}	0.9975
	298.15	500	0.0140	0.8534	1.5360 x10^{-3}	0.9992
	328.15	500	0.0174	0.9541	3.2011 x10^{-3}	0.9996
	298.15	1000	0.0214	0.8114	1.3823 x10^{-3}	0.9996
	328.15	1000	0.0262	0.9313	2.6223 x10^{-3}	0.9976
Chitosan	298.15	100	0.0108	0.7387	1.0004x10^{-3}	0.9987
	328.15	100	0.0132	0.9381	1.3281 x10^{-3}	0.9991
	298.15	500	0.0155	0.9658	1.2361x10^{-3}	0.9996
	328.15	500	0.0167	0.9215	1.5067 x10^{-3}	0.9996
	298.15	1000	0.0231	0.9351	0.9314 x10^{-3}	0.9994
	328.15	1000	0.0251	0.9576	1.1184 x10^{-3}	0.9994

4.4.3.5.4. Nickel (Ni^{2+})

The values of pseudo first order and second order rate constants of Ni^{2+} ion adsorption by chitin and chitosan are given in Table 4.8. Like in the cases of the Cu^{2+}, Pb^{2+} and Cd^{2+} , the pseudo second order model is seem to provide better correlation with the adsorption data of Ni^{2+} and rate of adsorption is increased with temperature. The corresponding linear fits are shown in Figures 4.39. a-b, 4.40. a-b, 4.41. a-b and 4.42. a-b.

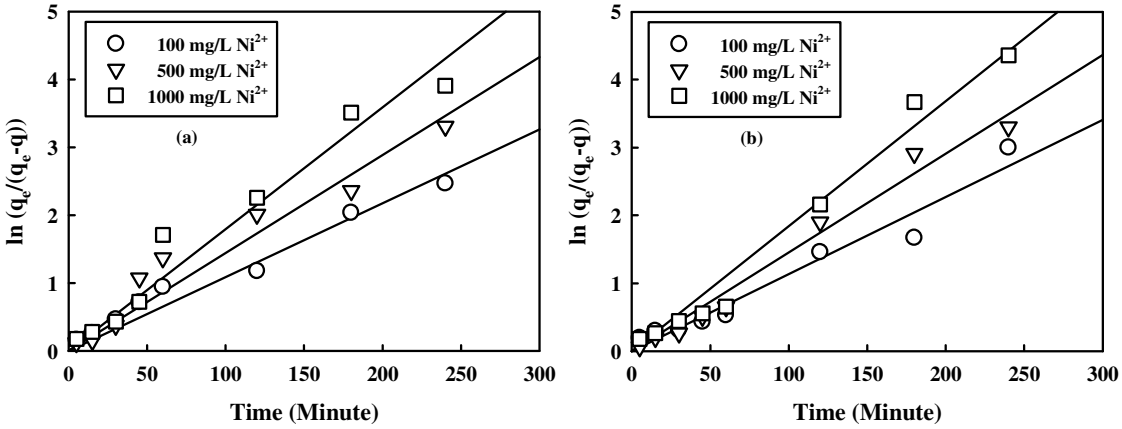

Figure 4.39. Pseudo first order kinetic plots of Ni^{2+} for chitin a) 298.15 K b) 328.15 K.

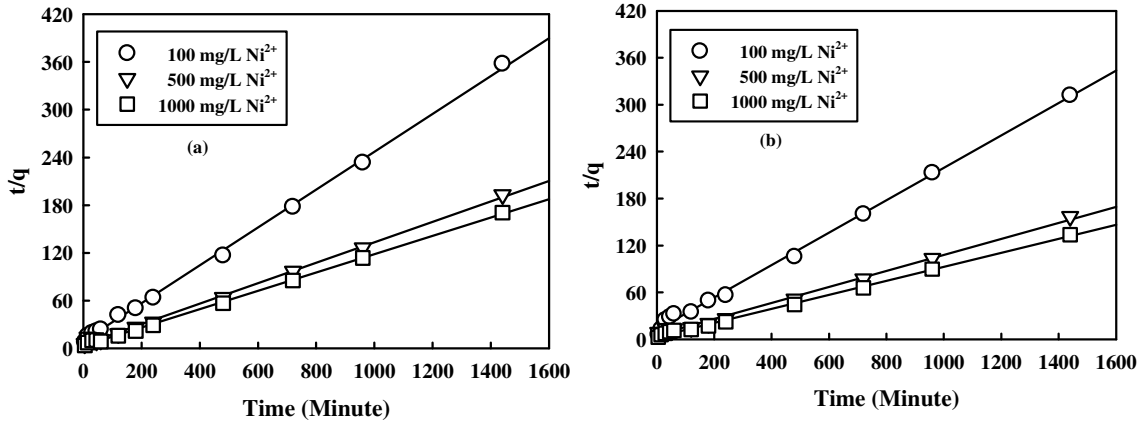

Figure 4.40. Pseudo second order kinetic plots of Ni^{2+} for chitin a) 298.15 K b) 328.15 K.

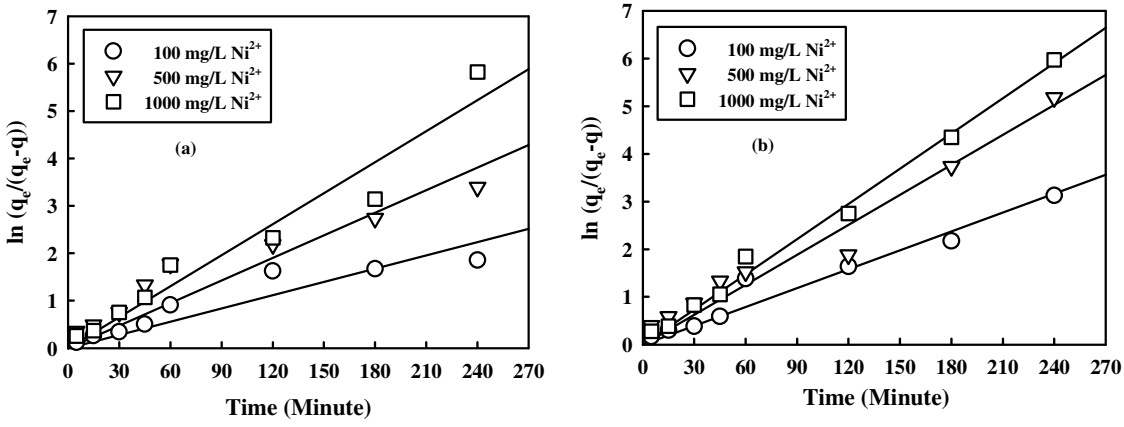

Figure 4.41. Pseudo first order kinetic plots of Ni^{2+} for chitosan a) 298.15 K b) 328.15 K.

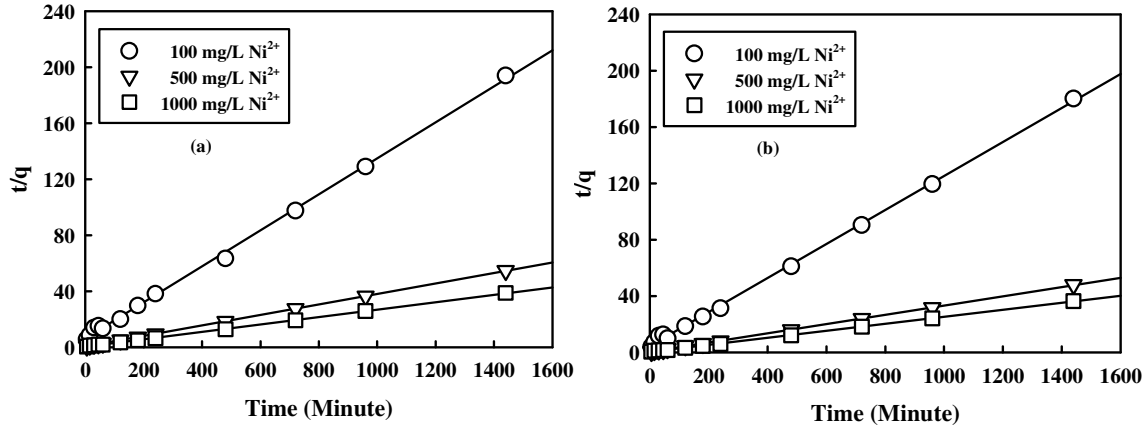

Figure 4.42. Pseudo second order kinetic plots of Ni^{2+} for chitosan a) 298.15 K b) 328.15 K.

Table 4.8. Pseudo first order and pseudo second order rate constants for the adsorption of Ni^{2+} on chitin and chitosan.

Adsorbent	Temp. (K)	C_o (mg/L)	k_1 (min^{1-})	R_1^2	k_2 ($g/mg^{1-}\ min^{1-}$)	R_2^2
Chitin	298.15	100	0.0109	0.9544	3.4273×10^{-3}	0.9988
	328.15	100	0.0114	0.9576	6.7763×10^{-3}	0.9971
	298.15	500	0.0144	0.9347	1.8163×10^{-3}	0.9971
	328.15	500	0.0145	0.9762	3.4100×10^{-3}	0.9957
	298.15	1000	0.0179	0.9559	2.3786×10^{-3}	0.9988
	328.15	1000	0.0184	0.9778	4.0992×10^{-3}	0.9978
Chitosan	298.15	100	0.0093	0.8409	2.5631×10^{-3}	0.9984
	328.15	100	0.0132	0.9463	3.2433×10^{-3}	0.9989
	298.15	500	0.0159	0.8187	1.9885×10^{-3}	0.9999
	328.15	500	0.0209	0.9564	2.2799×10^{-3}	0.9998
	298.15	1000	0.0218	0.9471	1.4834×10^{-3}	0.9996
	328.15	1000	0.0246	0.9924	1.5841×10^{-3}	0.9996

4.4.3.6. Determination of the Activation Energy of Adsorption

The activation energy can be though of as the minimum kinetic energy required for a particular reaction to occur, and as such, it provides a measure of the energetic barrier that the adsorbate ions have to overcome prior to being fixed by the adsorption sides. The activation energy of the adsorption (Ea;J/mol) can be calculated, as discussed in Chapter 2, using the following equation: (Levine 1988)

$$\ln \frac{k(T_2)}{k(T_1)} = -\frac{E_a}{R}\left(\frac{1}{T_2} - \frac{1}{T_1}\right) \qquad (2.24)$$

where k : apperant rate constant

E_a : activation energy

R : gas constant (8.314 J/mole.K)

T : temperature (K)

The kinetics analysis of heavy metal ions adsorption on both biopolymers showed that pseudo second order kinetic model correlates better with the experimental data. To determine the activation energy of the adsorption process of heavy metal ions by chitin and chitosan, pseudo-second-order rate constants are used . The values of k_2 and q_e obtained at the all initial concentrations and temperatures of Cu^{2+}, Pb^{2+}, Cd^{2+}, Ni^{2+} are shown in Table 4.9. In addition this table show the calculated activation energies of all metal ions adsorption by chitin and chitosan biopolymers.

As seen from the table, the values related with adsorption of Cu^{2+} and Pb^{2+} ions on chitosan biopolymers are greater than chitin related with fixation on chitosan , indicating the energetic barrier against adsorption on chitosan is easier to overcome when compared with chitin. However this situation is different for Cd^{2+} and Ni^{2+} ion adsorption on chitin and chitosan.

Table 4.9. The pseudo second order kinetic parameters obtained from the linear fits of experimental data to the second order rate equation for Cu^{2+} and Pb^{2+} ions.

Adsorbent	**Temp. (K)**	**Metal Ion**	**C_o (mg/L)**	**q_e (mg/L)**	**E_a (kJ/mol)**
Chitin	298.15	Cu^{2+}	100	8.41	12.40
	328.15		100	9.72	
	298.15		500	28.98	9.25
	328.15		500	31.47	
	298.15		1000	37.67	4.88
	328.15		1000	42.56	
Chitosan	298.15	Cu^{2+}	100	10.09	34.59
	328.15		100	10.38	
	298.15		500	43.63	32.67
	328.15		500	48.27	
	298.15		1000	68.04	16.21
	328.15		1000	71.17	
Chitin	298.15	Pb^{2+}	100	8.21	6.74
	328.15		100	8.98	
	298.15		500	14.32	6.54
	328.15		500	15.08	
	298.15		1000	35.72	5.51
	328.15		1000	37.62	
Chitosan	298.15	Pb^{2+}	100	10.02	14.39
	328.15		100	10.11	
	298.15		500	37.23	10.86
	328.15		500	40.01	
	298.15		1000	52.65	6.53
	328.15		1000	57.67	

Table 4.10. The pseudo second order kinetic parameters obtained from the linear fits of experimental data to the second order rate equation for Cd^{2+} and Ni^{2+} ions.

Adsorbent	**Temp. (K)**	**Metal Ion**	**C_o (mg/L)**	**q_e (mg/L)**	**E_a (kJ/mol)**
Chitin	298.15	Cd^{2+}	100	5.37	19.14
	328.15		100	7.75	
	298.15		500	12.33	19.91
	328.15		500	18.59	
	298.15		1000	19.12	17.35
	328.15		1000	22.62	
Chitosan	298.15	Cd^{2+}	100	8.05	7.68
	328.15		100	8.62	
	298.15		500	31.06	5.37
	328.15		500	33.22	
	298.15		1000	42.92	4.96
	328.15		1000	50.25	
Chitin	298.15	Ni^{2+}	100	4.03	18.48
	328.15		100	4.83	
	298.15		500	7.79	17.08
	328.15		500	9.77	
	298.15		1000	10.68	14.76
	328.15		1000	11.17	
Chitosan	298.15	Ni^{2+}	100	7.78	6.38
	328.15		100	8.29	
	298.15		500	28.25	3.71
	328.15		500	30.58	
	298.15		1000	37.74	1.78
	328.15		1000	40.16	

4.4.3.7. Intraparticle Diffusion

Prediction of the rate-limiting step is an important factor to be considered in adsorption proceses. For solid–liquid adsorption process, the solute transfer process was usually characterized by either external mass transfer (boundary layer diffusion) or intraparticle diffusion or both. The adsorption dynamics can be described by the following three consecutive steps which are as follows: (Vadivelan and Kumar 2005)

- Transport of the solute from bulk solution through liquid film to the adsorbent exterior surface.
- Solute diffusion into the pore of adsorbent except for a small quantity of adsorption on the external surface. Parallel to this is the intraparticle transport mechanism of the surface diffusion.
- Adsorption of solute on the interior surfaces of the pores and capillary spaces of the adsorbent.

The last step is considered to be an equilibrium reaction. Out of three steps, the third step is assumed to be rapid and considered to be negligible. The overall rate of adsorption will be controlled by the slowest step, which would be either film diffusion or pore diffusion. However, the controlling step might be distributed between intra-particle and external transport mechanism. Whatever may be the case external diffusion will be involved in the adsorption process. The adsorption of heavy metal ions onto chitin and chitosan biopolymer may be controlled due to film diffusion at earlier stages and as the adsorbent particles gets loaded with metal ions, the adsorption process may be controlled due to intraparticle diffusion (Vadivelan and Kumar 2005).

The intraparticle diffusion coefficients for the adsorption of heavy metal ions on chitin and chitosan biopolymers were calculated from the slope of the plot between square root of time ($min^{0.5}$) versus amount of metal ion adsorbed (mg/g). Previous studies by various researchers showed that the plot between q_t versus $t^{0.5}$ represents multi linearity, which characterizes the two or more steps involved in adsorption process (Sun and Yang 2003, Sivaraj et. al 2003). Figures 4.43. a-b, 4.44. a-b, 4.45. a-b, 4.46. a-b, 4.47. a-b, 4.48. a-b, 4.49. a-b and 4.50. a-b show the plot between q_t versus $t^{0.5}$ for heavy metal ions onto chitin and chitosan biopolymers. From these figures, at all initial metal ion concentrations, the adsorption process tends to be followed by two phases. It was found that an initial linear portion ended with a smooth curve followed by second linear portion. The two phases in the

intraparticle diffusion plot suggests that the adsorption process proceeds by surface adsorption and the intraparticle diffusion. The initial curved portion of the plot indicates boundary layer effect while the second linear portion is due to intra-particle or pore diffusion. The slope of second linear portion of the plot has been defined as the intra-particle diffusion parameter K_i (mg/g $min^{0.5}$). On the other hand, the intercept of the plot reflects the boundary layer effect. Larger the intercept, greater is the contribution of the surface adsorption in the rate limiting step (Vadivelan and Kumar 2005). The calculated intraparticle diffusion coefficient K_i value at different initial heavy metal ion concentrations of Cu^{2+}, Pb^{2+}, Cd^{2+} and Ni^{2+} on chitin and chitosan biopolymers are shown in Table 4.11, Table 4.12, Table 4.13. and Table 4.14. respectively.

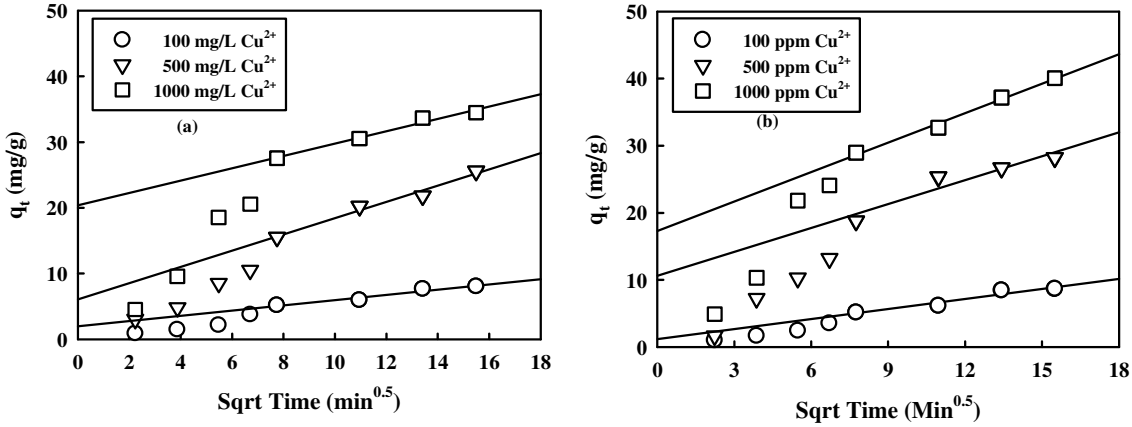

Figure 4.43. Intraparticle diffusion plot for Cu^{2+} adsorption on chitin a) 298.15 K b) 328.15 K (pH= 6, S/L= 0.01 g/mL, agitation rate= 600 rpm).

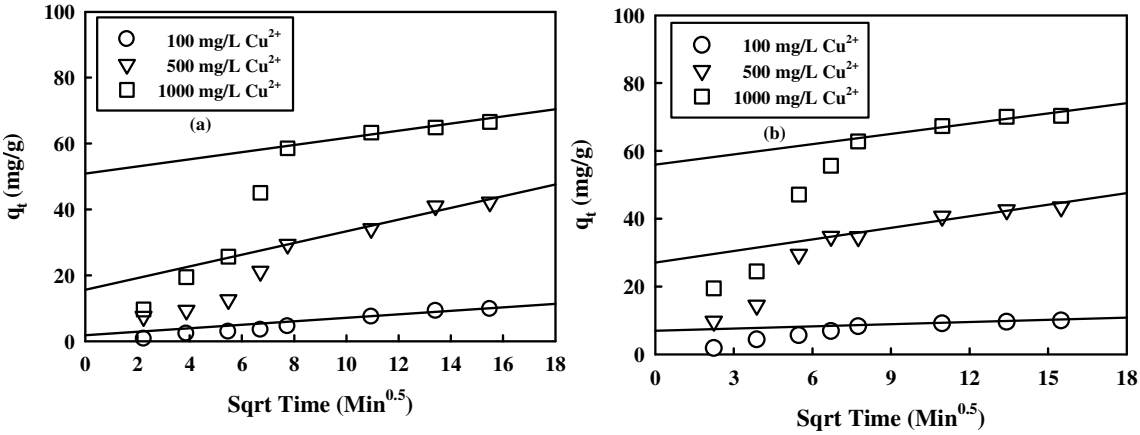

Figure 4.44. Intraparticle diffusion plot for Cu^{2+} adsorption on chitosan a) 298.15 K b) 328.15 K (pH= 6, S/L= 0.01 g/mL, agitation rate= 600 rpm).

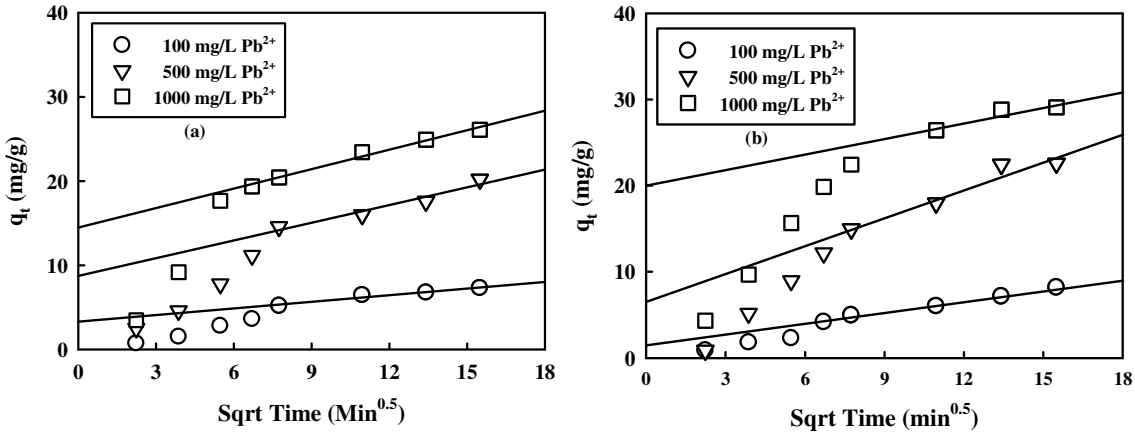

Figure 4.45. Intraparticle diffusion plot for Pb^{2+} adsorption on chitin a) 298.15 K b) 328.15 K (pH= 6, S/L= 0.01 g/mL, agitation rate= 600 rpm).

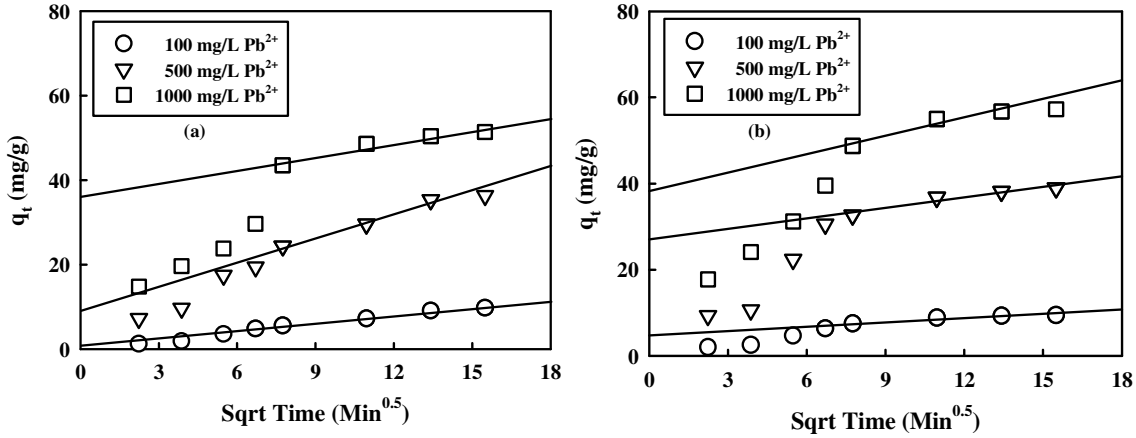

Figure 4.46. Intraparticle diffusion plot for Pb^{2+} adsorption on chitosan a) 298.15 K b) 328.15 K (pH= 6, S/L= 0.01 g/mL, agitation rate= 600 rpm).

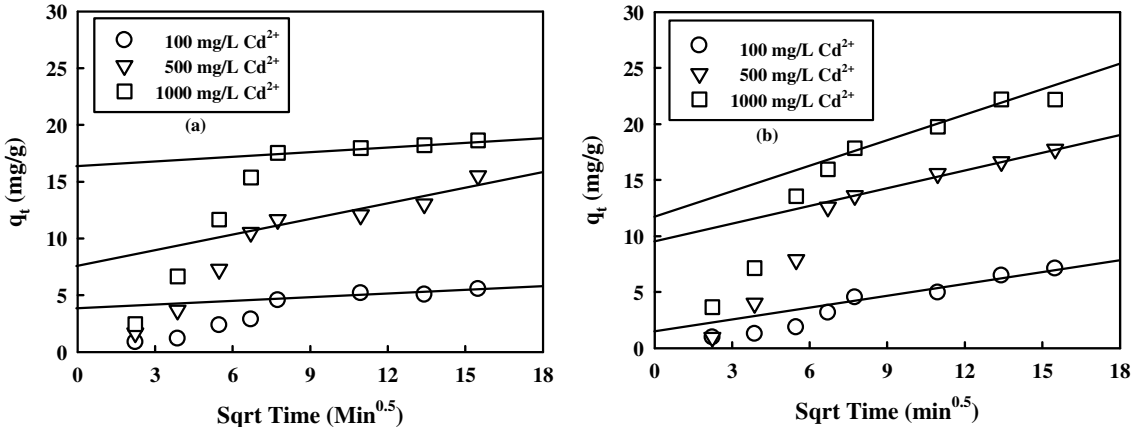

Figure 4.47. Intraparticle diffusion plot for Cd^{2+} adsorption on chitin a) 298.15 K b) 328.15 K (pH= 7, S/L= 0.01, agitation rate= 600 rpm).

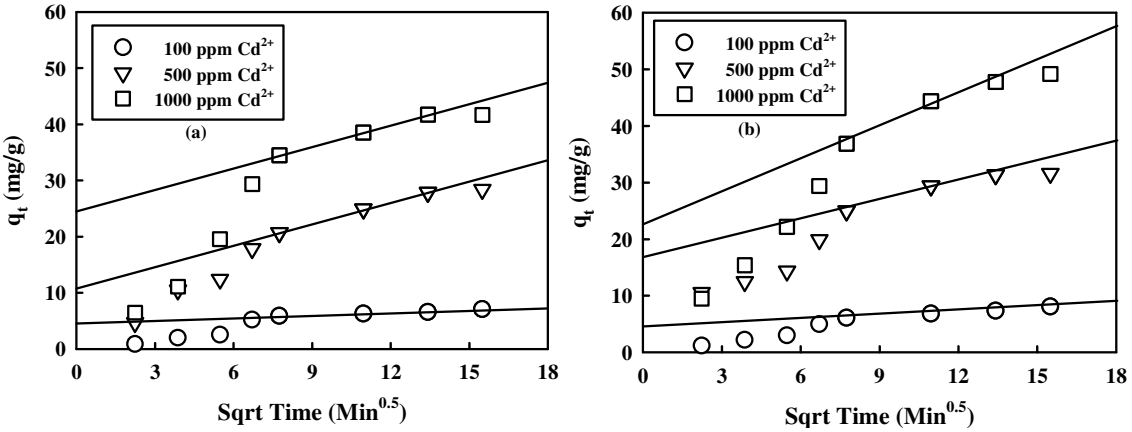

Figure 4.48. Intraparticle diffusion plot for Cd^{2+} adsorption on chitosan a) 298.15 K b) 328.15 K (pH= 7, S/L= 0.01, agitation rate= 600 rpm).

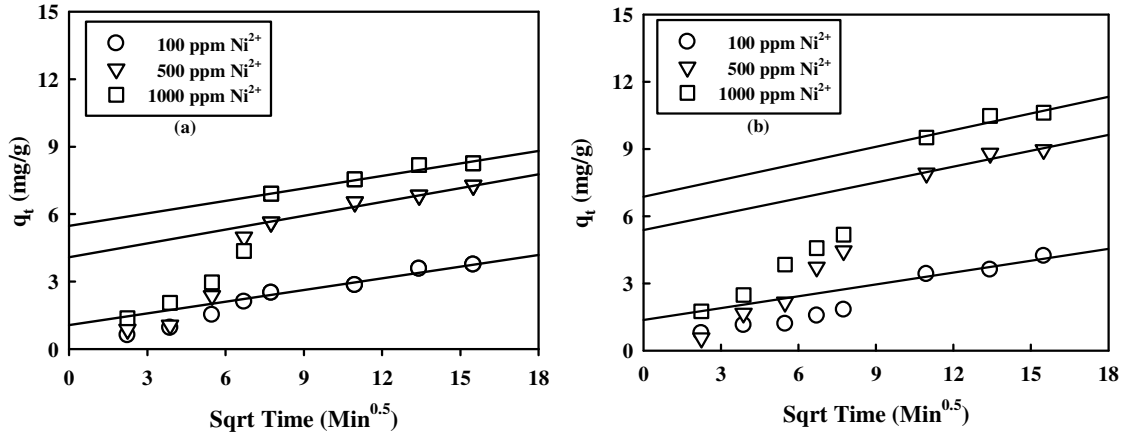

Figure 4.49. Intraparticle diffusion plot for Ni^{2+} adsorption on chitin a) 298.15 K b) 328.15 K (pH= 6, S/L= 0.01, agitation rate= 600 rpm).

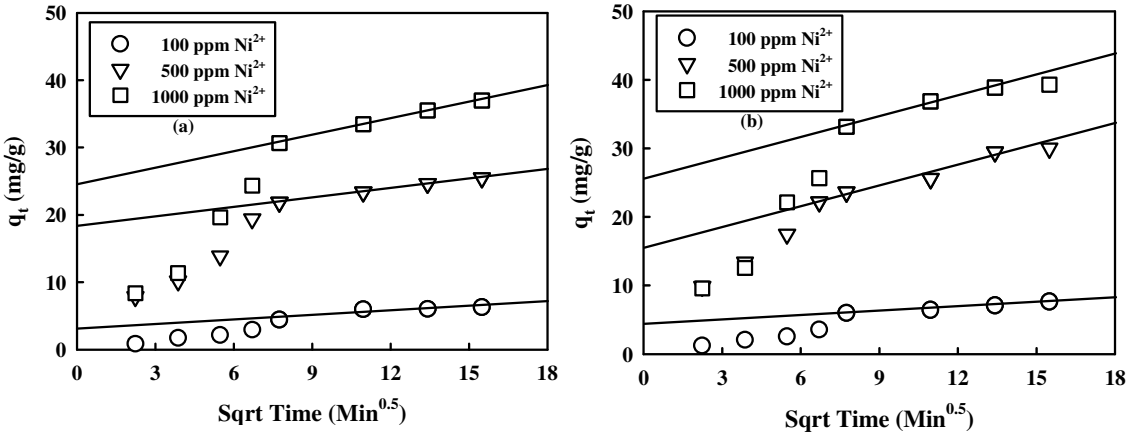

Figure 4.50. Intraparticle diffusion plot for Ni^{2+} adsorption on chitosan a) 298.15 K b) 328.15 K (pH= 6, S/L= 0.01, agitation rate= 600 rpm).

Table 4.11. Intraparticle diffusion coefficients for Cu^{2+} ion on chitin and chitosan.

Adsorbent	Temperature (K)	C_o (mg/L)	K_i (mg/gmin$^{0.5}$)
Chitin	298.15	100	0.3986
	328.15	100	0.5001
	298.15	500	1.2348
	328.15	500	1.1854
	298.15	1000	0.9372
	328.15	1000	1.4624
Chitosan	298.15	100	0.5246
	328.15	100	0.2163
	298.15	500	1.7734
	328.15	500	1.1364
	298.15	1000	1.0836
	328.15	1000	1.0103

Table 4.12. Intraparticle diffusion coefficients for Pb^{2+} ion on chitin and chitosan.

Adsorbent	Temperature (K)	C_o (mg/L)	K_i (mg/gmin$^{0.5}$)
Chitin	298.15	100	0.2619
	328.15	100	0.4165
	298.15	500	0.7015
	328.15	500	1.0782
	298.15	1000	0.7703
	328.15	1000	0.6002
Chitosan	298.15	100	0.5736
	328.15	100	0.3344
	298.15	500	0.8137
	328.15	500	1.9087
	298.15	1000	1.0205
	328.15	1000	1.4315

Table 4.13. Intraparticle diffusion coefficients for Cd^{2+} ion on chitin and chitosan.

Adsorbent	Temperature (K)	C_o (mg/L)	K_i (mg/gmin$^{0.5}$)
Chitin	298.15	100	0.1099
	328.15	100	0.3523
	298.15	500	0.4651
	328.15	500	0.5266
	298.15	1000	0.1371
	328.15	1000	0.7577
Chitosan	298.15	100	0.1494
	328.15	100	0.2528
	298.15	500	1.2683
	328.15	500	1.1422
	298.15	1000	1.2724
	328.15	1000	1.9469

Table 4.14. Intraparticle diffusion coefficients for Ni^{2+} ion on chitin and chitosan.

Adsorbent	Temperature (K)	C_o (mg/L)	K_i (mg/gmin$^{0.5}$)
Chitin	298.15	100	0.1730
	328.15	100	0.1761
	298.15	500	0.2050
	328.15	500	0.2354
	298.15	1000	0.1852
	328.15	1000	0.2481
Chitosan	298.15	100	0.2269
	328.15	100	0.2143
	298.15	500	0.4695
	328.15	500	1.0110
	298.15	1000	0.8197
	328.15	1000	1.0142

4.4.4. Adsorption Isotherm Models

The analysis and design of the adsorption process requires the relevant adsorption equilibria, which is the most important piece of information in understanding an adsorption process. Adsorption equilibria provide fundamental physicochemical data for evaluating the applicability of the adsorption process as a unit operation (Vadivelan and Kumar 2005). In this study, investigation the equilibrium data were analyzed using the Freundlich, Langmuir and Temkin isotherm expression.

Freundlich isotherm was discussed in Chapter 2 and its linear form is given by the equation;

$$\log q_e = \log K_f + \frac{1}{n} \log C_e \tag{2.6}$$

The Freundlich isotherm parameters obtained by the fitting of the adsorption data are described by the elemental concentration in solid and liquid are in equilibrium at the end of the experiments (6 hours). The magnitude of the Freundlich parameters K_f gives the quantitative information on the relative adsorption affinity towards the adsorbed cation and the magnitude of constant 1/n provides the information about linearity of adsorption. Nonlinear behavior of adsorption indicates that adsorption energy barrier increase exponentially with increasing fraction of filled sites on the chitin and chitosan biopolymer. (Schwarzenbach 2003).

Langmuir isotherm was discussed in Chapter 2 and its linear form is given by the equation;

$$\frac{C_e}{q_e} = \frac{1}{q_0 K_L} + \frac{C_e}{q_0} \tag{2.7}$$

The Langmuir isotherm parameters obtained by the fitting the data of adsorption are described by the elemental concentration in solid and liquid are equilibrium at the end of the experimens (6 hours). The magnitude of the Langmuir parameters K_L is correlated with the heat of adsorpt,on. The q_0 represents the total number of surface sites per mass of adsorbent (Fingueneisel 1998).

The Temkin isotherm in its linear form is given by the equation;

$$q_e = Bt \log K_T + Bt \log C_e \tag{2.8}$$

Temkin isotherm assumes that (i) the heat of adsorption of all the molecules in the layer decreases linearly with coverage due to adsorbate–adsorbate interactions and (ii) adsorption is characterized by a uniform distribution of binding energies, up to some maximum binding energy. The Temkin isotherm parameters obtained by fitting the data of adsorption are described by asuming the elemental concentration in solid and liquid are described by assuming the the elemental concentration in solid and liquid are equilibrium at the end of the experiments (6 hours) The magniude of the Temkin parameters B_T is the related to the heat of adsorption and K_T is equilibrium binding constant.(Sristeva et al. 2006)

Figures 4.51. a-b, 4.52. a-b, 4.53. a-b, 4.54. a-b, 4.55. a-b, 4.56. a-b, 4.57. a-b and 4.58. a-b show the Freundlich, Langmuir and Temkin curves for metal ions adsorption on chitin and chitosan biopolymers at a constant solution tempereature of 298.15 K and 328.15 K, respectively, along with the experimental data. Based on the isotherm parameters, Freundlich, Langmuir and Temkin isotherm equations are given in Table 4.18.

The Freundlich, Langmuir and Temkin adsorption constants evaluated from the isotherms with the correlation coefficients are also given in Table. 4.15, 4.16. and 4.17. As seen from the tables, regression correlation coefficients for all the adsorbate–adsorbent systems are very high for Freundlich and Langmuir models.

According to the 1/n values in Table 4.15, the deviation from linear adsorption is higher in the case of Ni^{2+} uptake by chitin and Cu^{2+} uptake by chitosan. The magnitude of K_F values indicate that both biopolymers favors the adsorption of Cu^{2+} over that of Pb^{2+}, Cd^{2+} and Ni^{2+}. Moreover, chitosan is seen to posses higher adsorption affinity towards Cu^{2+}, Pb^{2+}, Cd^{2+} and Ni^{2+} compared with chitin.

The value of q_o (i.e. maximum uptake) appears to be significantly higher for the Cu^{2+}-chitosan system in comparison with the uptake of Cu^{2+} on the chitin. A large value of K_L also implied strong bonding of Cu^{2+} to the chitosan. Langmuir parameters of chitin also indicated a maximum adsorption capacity of 41.32 mg/g for Cu^{2+}, 30.39 mg/g for Pb^{2+}, 21.98 mg/g for Cd^{2+} and 11.14 mg/g for Ni^{2+} at 328.15 K. These values are 69.97 mg/g for Cu^{2+}, 54.95 mg/g for Pb^{2+}, 48.78 mg/g for Cd^{2+} and 43.86 mg/g for chitosan at 328.15 K.

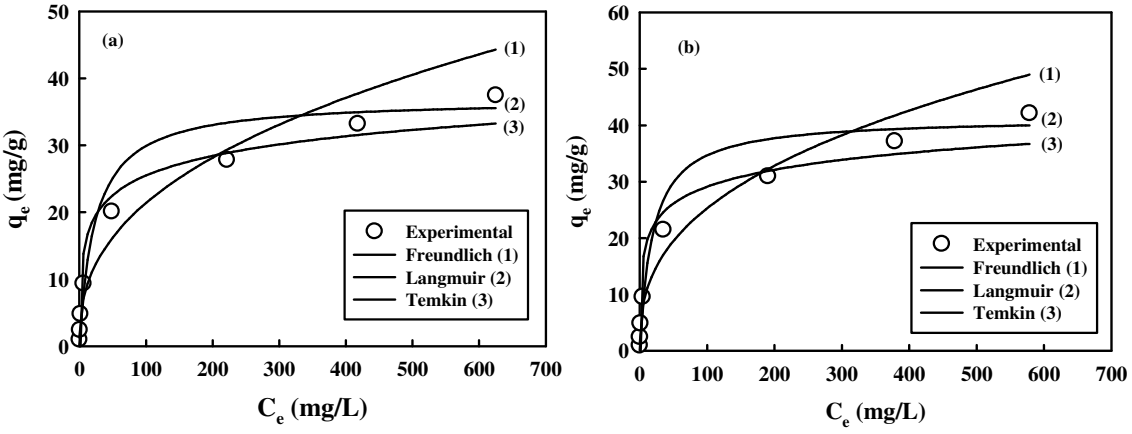

Figure 4.51. Equilibrium isotherms curves for the adsorption of Cu^{2+} on chitin a) 298.15 K b) 328.15 K (pH= 6, S/L= 0.01, agitation time= 6h, agitation rate= 600 rpm).

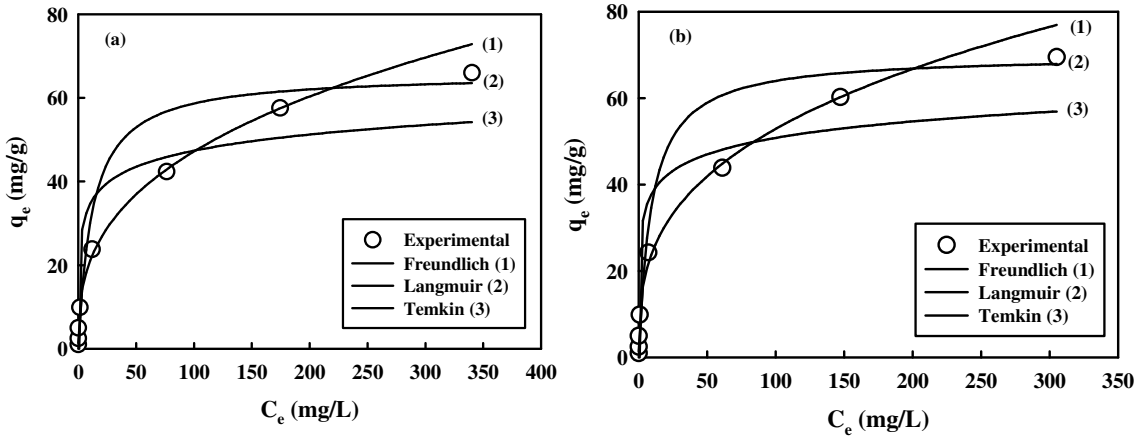

Figure 4.52. Equilibrium isotherms curves for the adsorption of Cu^{2+} on chitosan a) 298.15 K b) 328.15 K (pH= 6, S/L= 0.01, agitation time= 6h, agitation rate= 600 rpm).

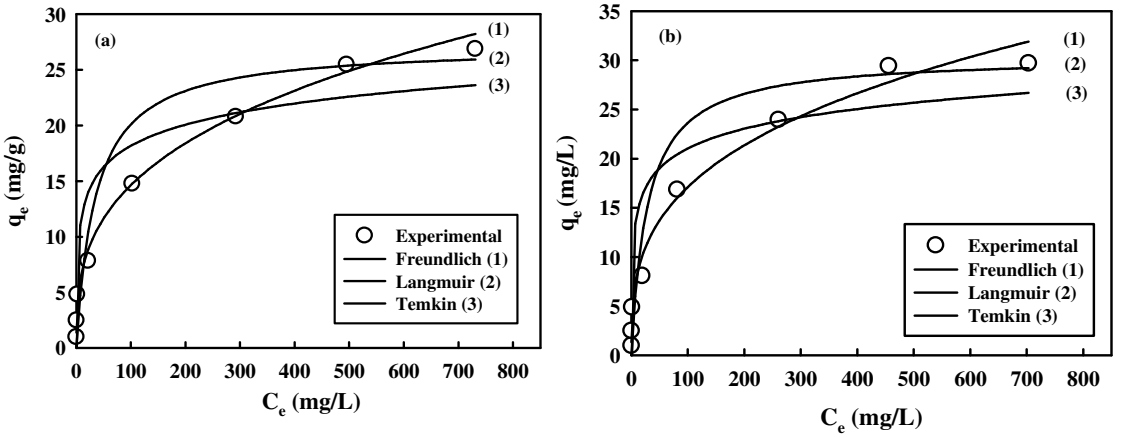

Figure 4.53. Equilibrium isotherms curves for the cdsorption of Pb^{2+} on chitin a) 298.15 K b) 328.15 K (pH= 6, S/L= 0.01, agitation time= 6h, agitation rate= 600 rpm).

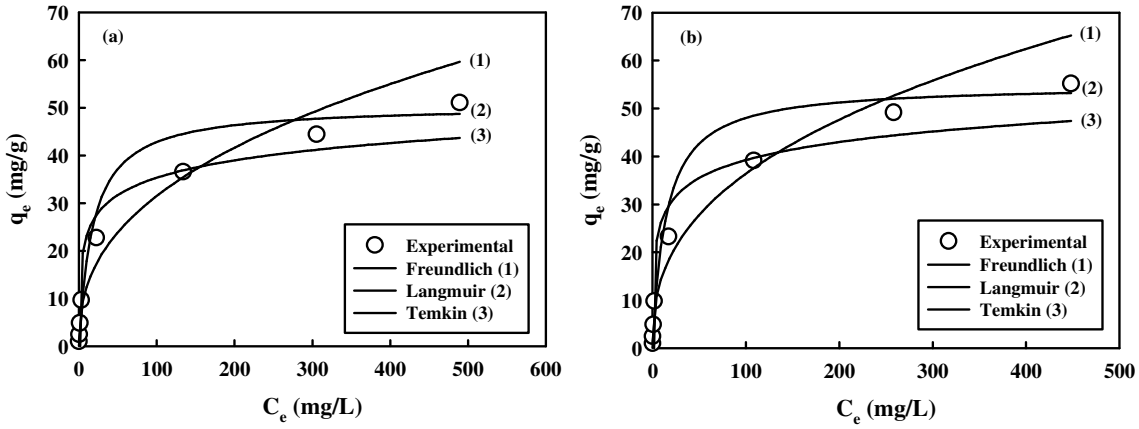

Figure 4.54. Equilibrium isotherms curves for the adsorption of Pb^{2+} on chitosan a) 298.15 K b) 328.15 K (pH= 6, S/L= 0.01, agitation time= 6h, agitation rate= 600 rpm).

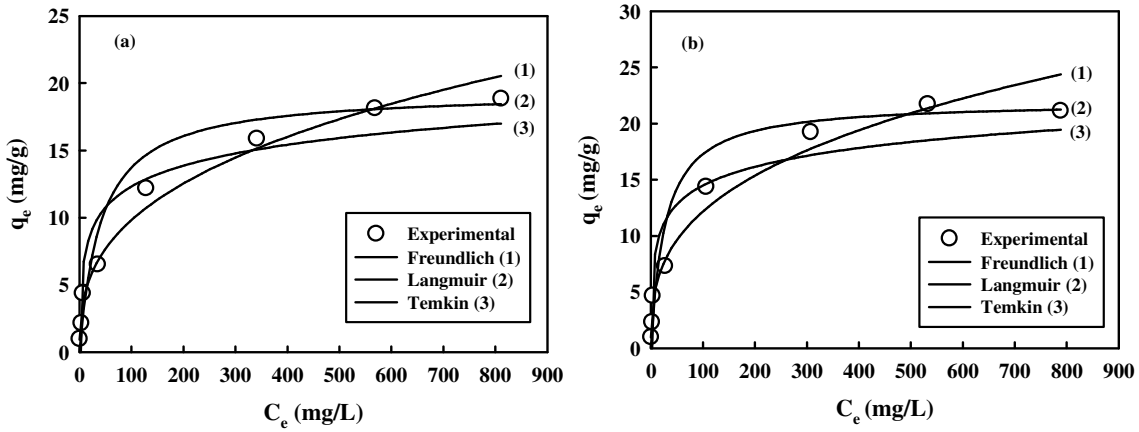

Figure 4.55. Equilibrium isotherms curves for the adsorption of Cd^{2+} on chitin a) 298.15 K b) 328.15 K (pH= 7, S/L= 0.01, agitation time= 6h, agitation rate= 600 rpm).

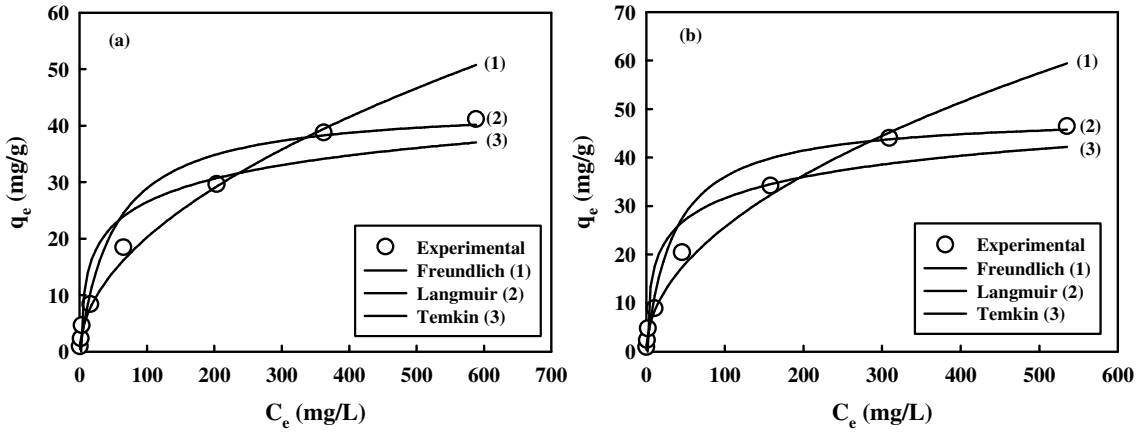

Figure 4.56. Equilibrium isotherms curves for the adsorption of Cd^{2+} on chitosan a) 298.15 K b) 328.15 K (pH= 7, S/L= 0.01, agitation time= 6h, agitation rate= 600 rpm).

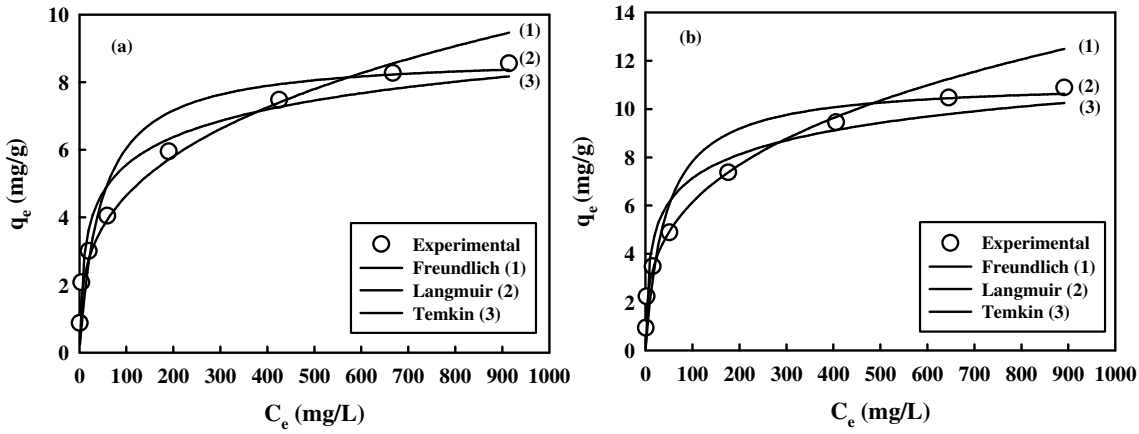

Figure 4.57. Equilibrium isotherms curves for the adsorption of Ni^{2+} on chitin a) 298.15 K b) 328.15 K (pH= 6, S/L= 0.01, agitation time= 6h, agitation rate= 600 rpm).

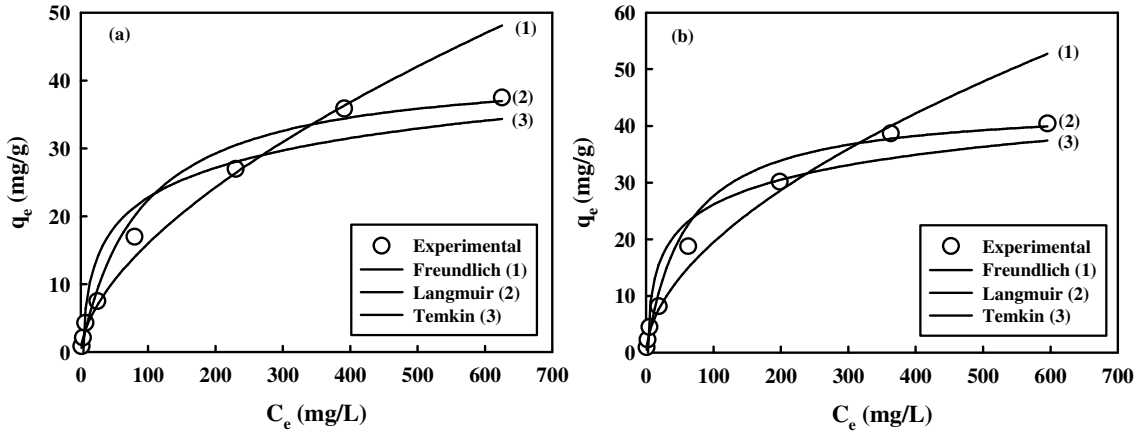

Figure 4.58. Equilibrium isotherms curves for the adsorption of Ni^{2+} on chitin a) 298.15 K b) 328.15 K (pH= 6, S/L= 0.01, agitation time= 6h, agitation rate= 600 rpm).

Table 4.15. Freundlich isotherm constants for heavy metal ions adsorption on chitin and chitosan.

Adsorbent	Temperature (K)	Metal Ion	Freundlich isotherm parameters		
			K_f (mg/g)(L/g)	1/n	R^2
Chitin	298.15	Cu^{2+}	3.4293	0.3974	0.9782
	328.15		4.4525	0.3770	0.9862
	298.15	Pb^{2+}	3.1944	0.3304	0.9757
	328.15		3.9364	0.3192	0.9760
	298.15	Cd^{2+}	1.9373	0.3525	0.9807
	328.15		2.5793	0.3368	0.9803
	298.15	Ni^{2+}	1.0585	0.3213	0.9717
	328.15		1.3778	0.3245	0.9768
Chitosan	298.15	Cu^{2+}	9.2215	0.3545	0.9827
	328.15		11.2642	0.3358	0.9837
	298.15	Pb^{2+}	4.9602	0.4015	0.9876
	328.15		6.0730	0.3889	0.9866
	298.15	Cd^{2+}	1.8518	0.5191	0.9809
	328.15		2.5663	0.5001	0.9825
	298.15	Ni^{2+}	1.0039	0.6011	0.9779
	328.15		1.4879	0.5583	0.9816

Table 4.16. Langmuir isotherm constants for heavy metal ions adsorption onto chitin and chitosan.

Adsorbent	Temperature (^oC)	Metal Ion	Langmuir isotherm parameters		
			K_L	q_o (mg/g)	R^2
Chitin	298.15	Cu^{2+}	0.0427	36.90036	0.9872
	328.15		0.0528	41.32231	0.9874
	298.15	Pb^{2+}	0.0283	27.17391	0.9826
	328.15		0.0349	30.39513	0.9878
	298.15	Cd^{2+}	0.0243	19.37984	0.9917
	328.15		0.0368	21.97802	0.9946
	298.15	Ni^{2+}	0.0221	8.78735	0.9928
	328.15		0.0236	11.13586	0.9920
Chitosan	298.15	Cu^{2+}	0.0824	65.7895	0.9838
	328.15		0.1069	69.9655	0.9858
	298.15	Pb^{2+}	0.0556	50.5051	0.9883
	328.15		0.0693	54.9450	0.9904
	298.15	Cd^{2+}	0.0196	43.6681	0.9836
	328.15		0.0282	48.7805	0.9885
	298.15	Ni^{2+}	0.0113	42.1940	0.9850
	328.15		0.0170	43.8596	0.9894

Table 4.17. Temkin isotherm constants for heavy metal ions adsorption onto chitin and chitosan.

Adsorbent	Temperature (^oK)	Metal Ion	Temkin isotherm parameters		
			K_T (L/mg)	B_t	R^2
Chitin	298.15	Cu^{2+}	4.1130	9.7495	0.9406
	328.15		8.2323	9.9824	0.9224
	298.15	Pb^{2+}	6.7019	6.3211	0.8926
	328.15		12.5364	6.6545	0.8769
	298.15	Cd^{2+}	2.4635	5.1514	0.8836
	328.15		4.9129	5.5491	0.8788
	298.15	Ni^{2+}	1.0982	2.7225	0.9649
	328.15		1.4868	3.2835	0.9547
Chitosan	298.15	Cu^{2+}	48.6209	12.8491	0.8681
	328.15		103.575	12.6502	0.8667
	298.15	Pb^{2+}	8.3654	12.0882	0.8922
	328.15		13.949	12.4790	0.8850
	298.15	Cd^{2+}	0.8665	13.6730	0.9171
	328.15		1.4829	14.5571	0.9154
	298.15	Ni^{2+}	0.3661	14.5540	0.9216
	328.15		0.6196	14.5750	0.9231

Table 4.18. Equilibrium isotherm expressions for the adsorption of heavy metal ions on chitin and chitosan.

Sorbent	Metal Ion	Temp. (K)	Predicted Freundlich Isotherm	Predicted Langmuir Isotherm	Predicted Temkin Isotherm
Chitin	Cu^{2+}	298.15	$q_e = 3.4293 C_e^{0.3974}$	$q_e = \frac{1.5749 C_e}{1 + 0.0427 C_e}$	$q_e = 13.7872 + 9.7495 \log C_e$
		328.15	$q_e = 4.4525 C_e^{0.3770}$	$q_e = \frac{2.1492 C_e}{1 + 0.0528 C_e}$	$q_e = 21.0436 + 9.9825 \log C_e$
Chitosan	Cu^{2+}	298.15	$q_e = 9.2215 C_e^{0.3545}$	$q_e = \frac{5.4210 C_e}{1 + 0.0824 C_e}$	$q_e = 49.9062 + 12.8491 \log C_e$
		328.15	$q_e = 11.2642 C_e^{0.3358}$	$q_e = \frac{4.4793 C_e}{1 + 0.1069 C_e}$	$q_e = 58.6997 + 12.6502 \log C_e$
Chitin	Pb^{2+}	298.15	$q_e = 3.1944 C_e^{0.3304}$	$q_e = \frac{0.7701 C_e}{1 + 0.0283 C_e}$	$q_e = 12.0252 + 6.3211 \log C_e$
		328.15	$q_e = 3.9364 C_e^{0.3192}$	$q_e = \frac{1.0626 C_e}{1 + 0.0349 C_e}$	$q_e = 16.8268 + 6.6546 \log C_e$
Chitosan	Pb^{2+}	298.15	$q_e = 4.9602 C_e^{0.4015}$	$q_e = \frac{2.8080 C_e}{1 + 0.0556 C_e}$	$q_e = 25.6762 + 12.0882 \log C_e$
		328.15	$q_e = 6.0730 C_e^{0.3889}$	$q_e = \frac{3.8877 C_e}{1 + 0.0693 C_e}$	$q_e = 32.8876 + 12.4790 \log C_e$
Chitin	Cd^{2+}	298.15	$q_e = 1.9373 C_e^{0.3325}$	$q_e = \frac{0.4703 C_e}{1 + 0.0243 C_e}$	$q_e = 4.6444 + 5.1514 \log C_e$
		328.15	$q_e = 2.5793 C_e^{0.3368}$	$q_e = \frac{0.8077 C_e}{1 + 0.0368 C_e}$	$q_e = 8.8334 + 5.5491 \log C_e$
Chitosan	Cd^{2+}	298.15	$q_e = 1.8518 C_e^{0.5191}$	$q_e = \frac{0.8558 C_e}{1 + 0.0196 C_e}$	$q_e = -0.8504 + 13.6730 \log C_e$
		328.15	$q_e = 2.5663 C_e^{0.5001}$	$q_e = \frac{1.3756 C_e}{1 + 0.0282 C_e}$	$q_e = 2.4909 + 14.5571 log C_e$
Chitin	Ni^{+2}	298.15	$q_e = 1.0585 C_e^{0.3213}$	$q_e = \frac{0.1939 C_e}{1 + 0.0221 C_e}$	$q_e = 0.1107 + 2.7225 \log C_e$
		328.15	$q_e = 1.3778 C_e^{0.3245}$	$q_e = \frac{0.2627 C_e}{1 + 0.0236 C_e}$	$q_e = 0.5656 + 3.2835 \log C_e$
Chitosan	Ni^{+2}	298.15	$q_e = 1.0039 C_e^{0.6011}$	$q_e = \frac{0.4768 C_e}{1 + 0.0113 C_e}$	$q_e = 6.3514 + 14.5540 \log C_e$
		328.15	$q_e = 1.4879 C_e^{0.5583}$	$q_e = \frac{0.7456 C_e}{1 + 0.0170 C_e}$	$q_e = -3.0299 + 14.5750 \log C_e$

Another essential characteristics of the Langmuir isotherm can be expressed in terms of dimensionless constant separation factor or equilibrium parameters R_L, and given by following equation;

$$R_L = \frac{1}{(1 + K_L C_0)} \tag{4.1}$$

The parameter R_L indicated the shape of isotherm as follows:

Value of R_L	Type of Isotherm
$R_L > 1$	Unfavorable
$R_L = 1$	Linear
$0 < R_L < 1$	Favorable
$R_L = 0$	Irreversible

The calculated R_L values versus initial solute concentration at two different temperatures were represented in Figures 4.59, 4.60, 4.61. and 4.62. for heavy metal ions adsorption on chitin and chitosan biopolymers. From the Figures it is observed that all temperature conditions adsorption of heavy metal ions on chitin and chitosan biopolymers was found to be more favorable at higher concentrations. Also the value of R_L being in the 0-1 range at all initial heavy metal ion concentrations and both temperatures confirm that uptake of heavy metals on chitin and chitosan biopolymers, is favorable under various conditions.

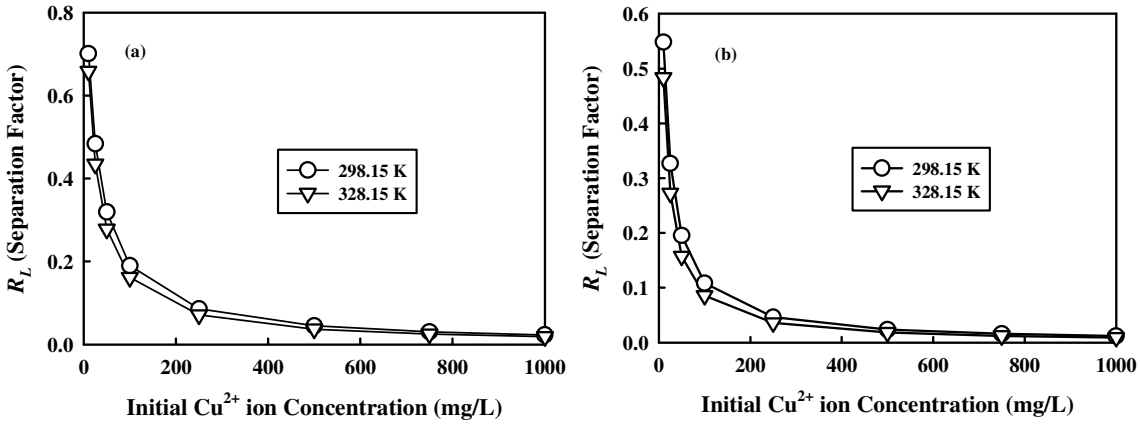

Figure 4.59. Separation factors for Cu^{2+} ion adsorption on chitin and chitosan a) chitin, b) chitosan (pH= 6, S/L= 0.01, agitation time= 6h, agitation rate= 600 rpm).

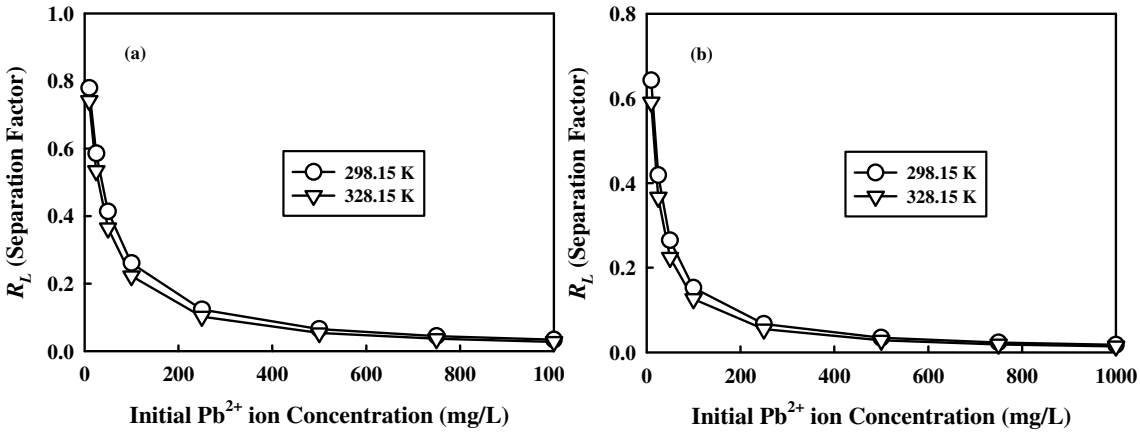

Figure 4.60. Separation factors for Pb^{2+} ion adsorption on chitin and chitosan a) chitin, b) chitosan (pH= 6, S/L= 0.01, agitation time= 6h, agitation rate= 600 rpm)

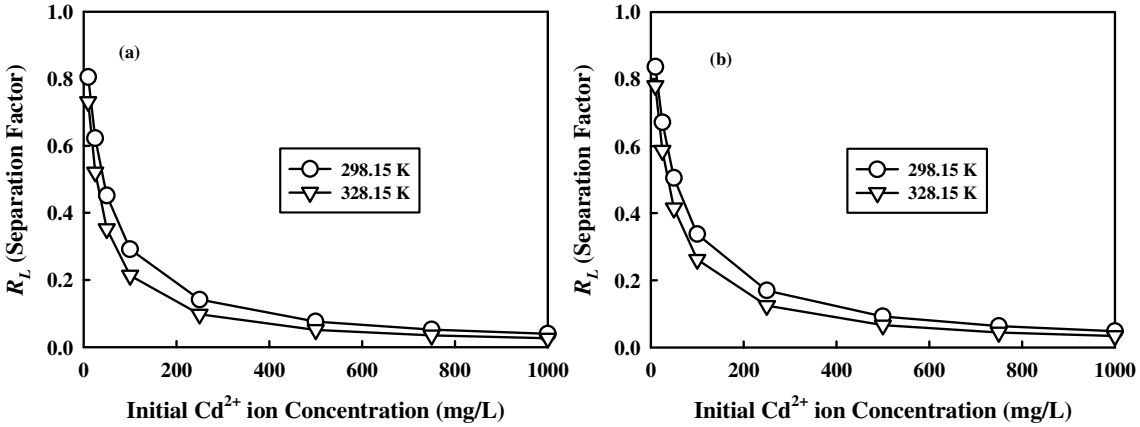

Figure 4.61. Separation factors for Cd^{2+} ion adsorption on chitin and chitosan a) chitin, b) chitosan (pH= 7, S/L= 0.01, agitation time= 6h, agitation rate= 600 rpm).

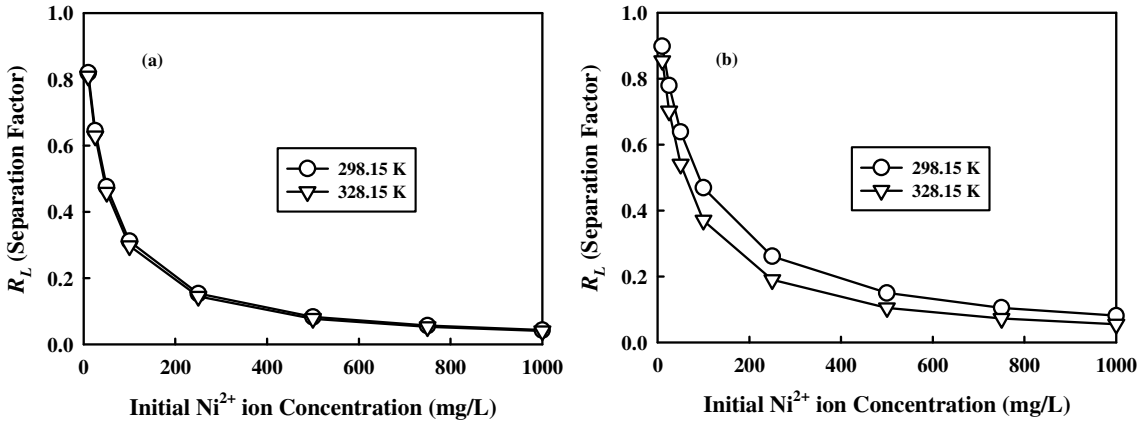

Figure 4.62. Separation factors for Ni^{2+} ion adsorption on chitin and chitosan a) chitin, b) chitosan (pH=6, S/L= 0.01, agitation time= 6h, agitation rate= 600 rpm).

4.4.5. Thermodynamic Parameters

The thermodynamic parameters, the standard enthalpy change (ΔH^o), standart entropy change (ΔS^o), and standard Gibbs energy (ΔG^o) of adsorption are useful in defining whether the adsorption reaction is endothermic or exothermic, comment of the system undergoing adsorption, and spontaneity of the adsorption process. As was outlined in Chapter 2, these parameters can be calculated using the following equations;

$$\ln K_d = \frac{\Delta S^o}{R} - \frac{\Delta H^o}{RT} \tag{2.12}$$

$$K_d = \frac{q_e}{C_e} \tag{2.13}$$

$$\Delta G^o = -RT \ln K_d \tag{2.14}$$

The distribution constant in the above equation is an empirical equilibrium constant that is valid at particular initial concentration and reaction conditions. This constant was used in the evaluation of thermodynamic parameters in many studies (Vadivelan and Kumar 2005). Based on the distribution constant and utilizing the above equations (ΔH^o), (ΔS^o) and (ΔG^o) were calculated. The values of these parameters obtained for Cu^{2+}, Pb^{2+}, Cd^{2+} and Ni^{2+} ions uptake on chitin and chitosan biopolymers and are given in Tables 4.19. and 4.20, respectively.

It is seen from Tables 4.19. and 4.20. that all the adsorption cases involve negative (ΔG^o) values, indicating that the adsorption reactions of Cu^{2+}, Pb^{2+}, Cd^{2+} and Ni^{2+} ions on chitin and chitosan bipolymers favors the products. The extent of spontaneity is seen to increase with temperature and decrease with concentration.

The values of enthalpy changes (ΔH^o) of the uptake of Cu^{2+}, Pb^{2+}, Cd^{2+} and Ni^{2+} ions on chitin and chitosan depend on initial concentrations. This dependence stems from the fact that K_d, used in the evaluation of thermodynamic parameters is concentration dependent. Positive values were obtained for the all concentrations indicating that the adsorption processes are endothermic.

The values of the entropy change (ΔS^o) of the adsorption processes of Cu^{2+}, Pb^{2+}, Cd^{2+} and Ni^{2+} on chitin and chitosan biopolymers ranged from 40.89 J/molK to 172.52 J/molK at 298.15 K and 328.15 K and 45.12 J/molK to 183.11 J/molK at 298.15 K and 328.15 K, respectively. The positive value of the (ΔS^o) reflects the increasing the randomness at the solid-liquid interface during the adsorption of metal ions, basically due to the dehydration of metal ions in their way to adsorption sites (Vadivelan and Kumar 2005).

Table 4.19. Values of ΔH^o, ΔS^o and ΔG^o calculated from the adsorption data of heavy metal ions on chitin.

Metal Ion	C_o (mg/L)	ΔH^o (kJ/mol)	$\Delta S^o_{avg.}$ (J/molK)	ΔG^o (kJ/mol)	
				298.15 K	328.15 K
Cu^{2+}	10	24.15	166.17	-23.36	-28.40
	25	14.23	127.84	-22.03	-25.71
	50	11.03	109.34	-19.98	-23.13
	100	10.91	100.66	-17.64	-20.54
	250	9.08	83.98	-14.74	-17.16
	500	6.82	66.29	-11.98	-13.89
	750	5.19	56.53	-10.85	-12.47
	1000	4.96	53.04	-10.08	-11.61
Pb^{2+}	10	24.39	172.52	-24.54	-29.51
	25	18.49	147.59	-23.36	-27.62
	50	14.94	121.15	-19.43	-22.92
	100	10.24	65.32	-14.61	-16.48
	250	9.52	77.04	-12.33	-14.55
	500	6.79	61.21	-10.57	-12.33
	750	6.01	55.64	-9.77	-11.37
	1000	3.66	44.41	-8.94	-10.21
Cd^{2+}	10	27.79	168.25	-22.15	-27.01
	25	25.56	156.05	-16.45	-20.96
	50	18.42	122.45	-16.30	-19.84
	100	9.86	80.52	-12.97	-15.29
	250	9.36	72.81	-11.29	-13.39
	500	7.89	61.37	-9.52	-11.29
	750	6.55	53.37	-8.58	-10.12
	1000	3.79	40.88	-7.80	-8.97
Ni^{2+}	10	16.73	119.48	-17.15	-20.58
	25	11.43	94.54	-15.38	-18.10
	50	10.99	82.64	-12.44	-14.82
	100	9.037	68.75	-10.46	-12.44
	250	7.73	57.35	-8.53	-10.18
	500	7.46	51.37	-7.11	-8.59
	750	7.15	47.21	-6.24	-7.60
	1000	7.07	44.49	-5.54	-6.83

Table 4.20. Values of ΔH^o, ΔS^o and ΔG^o calculated from the adsorption data of heavy metal ions on chitosan.

Metal Ion	C_o (mg/L)	ΔH^o (kJ/mole)	$\Delta S^o_{avg.}$ (J/molK)	ΔG^o (kJ/mol)	
				298.15 K	328.15 K
Cu^{2+}	10	28.31	183.11	-30.26	-35.80
	25	21.19	168.72	-29.09	-34.16
	50	18.40	155.98	-28.08	-32.82
	100	15.71	119.11	-21.79	-25.39
	250	14.69	112.38	-18.79	-22.20
	500	6.86	75.55	-15.66	-17.94
	750	5.70	67.34	-14.37	-16.41
	1000	4.25	58.07	-13.06	-14.88
Pb^{2+}	10	18.41	151.76	-26.82	-31.41
	25	16.66	122.35	-22.81	-26.51
	50	15.97	105.93	-20.60	-23.80
	100	14.77	116.51	-19.95	-23.48
	250	7.65	83.22	-17.15	-19.66
	500	7.41	71.52	-13.90	-16.06
	750	7.14	65.39	-12.34	-14.32
	1000	4.39	53.39	-11.52	-13.13
Cd^{2+}	10	19.08	126.81	-18.71	-22.56
	25	14.38	108.92	-18.08	-21.38
	50	13.86	106.98	-18.02	-21.26
	100	12.66	94.63	-15.54	-18.41
	250	12.18	87.84	-14.00	-16.66
	500	10.45	76.52	-12.35	-14.67
	750	7.59	64.35	-11.58	-13.53
	1000	5.72	54.52	-10.53	-12.18
Ni^{2+}	10	18.19	115.16	-16.13	-19.62
	25	14.66	102.35	-15.84	-18.94
	50	11.38	91.47	-15.88	-18.65
	100	10.05	81.21	-14.15	-16.61
	250	9.19	75.414	-13.28	-15.56
	500	6.89	62.77	-11.81	-13.71
	750	3.99	50.97	-11.20	-12.74
	1000	3.30	45.12	-10.15	-11.51

4.4.6. Comments of Adsorption Mechanism

Based on the studies conducted on heavy metal ion adsorption on chitosan the amine sides are accepted as the main reactive groups for heavy metal ions (Randall 1979, McKay 1989). As discussed in literature this interaction was found to be very much depend on the type of metal ion, matrix of the solution and pH. It is found that the free electron doublet on nitrogen binds metal cations best when the surface is chargeless. This occurs at the PZC of these polymer surfaces which was shown in Figure 4.5. Below PZC since both surface and the metal ions carry positive charge there will be a repulsion between them and this will decrease the overall adsorption. In addition, the adsorption uptake order of metal ions is similar to the Irwing-Williams Series for $Cu^{2+} > Cd^{2+} > Ni^{2+}$ ions and there was a relation between the order of the second ionization potentials. This series refers to the relative stability of complexes formed by a metal ion and is independent of ligand choice.

There are no differences among metal ions in terms of their valency. They all have the same positive charge. Their hydrodynamic radius are also almost similar. Therefore, the effects of diffusion and pore size (which almost equal for chitin and chitosan) seem to be irrelevant. Moreover, the pore size is much larger compared to the hydrodynamic radius of the ions. Therefore explaining the adsorption trend based on Irwing-Williams series seems reasonable.

The other mechanism discussed in literature is the chelation of metal cations by ligands in solution and formation of metal anions, which therefore turns the chelation of chitosan to an electrostatic attraction mechanism on protaneted amine groups of the polymer.

The chelation mechanism is one of the mechanism based on the theory of hard and soft acids and bases (HSAB) which describes the ability of ions to interact or enter into coordinate bonding with other ions or with ligands and shows that this depends on the availability of their outermost electrons and empty molecular orbitals. This must be considered on top of any electrostatic effects due to ion-ion, ion-dipole, and ion-higher multipole interactions. The last type of effect is governed primarily by the charge and size of the ion. The first type of effect can be described by means of the softness parameters and the Lewis acid/base parameters of the ions. The HSAB concept provides a description of “the capacities of ions to prefer ligands of the same kind (soft–soft and

hard–hard) to those of different kinds when forming coordinative bonds. Softness of ions generally goes hand in hand with their polarizability, and hardness with their electrostatic field strength (Pearson et al. 1963).

It is also postulated in literature that hydroxyl groups (especially in the C-3 position) may contribute to adsorption. However, in a study done by (Zhu et al. 2004) pure cellulose which has several OH groups did not show any contribution of this OH groups for adsorption of Cu^{2+}, Pb^{2+} and Cd^{2+} ions. In addition, other investigators (Dambies et al. 2001) have used XPS to analyze Cu^{2+} ion adsorption on chitosan and concluded that there is no contribution of these groups on adsorption. However, NH_2 groups represent the principle adsorption sites and their protonation controls adsorption efficency. In addition chitin has limited NH_2 groups when compared with chitosan and this situation directly affect the adsorption capacity of this biopolymer.

CHAPTER 5

CONCLUSION

Chitosan was prepared from chitin with controlled experimental conditions and both biopolymers were characterized before the adsorption experiments of heavy metal ions (Cu^{2+}, Pb^{2+}, Cd^{2+} and Ni^{2+}) with some analytical and instrumental techniques.

- Nearly six hours is enough to prepare approximately 82.9 % deacetylated chitin (chitosan) from chitin with reaction of hot and concentrated NaOH solution under nitrogen atmosphere.
- Degree of deacetylation (DD) value of chitosan biopolymer appeared to be higly associated with the analytical and instrumental method employed.
- Potentiometric titration method gave the highest degree of decetylation (DD) value while FT-IR analysis gave lowest degree of deacetylation value for used chitosan sample used in this study.
- Molecular weight determination of chitin and chitosan biopolymer with viscosity measurements showed that molecular weight of chitin is nearly ten times greater than chitin in this study.
- SEM analysis showed that chitin and chitosan biopolymers posses porous and fibril structures and there are no significant morphological differences between them.
- XRD analysis showed that the crystallinity of chitin changes from 40.1 % to 26.8 % after chemicall treatment with hot alkali solution to produce chitosan.
- TGA/DTA analysis showed that one degradation stage are observed at 261.5 and 288.3^{o}C for chitin and chitosan biopolymers respectively indicating that the thermal behavior of these biopolymers is slightly different.

Adsorption studies were performed to investigate the adsorption capacity of chitin and chitosan biopolymers toward heavy metal ions (Cu^{2+}, Pb^{2+}, Cd^{2+}, and Ni^{2+}) under different conditions such as S/L ratio, pH, contact time, concentration and temperature. The kinetic studies were analyzed using the pseudo first order and pseudo second order kinetic models. The data on the effect of solution temperature were used in the determination of the thermodynamic parameters of adsorption of heavy metal ions

onto chitin and chitosan biopolymers such as Activation energy (E_a), Enthalpy of adsorption (ΔH^o), Entropy of adsorption (ΔS^o), and Free energy of adsorption (ΔG^o). The Freundlich Langmuir and Temkin isotherms were used for the mathematical description of the adsorption equilibrium of heavy metal ions on chitin and chitosan bioplymers.

- The amount of Cu^{+2}, Pb^{2+}, Cd^{2+} and Ni^{2+} adsorbed was found to vary with the initial solution pH, adsorbent dosage, contact time, concentration and temperature.
- The amount of Cu^{+}, Pb^{2+}, Cd^{2+} and Ni^{2+} ions uptake (mg/g) was found to increase in solution temperature, concentration and contact time.
- The maximum amount of Cu^{+2}, Pb^{2+}, Cd^{2+} and Ni^{2+} ions uptake at 328.15 K were 42.56, 30.40, 21.98 and 11.14 (mg/g) for chitin and 69.97, 54.94, 48.78 and 43.86 (mg/g) for chitosan.
- Chitosan biopolymer have significantly higher adsorption capacity towards Cu^{2+}, Pb^{2+}, Cd^{2+} and Ni^{2+}, then chitin biopolymer. In addition both of chitin and chitosan biopolymers are showing similar trends of fixation ability within the experimental conditions of this study. ($Cu^{2+} > Pb^{2+} > Cd^{2+} > Ni^{2+}$). Moreover, the uptake mechanism seems to be relateded with Irwing-Williams Series for Cu^{2+}, Cd^{2+} and Ni^{2+} ions.
- The adsorption data of Cu^{2+}, Pb^{2+}, Cd^{2+} and Ni^{2+} ions on chitin and chitosan biopolymers show that pseudo-second order model was more suitable than pseudo first order model. The calculated rate constants of the adsorption showed that adsorption of Cu^{2+} and Pb^{2+} ions are faster on chitin and this is also marked by lower activation energy.
- Kinetic experiments showed that the intra-particle diffusion seems to play a role at later stages of the adsorption of Cu^{2+}, Pb^{2+}, Cd^{2+} and Ni^{2+} onto chitin and chitosan biopolymers.
- Temkin model did not correlate well with the the adsorption data. On the contrary, Freundlich and Langmuir isotherm models described the adsorption data adequately.
- Positive Enthalpy (ΔH^o) values were obtained for heavy metal ions adsorption on chitin and chitosan biopolymers indicating that the uptake process is endothermic.

• The entropy change (ΔS^{o}) of the adsorption of heavy metal ions on chitin and chitosan was in the range of 40.9-172.5J/molK, and 45.1-183.1 J/mol K, respectively. These values show an increase randomness at the solid-liquid interface during the adsorption of metal ions onto chitin and chitosan biopolymers.

• The negative (ΔG^{o}) values obtained indicate that the adsorption reactions of heavy metal ions on chitin and chitosan biopolymers favors the products. The extent of spontaneity increases with temperature and decreases with concentration.

REFERENCES

Aiba, S. 1991. "Studies on chitosan: 3. Evidence for the presence of random and block copolymer structures in partially *N*-acetylated chitosans", *International Journal of Biological Macromolecules.* Vol. 13, pp. 40–44.

Argüelles-Monal, W., Goycoolea, F.M., Lizardi, J., Peniche C. and Higuera-Ciapara, I. 2003. "Chitin and chitosan in gel network systems" in *Polymer gels,* edited by H.B. Bohidar, P. Dubin and Y. Osada, (American Chemical Society, Washington D.C.), pp. 102–122.

Arof, L., Subban, R.H.Y. and Radhakrishna, S. 1995. "Polymer and Other Advanced Materials*" in Emerging Technologies and Business,* edited by P.N. Prasad, (Plenum Press, New York), p. 539.

Atkins, E.D.T., Dlugosz, J. and Foord, S. 1979. "Electron diffraction and electron microscopy of crystalline α-chitin from the grasping spines of the marine worm *Sagitta"*, *International Journal of Biological Macromolecules.* Vol.1, pp. 29–32.

Atkins, E.D.T. 1985. "Conformation in polysaccharides and complex carbohydrates", *Journal of Biosciences*. Vol. 8, pp. 375–387.

Atkins, P.V. 1994. *Physical Chemistry*. (Oxford University Press, 5th Edition, Oxford), pp. 324-326

Ayoub, G.M., Semerjian, L., Acra, A., El Fadel, M. and Koopman, B. 2001. "Heavy metal removal by coagulation with seawater liquid bittern", *Journal of Environmental Engineering.* Vol. 127. No: 3, pp. 196–202.

Bartnicki-Garcia, S., Persson, J. and Chanzy, H. 1994. "An electron microscope and electron diffraction study of the effect of calcofluor and congo red on the biosynthesis of chitin in vitro", *Archives of Biochemistry and Biophysics.* Vol. 310, pp. 6–15.

Baxter, A., Dillon, M., Taylor, K.D.A. and Roberts, G.A.F. 1992. "Improved method for IR determination of the degree of *N*-acetylation of chitosan", *International Journal of Biological Macromolecules.* Vol. 14, p. 166.

Blackwell, J., Parker, K.D. and Rudall, K.M. 1965. "Chitin in pogonophore tubes", *Journal of the Marine Biological Association of the U.K*. Vol. 45, pp. 659–661.

Bose, P., Bose, M.A. and Kumar, S. 2002. " Critical evaluation of treatment strategies involving adsorption and chelation for wastewater containing copper, zinc, and cyanide", *Advances in Environmental Research.* Vol.7 , pp. 179–195.

Brugnerotto, J., Desbrières, J., Roberts, G. and Rinaudo, M. 2001. "Characterization of chitosan by steric exclusion chromatography", *Polymer.* Vol. 42, pp. 9921–9927.

Cartier, N., Domard, A and Chanzy, H. 1990. "Single crystals of chitosan", *International Journal of Biological Macromolecules.* Vol.12, pp. 289–294.

Chang, K.L.B., Tsai, G., Lee, J. and Fu, W.R. 1997. "Heterogenous *N*-deacetylation of chitin in alkaline solution", *Carbohydrate Research.* Vol. 303, pp. 327-332

Chantawong, V., Harvey, N.W. and Bashkin, V.N. 2001. "Comparison of heavy metal adsorptions by thai kaolin and ballclay", *Asian Journal of Energy & Environmental.* Vol.1, pp. 33–48.

Chanzy, H. 1998. "Chitin crystals", in *Advances in chitin Science,* edited by A. Domard, G.A.F. Roberts and K.M. Vårum, (Jacques André, Lyon, France) pp. 11–21.

Chen, X.H., Gosset, T. and Thevenot, D.R. 1990. "Batch copper ion binding and exchange properties of peat", *Water Research.* Vol. 24, pp. 1463–1471

Chrétiennot-Dinet, M.J., Giraud-Guille, M.M., Vaulot, D., Putaux, J.L. and Chanzy, H. 1997. "The chitinous nature of filament ejected by *Phaeocystis* (Prymnesiophycae)", *Journal of Phycology.* Vol. 33, pp. 666–672.

Damibies, L., Guiman, C., Yiacoumi, S. and Guibal, E. 2001. "Characterization of metal ion interactions with chitosan by X-Ray photoelectron spectroscopy, *Colloids and Surfaces A: Physicochemical and Engineering Aspects.* Vol. 177, pp. 203-214

Dinger, D.R., 2005. *Characterization Techniques for Ceramists.* (Morris Publishing, U.S.A), pp.3-4, 71-72, 175-176, 223-224.

Dojlido, J.R. and Best, G. A. 1993. *Chemistry of Water and Water Pollution*. (Ellis Horwood Limited, Herts), pp. 65-69, 84-91, 108-114, 201-205

Domard, A., 1986. "Circular dichroism study on *N*-acetylglucosamine oligomers", *International Journal of Biological Macromolecules.* Vol. 8 , p. 243.

Domard, A. 1987. "pH and c.d. measurements on a fully deacetylated chitosan: application to Cu^{II}–polymer interactions", *International Journal of Biological Macromolecules.* Vol. 9, p. 98.

Domszy, J.G. and Roberts, G.A.F. 1985. " Evaluation of infrared spectroscopic techniques for analyzing chitosan", *Makromolekulare Chemie*. Vol. 186, pp. 1671-1677

Dutta, P.K. and Kumar, R.M.N.V. 1999. "Chitosan–amine oxide: thermal behavior of new gelling system", *Indian Journal of Chemical Technology.* Vol.6 , p. 55.

Dutta, P.K., Viswanathan, P., Mimrot, L. and Kumar, M.N.V.R. 1997. "Use of chitosan amine oxide gel as drug carrier", *Journal of Polymer Materials.* Vol.14 , p. 351.

Eckenfelder, W. W. 2000. *Industrial Water Pollution Control*, (McGraw-Hill Companies), pp. 451-457.

Einbu, A., Naess, S.N., Elgsaeter A. and Vårum, K.M. 2004. "Solution properties of chitin in alkali", *Biomacromolecules* . Vol. 5, pp. 2048–2054.

Elimelech, M. and O'Melia, C.R. 1990. " Kinetics of deposition of colloidal particles in porous media", *Environmental & Science Technology.* Vol. 24, pp. 1528–1536

Flory, P.J. 1953. *Principles of polymer chemistry*. (Cornell University Press, Ithaca, NY), pp. 266–316.

Gaill, F., Persson, J., Sugiyama, P., Vuong, R. and Chanzy, H. 1992. "The chitin system in the tubes of deep sea hydrothermal vent worms", *Journal of Structural Biology.* Vol. 109, pp. 116–128.

Gosset, T., Trancart, J.L. and Thevenot, D.R. 1986. "Batch metal removal by peat: kinetics and thermodynamics", *Water Research.* Vol. 20, pp. 21–26.

Goycoolea F.M., Arguelles-Monal W.M., Lizardi, J., Peniche, C., Heras, A., Galed, G. and Diaz E.I. 2006. "Temperature and pH-sensitive chitosan hydrogels: DSC, rheological and swelling evidence of a volume phase transition*", Polymer Bulletin.* Vol.58, pp. 225-234

Grant, D.C., Skriba, M.C. and Saha, A.K. 1987. "Removal of radioactive contaminants from west valley waste streams using national zeolites", *Environmental Progress.* Vol. 6 , pp. 104–109.

Gupta, D.C. and Tiwari, U.C. 1985. "Aluminium Oxide as adsorbent for removal of hexavalent chromium from aqueous waste", *Indian Journal of Environmental Health.* Vol. 27, pp. 205–215.

Helbert, W. and Sugiyama, J. 1998. "High-resolution electron microscopy on cellulose II and α-chitin single crystals", *Cellulose.* Vol. 5, pp. 113–122.

Herth, W., Mulisch, M. and Zugenmaier, P. 1986. "Comparison of chitin fibril structure and assembly in three unicellular organisms", in *Chitin in nature and technology*, edited by R. Muzzarelli, C. Jeuniaux and G.W. Gooday, (Plenum Publishing Corporation, New York), pp. 107–120.

Herth, W., Kuppel, A. and Schnepf, E. 1977. "Chitinous fibrils in the lorica of the flagellate chrysophyte *Poterioochromonas stipitata* (syn. *Ochromonas malhamensis*)", *Journal of Cell Biology.* Vol. 73, pp. 311–321.

Ho, Y.S. 2003. "Removal of copper ions from aqueous solution by tree fern", *Water Research.* Vol. 37, pp. 2323–2330.

Ho, S. and McKay, G. 1998. "The kinetics of sorption of basic dyes from sphagnum. moss peat", *Canadian Journal of Chemical Engineering.* Vol. 76, p. 822.

Ibrahim, K.M., NasserEd-Deen, T. and Khoury, H. 2002. "Use of natural chabazite-phillipsite tuff in wastewater treatment from electroplating factories in Jordan", *Environmental Geology.* Vol. 41, pp. 547–551.

Illum, L. 1998. "Chitosan and its use as pharmaceutical excipient", *Pharmaceutical Research.* Vol. 15, p. 1326.

Inbaraj, B.S., Selvarani, K. and Sulochana, N. 2002. "Evaluation of a carbonaceous sorbent prepared from pearl millet husk for its removal of basic dyes", *Journal of Scientific & Industrial Research*. Vol. 61, pp. 971–978.

Jokela, P. and Keskitalo, P. 1999. "Plywood mill water system closure by dissolved air flotation treatment", *Water Science &Technology.* Vol. 40, pp. 33–42.

Jüttner, K., Galla, U. and Schmieder, H. 2000. "Electrochemical approaches to environmental problems in the process industry", *Electrochimica Acta.* Vol. 45, pp. 2575–2594.

Kaifu, K., Nishi, N and Komai, T. 1981. "Preparation of hexanoyl, decanoyl and dodecanoyl chitin", *Journal of Polymer. Science Part A: Polymer Chemistry,* Vol.19, p. 2361.

Kannan, K. and Sundaram, M.M. 2001. "Kinetics and mechanism of removal of methylene blue by adsorption on various carbons—a comparative study", *Dyes and Pigments*. Vol. 51, pp. 25–40.

Kasaai, M.R., Arul, J. and Charlet, G. 2000. "Intrinsic viscosity–molecular weight relationship for chitosan", *Journal of Polymer Science and Polymer Physics*. Vol. 38, pp. 2591–2598.

Kawamura, Y., Mitsuhashi, M., Tanibe, H., Yoshida, H. 1993. "Adsorption of metal ions on polyaminated highly porous chitosan chelating agents". *Indian Engineering &Chemical Research*. Vol. 32, pp. 386–391.

Khan, S.A., Rehman, R. and Khan, M.A. 1995. "Adsorption of Cr(III), Cr(VI) and Ag(I) on bentonite", *Waste Management.* Vol. 15, pp. 271–282.

Khan, S.A., Rehman, R. and Khan, M.A. 1995. "Adsorption of strontium (II) on bentonite", *Waste Management.* Vol. 15 , pp. 641–650.

Knorr, D. 1991. "Recovery and utilization of chitin and chitosan in food processing waste management", *Food Technology.* Vol. 45, p. 114-122

Kubota, N. and Eguchi, Y. 1997. "Facile preparation of water-soluble N-acetylated chitosan and molecular weight dependence of its water-solubility", *Polymer Journal.* Vol. 29, pp. 123–127.

Kumar, M.N.V.R. 2000. “A review of chitin and chitosan applications”, *Reactive &. Functional Polymers.* Vol. 46, pp.1-27

Kumar, M.N.V.R, Singh , P. and Dutta, P.K. 1999. “Effect of swelling on chitosan–amine oxide gel in extended drug delivery”, *Indian Drugs.* Vol. 36, p. 393.

Kurniawan, T.A. and Babel, S. 2003. “A research study on Cr(VI) removal from contaminated wastewater using low-cost adsorbents and commercial activated carbon”, Proceedings of the 2nd International Conference on Energy Technology Towards a Clean Environment, Phuket, Thailand, (12–14 February 2003), *RCETE,* Vol. *2*, pp. 1110–1117.

Kurniawan, T.A., Chan, G.Y.S., Lo, W.H., Babel, S. 2006. “Physico–chemical treatment techniques for wastewater laden with heavy metals”, *Chemical Engineering Journal*. Vol.118, pp. 83–98

Lang, G. 1995. “Chitosan derivatives-preparation and potential uses” in *Chitin and Chitosan*, edited by M. B. Zakaria, W. M. Wan-Muda, A. Pauzi, (Bangi: Penerbit University Kebangsaan Malaysia), pp.109-118

Larry, H.L. 1998. “Biomaterials: a forecast for the future”, *Biomaterials.* Vol. 19 p. 1419.

Le, Y., Anand, S.C. and . Horrocks, A.R. 1997. “Recent developments in fibres and materials for wound management”. *Indian Journal of Fibre & Textile Research.* Vol. 22, p. 337.

Lee, V.F.P. 1974. “Solution and shear properties of chitin and chitosan”.(University of Washington USA), PhD dissortation

Levine, I.N. 1998. “Reaction kinetics and surface chemistry”, in *Phyical Chemistry*, edited by K.S. Misler, S. Tenney (McGraw Hill, third edition, Singapore), pp. 372-373, 537-540

Licskó, I. 1997. “Realistic coagulation mechanisms in the use of aluminium and iron(III) salts”, *Water Science and Technology.* Vol. 36, pp. 103–110.

Liu, D., Hsu, C., Chuang, C. 1995. "Ion-exchange and sorption kinetics of Cesium and Strontium in soils", *Applied Radiation and Isotopes.* Vol. 46, pp. 839-843.

Lima, I.S. and Airoldi, C. 2004. “A thermodynamic investigation on chitosan–divalent cation interactions”, *Thermochimica Acta*. Vol. 421, pp. 133-139

Lo, W.H., Chua, H., Lam, K.H. and Bi, S.P. 1999. “A comparative investigation on the biosorption of lead by filamentous fungal biomass”, *Chemosphere.* Vol.39, pp. 2723–2736.

Madhavan, P. 1992. *Chitin, Chitosan and their Novel Applications*. (*Science Lecture Series*, CIFT, Kochi) , p. 1.

Maghami, G.A. and Roberts, G.A.F. 1988. "Studies on the adsorption of anionic dyes on chitosan" *International Journal of Biological Macromololecules.* Vol. 189, p. 2239.

Malettas, W.G., Quingley, H.J. and Adickes, E.D. 1986. "*Chitin in Nature and Technology"*, edited by R.A.A. Muzzarelli, (Plenum Press, New York), p. 435.

Mall, I.D. and Upadhyay, S.N. 1998. "Studies on treatment of basic dyes bearing wastewater by adsorptive treatment using flyash", *Indian Journal of Environmental*. Vol. 40, p. 177.

Malliou, E., Malamis, M., Sakellarides, P.O. 1992. "Lead and cadmium removal by ionexchange", *Water Science and Technology.* Vol. 25, pp.133-138.

Marcus, Y. 1997. *Ion Properties*, (Marcel Dekker Inc., New York) p.259

Mark, H.F., Bikales, N.M., Overberger, C.G. and . Menges, A.C 1985. *Encyclopedia of Polymer Science and Engineering* , Vol. 1, (Wiley, New York), p. 20.

Markey, M.L., Bowman, M.L. and Bergamini, M.V.W. 1989. "*Chitin and Chitosan*" (Elsevier Applied Science, London), p. 713.

Mass W.A., Mass A. and Tighe B. 1998. "A review of biodegradable polymers: uses, current developments in the synthesis and characterization of biodegradable polyesters. Blends of biodegradable polymers and recent advances in biodegradation studies", *Polymer International.* Vol. 47 , p. 89.

Mathur, N.K. and Narang, C.K. 1990. "Chitin and chitosan, versatile polysaccharides from marine animals", *Journal of Chemical Education.* Vol. 67, pp. 938–942.

Matis, K.A., Zouboulis, A.I., Lazaridis, N.K. and Hancock, I.C. 2003. " Sorptive flotation for metal ions recovery", *International Journal of Mineral Processing*. Vol. 70, pp. 99–108.

McKay, G., Blair, H.S. and Findon, A. 1989. "Equilibrium studies for the sorption of metal ions onto chitosan", *Indian Journal of Chemistry*. Vol. 28, pp. 356–360.

McKay, G. 1996., "Use of adsorbents for the removal of pollutants from wastewaters" (CRR Press, U.S.A), pp. 40-41

Mellah, A. and Chegrouche, S. 1997. "The removal of zinc from aqueous solutions by natural bentonite", *Water Research.* Vol. 31, pp. 621–629.

Metcalf and Eddy, 2003. *Wastewater Engineering: Treatment and Reuse*. (McGraw Hill International Edition, New York). pp.478-483

Montgomery, J.M., 1985. *Water Treatment Principles and Design*, (Consulting Engineers Inc. USA). pp. 312-326

Muzzarelli, R.A.A., 1973. *Natural Chelating Polymers* (Pergamon Press, New York), p. 83.

Muzzarelli, R.A.A. 1997. "Human enzymatic activities related to the therapeutical administration of chitin derivatives", *Cellular and Molecular Life Sicences.* Vol. 53, p. 131.

Muzzarelli, R.A.A. 1998. "Management of hypercholesterolemia and overweight by oral administration of chitosans" in *New Biomedical Materials — Applied and Basic,* edited by D. Chapman, (POI Press, London).

Muzzarelli, R.A.A. 1999. "Clinical and biochemical evolution of chitosan for hypercholesterolemia and overweight control"*in Chitin and Chitinases*: edited by P. Jolles and R.A.A. Muzzarelli (Birkhauser, Basel)

Muzzarelli. R.A.A., Mark H.F., Bikales N.M., Overberger C.G. and Menges G., 1984. "*Encyclopedia of Polymer Science and Engineering*", Vol. 3, (Wiley, New York), p. 435.

Naseem, R. and Tahir, S.S. 2001. "Removal of Pb(II) aqueous/acidic solutions by using bentonite as an adsorbent", *Water Research.* Vol. 35, pp. 3982–3986.

Niola, F., Basora, N., Chornet, E. and Vidal, P.F. 1983 "A rapid method for the determination of the degree of *N*-acetylation of chitin–chitosan sample by acid hydrolysis and HPLC", *Journal of Thermal Analysis and Calorimetry.* Vol. 28, p. 189.

Nishi, N., Noguchi, J., Tokura, S. and Shiota, H. 1979. "Studies on chitin. I. Acetylation of chitin". *Polymer Journal.* Vol.11, p. 27.

Ogawa, K., Yui, T. and Miya, M. 1991. "Dependence on the preparation procedure of the polymorphism and crystallinity of chitosan membranes", *Bioscience Biotechnology and Biochemistry.* Vol. 56, pp. 858–862.

Ogawa, K. 1991. "Effect of heating an aqueous suspension of chitosan on the crystallinity and polymorphs", *Biological Chemistry.* Vol. 55, pp. 2375–2379.

Olivera, B.M., Hillyard, D.R., Marsh M. and Yoshikami, D. 1995. "Combinatorial peptide libraries in drug design: lesson from venomous cone snails",*TIBTECH.* Vol.13 , pp. 422–426.

Olsen, R., Schwartzmiller, A., Weppner, DW. and Winandy, R.1989." in *Chitin and Chitosan: Sources, Chemistry, Biochemistry, Physical Properties and Applications"* edited by G. Skjak-Brack, T. Anthonsen and P.A. Sandford (Elsevier Applied Science, New York), p 198.

Ouki, S.K., Cheeseman, C.R. and Perry, R. 1993. "Effects of conditioning and treatment of chabazite and clinoptilolite prior to lead and cadmium removal", *Environmental Science &. Technology.* Vol. 27, pp. 1108–1116.

Ouki, S.K. and Kavanagh, M. 1997. "Performance of natural zeolites for the treatment of mixed metal-contaminated effluents", *Waste Management and Research.* Vol. 15, pp. 383–394.

Panday, K.K., Prased, G. and Singh, V.N. 1985. "Copper (II) removal from aqueous solution by fly ash", *Water Research*. Vol. 19, pp. 869-873

Panday, K.K., Prasad, G. and Singh, V.N. 1984. "Removal of Cr(VI) from aqueous solutions by adsorption on fly ash-wollastonite", *Journal of Chemical Technology & Biotechnology*. Vol. 34A, pp. 367–374.

Pangburn, S.H., Trescony, P.V. and Heller, H.S. 1984. in "*Chitin, Chitosan and Related Enzymes",* edited by J.P. Zikakis , (Harcourt Brace Janovich, New York), p. 3.

Pearson, R.G. 1963. "Soft and Hard Acids and Bases", *Journal of American Chemical Society.* Vol. 12, pp. 3538 -3546.

Persin, F. and Rumeau, M. 1989. " Le traitement électrochimique des eaux et des effluents", *Tribune de l'eau.* Vol.3 No: 42, pp. 45–46.

Persson, J.E., Domard, A. and Chanzy, H. 1990. "Single crystals of α-chitin", *International Journal of Biological Macromolecules.* Vol.13, pp. 221–224.

Peter, M.G. 1995. "Aplications and environmental aspects of chitin and chitosan", *Journal of Macromolecular Science, Pure and applied chemistry* . Vol.32, pp. 629-640

Philippova, O.E., Volkov, E.V., Sitnikova, N.L., Desbrières, A. J. and Rinaudo, M. 2001. "Two types of hydrophobic aggregates in aqueous solutions of chitosan and its hydrophobic derivative", *Biomacromolecules*. Vol. 2, pp. 483–490.

Poirier, M. and Charlet, G. 2002. "Chitin fractionation and characterization in *N, N*-dimethylacetamide/lithium chloride solvent system", *Carbohydrate Polymer.* Vol. 50, pp. 363–370.

Randall, J.M., Randall, V.G., McDonald, G.M., Young, R.N. and Masri, M.S. 1979. "Removal of trace quantities of Nickel from solution", *Water Research*. Vol. 23, p. 727

Revol, J.F. and Chanzy, H. 1986. "High-resolution electron microscopy of β-chitin microfibrils", *Biopolymers*. Vol. 25 , pp. 1599–1601.

Rinaudo, M. 2006. "Chitin and Chitosan: Properties and applications", *Progress in Polymer Science.* Vol. 31, pp. 603-632

Rinaudo, M. and Domard, A. 1989. "Solution properties of chitosan." in *Chitin and chitosan. Sources, chemistry, biochemistry, physical properties and applications* edited by : G. Skjak-Braek, T. Anthonsen and P. Sandford, (Elsevier, London and New York), pp. 71–86.

Rinaudo, M., Pavlov, G. and Desbrières, J. 1999. "Influence of acetic acid concentration on the solubilization of chitosan", *Polymer*. Vol. 40, pp. 7029–7032.

Rinaudo, M., Milas, M. and Le Dung, P. 1993. "Characterization of chitosan: Influence of ionic strength and degree of acetylation on chain expansion", *International Journal of Biological Macromolecules.* Vol. 15, pp. 281–285.

Roberts G.A. and Domszy, J.G. 1982. "Determination of the viscometric constants for chitosan", *International Journal of Biological Macromolecules.* Vol. 4, pp. 374–377.

Rouquerol, F., 1999. *Adsorption by Powders and Porous Solids*. (Academic Press, London), pp. 1-21, 355-361, 378-382.

Rudall, K.M. 1969. "Chitin and its association with other molecules", *Journal of Polymer Science Part C*. Vol. 28, pp. 83–102.

Rudall, K.M. and Kenchington, W. 1973. "The chitin system", *Biological Reviews*. Vol. 40, pp. 597–636.

Rudall, K.M. 1979. *Molecular structure in arthropod cuticles*. (Elsevier Scientific, Amsterdam) , pp. 21–41.

Ruiz-Herrera, J., Sing, V.O., Van der Woude, W.J. and Bartnicki-Garcia, S. 1975. "Microfibril assembly by granules of chitin synthetase", Proceedings of the National Academy of Sciences of the U.S.A. Vol. 72, pp. 2706–2710.

Sakamoto, J., Sugiyama, J., Kimura, S., Imai, T., Itoh T. and Watanabe, T. 2000. "Artificial chitin spherulites composed of single crystalline ribbons of α-chitin via enzymatic polymerization", *Macromolecules*. Vol. 33, pp. 4155–4160.

Saito, Y., Putaux, J.L., Okano, T., Gaill, F. and Chanzy, H. 1997. "Structural aspects of the swelling of β-chitin in HCl and its conversion into α-chitin", *Macromolecules.* Vol. 30, pp. 3867–3873.

Saito, Y., Okano, T., Chanzy, H. and Sugiyama, J. 1995. "Structural study of α-chitin from the grasping spine of the arrow worm (*Sagitta* spp.), *Journal of Structural Biology.* Vol. 114, pp. 218–228.

Sannan, T., Kurita, K. and Iwakura, Y. 1975. "Studies on chitin 1", *Macromolecular Chemistry and Pyhsics.* Vol. 176, pp. 1191–1195.

Sannan, Y., Kurita, K. and Iwakura, Y. 1976. "Studies on chitin 2", *Macromolecular Chemistry and Pyhsics.* Vol. 177, pp. 3589–3600.

Sashiwa, H., Saimoto, H., Shigemasa, Y., Ogawa, R. and Tokura, S. 1991. "Distribution of the acetamido group in partially deacetylated chitins", *Carbohydrate Polymers.* Vol. 16, p. 291.

Sawyer, N.C., Mc Carty, P.L., Parkin, G.F., 1994. *Chemistry for Environmental Engineering.* (Mc. Graw Hill International Edition, Singapore).

Schwarzenbach, R.P, Gschwend, M.P, Imboden, D.M., 2003. *Environmental Organic Chemistry*. (John Wiley & Sons, Inc. Publication, Canada).

Semerjian, L. and Ayoub, G.M. 2003. "High-pH-magnesium coagulation–flocculation in wastewater treatment", *Advanced Environmental Research.* Vol.7, pp. 389–403.

Sen, A.K. and Arnab, K.D. 1987. "Adsorption of mercury on coal fly-ash", *Water Research.* Vol. 21, pp. 885–888.

Settle, F. 1997. *Handbook of Instrumental Techniques for Analytical Chemistry.* (Prentice-Hall, New Jersey), pp.341-342

Shammas, N.K., 2004 "Coagulation and flocculation" in *Physicochemical Treatment Processes*, edited by L.K. Wang, Y.T. Hung and N.K. Shammas, (Humana Press, New Jersey), pp. 103–140.

Sharma, D.C. and Forster, C.F. 1993. "Removal of hexavalent chromium using sphagnum moss peat", *Water Research.* Vol. 27, pp. 1201–1208

Sharma, D.C. and Forster, C.F. 1995. "Continuous adsorption and desorption of chromium ions by sphagnum moss peat", *Process Biochemistry*. Vol. 30, pp. 293–298.

Singh, A.K., Singh, D.P. and Singh, V.N. 1998. "Removal of Zn(II) from water by adsorption on China clay*", Environmental Technology Letters.* Vol. 9, pp. 1153–1162.

Sivaraj, R., Namasivayam, C. and Kadirvelu, K. 2001. "Orange peel as an adsorbent in the removal of acid violet 17 (acid dye) from aqueous solution", *Waste Management*. Vol. 21, pp. 105.-110

Srivastava, V.C., Swamy, M.M., Mall, I.D., Prasad, B., Mishra, I.M. 2006. "Adsorptive removal of phenol by bagasse fly ash and activated carbon: equilibrium, kinetics and thermodynamics", *Colloids and Surface A: Physicochemical and Engineering Aspects.* Vol. 272, pp. 89–104.

Srivastava, S.K., Tyagi, R. and Pal, N. 1989. "The application of nature absorbents for heavy metals uptake from contaminated water", *Environmental Technology*. Vol. 10, pp. 275–282.

Srivastava, S.K., Bhattacharjee, G., Tyagi, R., Pant N. and Pal, N. 1988. "Studies on the removal of some toxic metal-ions from aqueous-solutions and industrial-waste. 1. (Removal of lead and cadmium by hydrous iron and aluminum-oxide)", *Environmental Technology Letters.* Vol. 9, pp. 1173–1185.

Sun, Q. and Yang, L. 2003. "The adsorption of basic dyes from aqueous solutions on modified peat–resin particle", *Water Research.* Vol.37, pp. 1535–1544.

Tamura, H., Hamaguchi, T. and Tokura, S. 2003. "Destruction of rigid crystalline structure to prepare chitin solution", *Advances in chitin science.* Vol. 7, (ISM BioPolymer Inc.) , pp. 84–87.

Tanford, C. 1961. *Physical chemistry of macromolecules*. (John Wiley Press, New York), pp. 390–412

Terbojevich, M., Carraro, C. and Cosani, A. 1988. "Solution studies of the chitin-lithium chloride-N, N-dimethylacetamide system", *Carbohydrade Research.* Vol. 180, pp. 73–86.

Tolaimate, A., Desbrières, J., Rhazi, M., Alagui, A., Vincendon, M. and Vottero, P. 2000. "On the influence of deacetylation process on the physicochemical characteristics of chitosan from squid chitin", *Polymer*. Vol. 41, pp. 2463-2469

Trivedi, P., Axe, P. and Dyer, J. 2001. "Adsorption of metal ions onto goethite: single-adsorbate and competitive systems", *Colloids and Surfaces A: Physicochemical and Engineering Aspects.* Vol. 191 , pp. 107-121

Tyson, J.F., Haswell, S.J., 1991. "Basic Principles and Instrumental Requirements and optimization" in *Atomic Absorption Spectrometry*, edited by S.J. Haswell (Elsevier Publishing, New York), pp. 9-10, 14-17, 21-40

Undaybeytia, T., Morillo, E. and Maqueda, C. 1996. "Adsorption of Cd and Zn on montmorillonite in the presence of a cationic pesticide", *Clays and Clay Minerals.* Vol. 31 , pp. 485–490.

Vaca-Mier, M., Callejas, R.L., Gehr, R., Cineros, B.E.J., Alvarez. P.J.J. 2001. " Heavy metal removal with Mexican clinoptilolite:multi-component ionic exchange," *Water Research.* Vol.35, pp. 373-378.

Vadivelan, V., Kumar, K.V. 2005. "Equilibrium, kinetics, mechanism, and process design for the sorption of methylene blue onto rice husk", *Journal of Colloid and Interface Science*. Vol. 286, pp. 90-100.

Vasconcelos, M.T.S.D., Leal, M.F.C. and Soares, H.M.V.M. 1996. "Influence of the ratio Copper(II) to ligand concentrations and nature of entering and leaving ligands on the lability of copper complexes", *Analytica Chimica Acta*. Vol. 330, pp. 273-281

Vik, E.I., Carlsoon, D.A., Eikum A.S. and Gjessing, E.T. 1984. "Electrocoagulation of potable water", *Water Research.* Vol.18, pp. 1355–1360.

Vincendon, M. 1994. "Solution of chitin in phosphoric acid" in *Chitin world*, edited by S.Z. Karniki (Wirtschaftsverlag NW, Bremerhaven, Germany), pp. 91–97.

Wadstein, J., Thom, E., Heldman, E., Gudmunsson, S. and Lilja, B. 2000. "Biopolymer L 112, a chitosan with fat binding properties and potential as a weight reducing agent: a review of in vitro and in vivo experiments" in *From Dietary Supplement To Drug Carrier* edited by R.A.A. Muzzarelli, (Grottammare, Italy), pp. 22-36

Wang, L.K., Fahey, E.M. and Wu, Z.C. 2004., "Dissolved air flotation" in , *Physicochemical Treatment Processes*. edited by L.K. Wang, Y.T. Hung and N.K. Shammas, (Humana Press, New Jersey), pp. 431–500.

WEB_1, 2007. Chemical Engineering Tools and Information, 08/06/2007 http://www.cheresources.com/biosorption.shtml

WEB_2, 2007. TMMOB Çevre Mühendisleri Odası, 01/06/2007. http://www.cmo.org.tr/mevzuat/dosya/su_kir_kont_yon.pdf

WEB_3, 2007. Lenntech Water Treatment&Air Purification, 11/06/2007. http://www.lenntech.com/heavy-metals.htm

WEB_4, 2007. Dalwoo-Chitosan Corporation, 19/05/2007 http://members.tripod.com/~Dalwoo/structure.htm

WEB_5, 2007. Cornell University, 10/05/2007 http://www.nbtc.cornell.edu/facilities/downloads/Zetasizer%20chapter%2016.pdf

WEB_6, 2007. The University of Wet Indies, 13/06/2007 http://wwwchem.uwimona.edu.jm:1104/courses/IrvWill.html

Weber W.J. and Morris, J.C. 1963. "Kinetics of adsorption on carbon from solution", *Water Research.* Vol. 89, pp. 31–59.

Wei, Y.C. and Hudson, S.M. 1993. "Binding of sodium dodecyl sulfate to a polyelectrolyte based chitosan", *Macromolecules.* Vol. 26, p. 4151.

Welz, B., Sperling, M., 1998. *Atomic Absorption Spectrometry*. (Wiley-VCH, Weinheim), pp. 103-105, 113, 149-171.

Wingenfelder, U., Hansen, C., Furrer, G. and Schulin, R. 2005. "Removal of heavy metals from mine water by natural zeolites", *Environmental. Science and. Technology*. Vol. 39, pp. 4606–4613.

Yang, X.J., Fane, A.G. and MacNaughton, S. 2001. " Removal and recovery of heavy metals from wastewater by supported liquid membranes", *Water Science and Technology.* Vol. 43, pp. 341–348.

Yannas, I.V., Burke, H.F., Orgill, D.P. and Skrabut, E.M. 1982. "Wound tissue can utilise a polymeric template to synthesise a functional extension of skin", *Science*. Vol. 215, p. 174.

Zabel, T., 1984., “Flotation in water treatment” in *The Scientific Basis of Flotation*, edited by K.J. Ives, (Martinus Nijhoff Publishers, The Hague), pp. 349–378.

Zamzow, M.J.R., Eichbaum, B.R. and Shanks, D.E. 1990. “Removal of heavy metals and other cations from wastewater using zeolites”, *Separation Science and Technology*. Vol. 25, pp.1555–1569.

Zhang, Y., Xue, C., Xue, Y., Gao, R. and Zhang, X. 2005. “Determination of the degree of deacetylation of chitin and chitosan by X-ray powder diffraction”, *Carbohydrate Research.* Vol. 11, pp. 1914-1917